

Title	分子触媒と固体触媒の概念を融合したオレフィン重合触媒の開発
Author(s)	馬場, 竜希
Citation	
Issue Date	2019-03
Type	Thesis or Dissertation
Text version	ETD
URL	http://hdl.handle.net/10119/15799
Rights	
Description	Supervisor: 谷池 俊明, 先端科学技術研究科, 博士

Doctoral Dissertation

Development of Olefin Polymerization Catalysts by
Bridging Molecular and Solid Catalyst Concepts

Ryuki Baba

Supervisor: Associate Professor Dr. Toshiaki Taniike

Graduate School of Advanced Science and Technology

Japan Advanced Institute of Science and Technology

[Materials Science]

March 2019

Referee-in-chief: **Associate Professor Dr. Toshiaki Taniike**
Japan Advanced Institute of Science and Technology

Referees: **Professor Dr. Shinya Maenosono**
Japan Advanced Institute of Science and Technology

Associate Professor Dr. Shinohara Ken-ichi
Japan Advanced Institute of Science and Technology

Associate Professor Dr. Shun Nisimura
Japan Advanced Institute of Science and Technology

Professor Dr. Hideki Kurokawa
Saitama University

Contents

Chapter 1 General Introduction

1.1	Catalysis	2
1.2	Olefin Polymerization Catalyst	8
1.3	Approaches Using Heterogeneous and Homogeneous Catalysts	22
1.4	Bridging Catalysts in Olefin Polymerization	36
1.5	Purpose of the Present Research	40

Chapter 2 Synthesis of Silsesquioxane-Supported Chromium Catalysts as a Homogeneous Analogue to Phillips Catalyst

2.1	Introduction	52
2.2	Experimental	55
2.3	Results and Discussion	62
2.4	Conclusions	75
2.5	References	76
	Appendix	79

Chapter 3 Active Site Nature of a Silsesquioxane-Supported Homogeneous Phillips Catalyst

3.1	Introduction	94
3.2	Experimental	96
3.3	Results and Discussion	98

3.4	Conclusions	108
3.5	References	109
Chapter 4	Tandem Catalysis by Soluble Polynorbornene Supported Half-Titanocene Catalysts for Olefin Polymerization	
4.1	Introduction	113
4.2	Experimental	117
4.3	Results and Discussion	121
4.4	Conclusions	129
4.5	References	130
Chapter 5	General Conclusions	132
	Acknowledgments	135
	Achievements	136

Chapter 1

General Introduction

1.1 Catalysis

Definition

Catalyst is a substance that increases the rate of a chemical reaction while it does not convert itself during the reaction. It is defined as follows: 1) It is a substance which promotes a chemical reaction in a relatively less amount than the reactant. 2) It does not appear in a stoichiometric equation since it does not change through the reaction. 3) It can accelerate a reaction by lowering activation energy and creating a new pathway. Heat and light can also promote a chemical reaction; however, they are not regarded as a catalyst because they are nonmaterial. Catalyst can be in any state: solid, liquid or gas.

Catalysis in chemical reaction

The equilibrium of the chemical reaction is determined by the state before and after the reaction. Since the final free energy does not change if the products are the same, the equilibrium position is determined only by the stoichiometric equation. Therefore, the catalyst does not affect the equilibrium but only increases the speed for approaching equilibrium. When the reactants A and B changes to the product C, the chemical reaction formula is expressed by eq. (1).



The equilibrium of the chemical reaction is determined by Gibbs free energy change (ΔG°), and the relationship between the equilibrium constant $K_p = [C]/[A][B]$ and ΔG° is expressed by the following equation,

$$\Delta G^\circ = -RT \ln K_p \quad \text{Eq. (2).}$$

where $\Delta G^\circ = \Delta H^\circ - T\Delta S^\circ$. The temperature dependence of K_p is represented by the van't

Hoff equation as:

$$\ln K_p = -\frac{\Delta H^0}{RT} + \frac{\Delta S^0}{R} \quad \text{Eq. (3).}$$

Subsequently, as for the activation energy, the state at a maximum energy of the reaction is called a transition state. In the reaction between A and B, the activated-complex AB^\ddagger is formed in the transition state and becomes product C with the rate constant k^\ddagger .



The concentration of AB^\ddagger is expressed by $[AB^\ddagger] = K^\ddagger[A][B]$ using the equilibrium constant K^\ddagger , and the reaction rate equation is $d[C]/dt = k^\ddagger[AB^\ddagger] = k^\ddagger K^\ddagger[A][B]$. Therefore, the rate constant of overall the reaction is $k = k^\ddagger K^\ddagger$. Since the ratio at which the activated complex passes through the transition state is proportional to the frequency of vibration in the direction of the reaction coordinate, it is expressed by $k^\ddagger = \kappa\nu$ (κ : transmission coefficient). On the other hand, the equilibrium constant K^\ddagger is expressed by the following equation [Eq. (5)] using activation free energy ΔG^\ddagger .

$$K^\ddagger = \exp\left(-\frac{\Delta G^\ddagger}{RT}\right) \quad \text{Eq. (5).}$$

The rate of product formation from AB^\ddagger is the rate at which the chemical bond of the active complex is cleaved. The frequency of transcending this energy barrier is equal to the frequency of vibration ν . According to the theory of statistical thermodynamics, it is expressed by the following equation using the vibration distribution function if $h\nu \ll k_B T$ in the transition state.

$$K^\ddagger = \frac{1}{1 - \exp\left(\frac{-h\nu}{k_B T}\right)} \exp\left(-\frac{\Delta G^\ddagger}{RT}\right) \cong \frac{k_B T}{h\nu} \exp\left(-\frac{\Delta G^\ddagger}{RT}\right) \quad \text{Eq. (6).}$$

Where h is the Plank constant, k_B is the Boltzmann constant. Eyring equation [Eq. (7)] can be obtained from $k = k^\ddagger K^\ddagger$, $k^\ddagger = \kappa\nu$ and Eq. (6).

$$k = \kappa \frac{k_B T}{h} \exp\left(-\frac{\Delta G^\ddagger}{RT}\right) = \kappa \frac{k_B T}{h} \exp\left(-\frac{\Delta H^\ddagger}{RT} + \frac{\Delta S^\ddagger}{R}\right) \quad \text{Eq. (7).}$$

Eyring equation can be expressed by the enthalpy (ΔH^\ddagger) and the entropy of activation (ΔS^\ddagger). The ΔH^\ddagger and ΔS^\ddagger can be calculated by plotting $\ln(k/T)$ vs. $1/T$, which give a straight line with the slope as $-\Delta H^\ddagger/R$ and the intercept as $\ln(\kappa k_B/h) + \Delta S^\ddagger/R$. A catalyst influences both the ΔH^\ddagger and ΔS^\ddagger of a reaction so as to minimize the ΔG^\ddagger as compared to a non-catalyzed reaction. An energy profile in catalytic and non-catalytic reactions is illustrated in **Figure 1**.

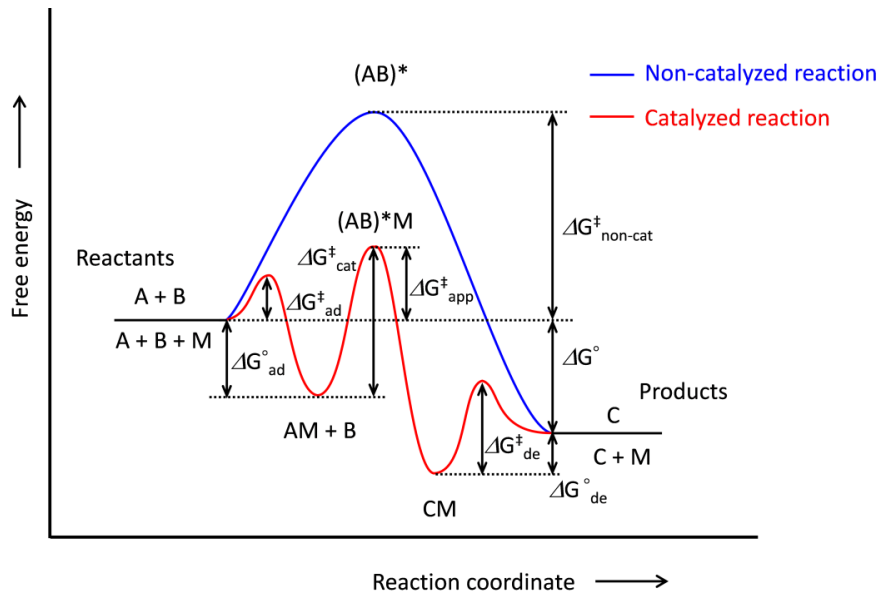


Figure 1 Energy profile in a chemical reaction ($A + B \rightarrow C$) with catalyst or no catalyst.

In the non-catalytic reaction, the reaction does not proceed unless it exceeds the energy barrier of $\Delta G^\ddagger_{\text{non-cat}}$. On the other hand, when the catalyst is present, the activation energy is lowered as a consequence of stabilization of the energy transition state. In the case of a heterogeneous catalyst, reaction molecules diffuse to the surface of a catalyst and then, it exceeds the activation free energy $\Delta G^\ddagger_{\text{ad}}$ and releases the adsorption free energy $\Delta G^\circ_{\text{ad}}$ so as to be adsorbed on the catalyst surface ($AM + B$).

Subsequently, it absorbs the activation free energy $\Delta G_{\text{cat}}^{\ddagger}$ and forms the adsorption activated complex $[(AB)^*M]$ and then, converted into the product adsorbed at the active site (CM). The adsorbed product diffuses (C + M) transcending the activation free energy of desorption $\Delta G_{\text{de}}^{\ddagger}$ thus, one catalytic reaction cycle is completed. The activation free energy obtained using the Eyring equation from the measured values is the apparent activation free energy $\Delta G_{\text{app}}^{\ddagger}$, which corresponds to the difference between the highest energy in the sequential process and reactant energy. In **Figure 1**, it is expressed as $\Delta G_{\text{app}}^{\ddagger} = \Delta G_{\text{cat}}^{\ddagger} - \Delta G_{\text{ad}}^{\circ}$ and the energy level is lower than that of the activated complex in a non-catalytic reaction. In contrast, the overall free energy change is constant in both for a catalyzed and non-catalyzed reaction. Therefore, the main role of a catalyst is to minimize the activation energy and accelerate a chemical reaction.

Classification

(1) Phase of a catalyst system (homogeneous/heterogeneous catalyst)

A catalyst whose phase is different from the reaction system is called a heterogeneous catalyst, and a catalyst of the same phase with the reaction system is referred to a homogeneous catalyst. Molecular catalysts such as a metal complex are regarded as homogeneous catalysts because they are usually applied for liquid phase reactions as solutes. On the other hand, solid catalysts (including supported molecular catalysts) are generally regarded as heterogeneous catalysts since they are usually used for dual phase reactions like gas-solid or liquid-solid.

(2) Catalyst materials

Catalysts can be classified according to the materials, *i.e.* metal catalysts, metal oxide catalysts, metal complex catalysts, acid-base catalysts. If a metal catalyst is

supported on an oxide, even metal loading is low (less than few wt%), that catalyst is classified as a metal catalyst as long as the active site is the metal species.

(3) Chemical reaction types and application

Catalysts are also classified according to the reaction the catalysts applied to, e.g. oxidation catalysts, reduction catalysts, isomerization catalyst, and so on. Also, they can be categorized according to their applications such as desulfurization catalysts for removing sulfur compounds in petroleum and denitrification catalyst for removing nitrogen oxides contained in automobile exhaust gas.

(4) Energy to use

In order to promote a chemical reaction, it is necessary to supply energy for exceeding the activation energy. A general catalyst utilizes thermal energy. In the contrast, catalysts that utilize light or electric energy are called a photocatalyst or an electrochemical catalyst, respectively.

Social significance of catalyst

Catalysts are widely used in modern chemical industry and are indispensable tools. There are many examples where the discovery of new catalysts has made major innovations to the society. For example, an iron catalyst synthesizing ammonia from nitrogen and hydrogen was discovered in 1905, and a large amount of nitrogen fertilizer was produced from ammonia. As a result, the production of agricultural crops increased dramatically and it made a great contribution to the solution of food problems accompanying the rapid increase in the world population. In the petrochemistry, fluid catalytic cracking (FCC) process using solid acid catalyst enabled efficient production of fuel oil and hydrocarbon compounds to expanded energy supply and chemical

products. Also, the invention of olefin polymerization catalyst by Ziegler and Natta contributed greatly to the development of plastic materials. As described above, the catalyst is closely related to the chemical industry and the invention of a new catalyst contributes greatly to not only the development of the chemical industry, but also the life of human being. From the viewpoint of global exhaustion of resources and environmental pollution problems, a development of efficient a catalytic reaction that does not employ harmful raw materials and generate byproducts is required. Thus, catalysts play a crucial role and have a great impact on our society.

1.2 Olefin Polymerization Catalyst

Ziegler-Natta catalysts

In 1953, Ziegler and colleagues found that ethylene was polymerized under mild conditions at normal temperature and normal pressure in a catalyst system combining titanium tetrachloride (TiCl_4) and an alkylaluminum compound (AlR_3).^{1,2} Based on this discovery, Natta *et al.* found that stereo regular polypropylene (PP) can be synthesized using crystalline titanium trichloride (TiCl_3) instead of TiCl_4 in 1954.³⁻⁴ The revolutionary discovery by Ziegler and Natta is the basis for the present development of polyolefin materials and these catalysts are collectively referred to as Ziegler-Natta catalysts. In an industrial process, a high activity was attained using MgCl_2 as a support and the stereoregularity of propylene polymerization was improved by the addition of Lewis basic compounds (donors). At present, it is common to use a catalyst prepared based on ($\text{TiCl}_4/\text{AlR}_3/\text{MgCl}_2$) as a Ziegler-Natta catalyst. Polyethylene (PE) synthesized with Ziegler-Natta catalyst has a basically non-branched structure and it termed as high density polyethylene (HDPE). As for molecular weight, by changing the introduction amount of hydrogen as a chain transfer agent, it is possible to synthesize various PEs up to the high million area. The molecular weight distribution is somewhat narrow in the range of 4 to 6 in M_w/M_n , and it can be adjusted by multistage polymerization process.⁵

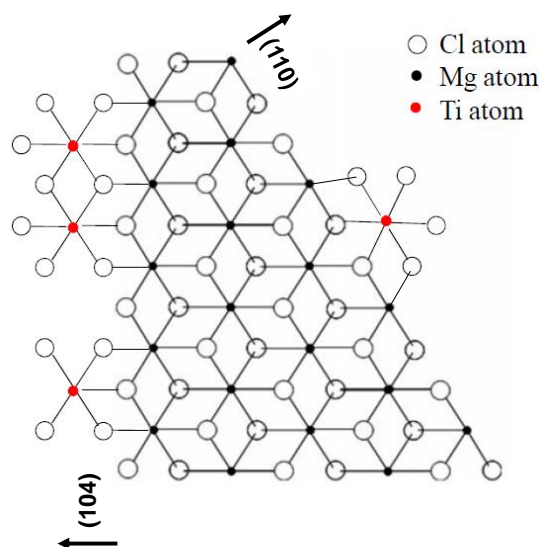
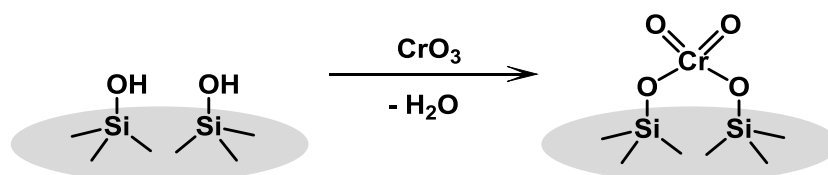


Figure 2 Structure of MgCl₂-supported Ziegler-Natta catalysts.

Phillips catalyst

The Phillips catalyst was a polymerization catalyst that is chromium oxide (VI) supported on amorphous silica and was discovered by Hogan and Banks at Phillips Petroleum Co. in 1951 (**Scheme 1**).⁶⁻⁹ About 40% or more of the world's HDPE is manufactured by Phillips catalyst. The PE produced using Phillips catalyst has a broad molecular weight distribution (MWD = 10-30) as compared with that produced by Ziegler-Natta catalyst and metallocene catalyst and contains long/short chain branching structure. Particularly, PE possessing a long chain branch is excellent in moldability since it shows high elasticity at high shear rate. Therefore the PE is widely used in the blow molding process for plastic containers and automobile fuel tanks.



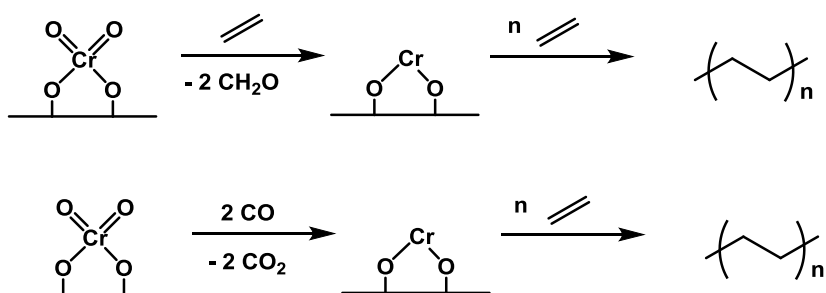
Scheme 1 Hexavalent chromate species on silica surface in Phillips catalyst.

Although the Phillips catalyst is made of simple composition, it generates a variety of unique structures such as a very broad molecular weight distribution as well as long and short chain branches. In other words, it is considered that a plurality of chromium active species having different catalytic properties exist on silica in the Phillips catalyst. The origin of causing such multifunctionality from a single metal element is quite interesting. Further, even when alkylaluminum is not employed as an activator, the ethylene polymerization can progress unlike the Ziegler-Natta catalyst and metallocene catalyst. However, alkylaluminum is often added in practical polymerization for the productivity to remove impurities from the reactor.

However, the active site structure and polymerization mechanism are still unclear as well as the origin of multifunctionality of Phillips catalyst since it was discovered in 1951. Even though huge experimental efforts have been devoted such as infrared (IR) spectroscopy^{10,11}, ultraviolet-visible (UV-Vis) spectroscopy¹²⁻¹⁴, Raman spectroscopy¹⁵⁻²⁰, high resolution solid-state nuclear magnetic resonance (Solid-state NMR)^{21,22}, X-ray photoelectron spectroscopy (XPS)²³⁻²⁵, electron probe microanalysis (EPMA)^{20,23,26-27}, secondary ion mass spectrometry (SIMS)²⁷, extended X-ray absorption fine structure (EXAFS)²⁸, electron spin resonance (ESR)²¹ and so on, it is difficult to fully clarify the active site structure in the Phillips catalyst as with the other heterogeneous catalysts.

Even under these circumstances, McDaniel *et al.* revealed that the active site precursor is a structure in which the chromate structure is reduced from chromium (VI) species to chromium (II) species by ethylene via XPS measurement (**Scheme 2**).²⁹ It is believed that polymerization proceeds by reaction of this active site precursor with ethylene. In addition, Baker *et al.* have confirmed that formaldehyde is formed as a

by-product upon reduction by Phillips catalyst with ethylene.^{30,31} In the ethylene polymerization, there is an induction period in which ethylene is not consumed during the period from the introduction of ethylene to the start of polymerization, which is considered to be the time required for the reduction by ethylene. Furthermore, it is known that even when reduced with carbon monoxide, a similar structure is formed and the induction period disappears.^{12,13,17,29-31}



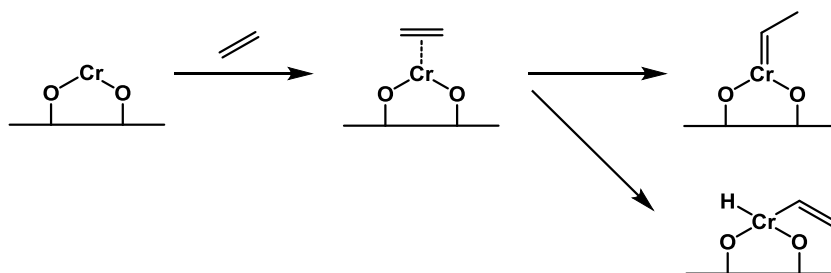
Scheme 2 Reduction of Cr(VI) species by ethylene or carbon monoxide.

Ethylene polymerization mechanism in Phillips catalyst

Initiation reaction

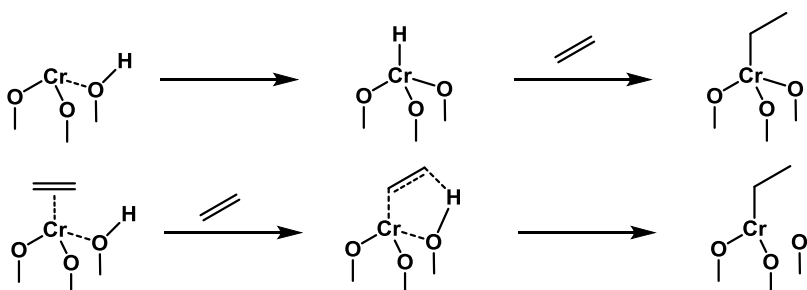
Phillips catalyst does not require cocatalysts unlike Ziegler-Natta catalysts and metallocene catalysts. For this reason, there is a mechanism by which a chromium-carbon bond is generated by the reaction of the active site precursor and ethylene, and a mechanism for generating various active site structures has been proposed. For example, the mechanism in which one molecule of ethylene is coordinated to the active site precursor to generate alkylidene chromium species or alkyl chromium species has been proposed (**Scheme 3**).³²⁻³⁴ Some experimental reports show that carbene species are formed in ethylene polymerization using a chromium polymerization catalyst. For this reason, it is considered that alkylidene chromium

species is formed in initiation reaction. Furthermore, alkyl chromium species that formed by the extraction of hydrogen of ethylene to chromium is also considered as initial active species since PE having a terminal vinyl and methyl groups are likely to be formed.



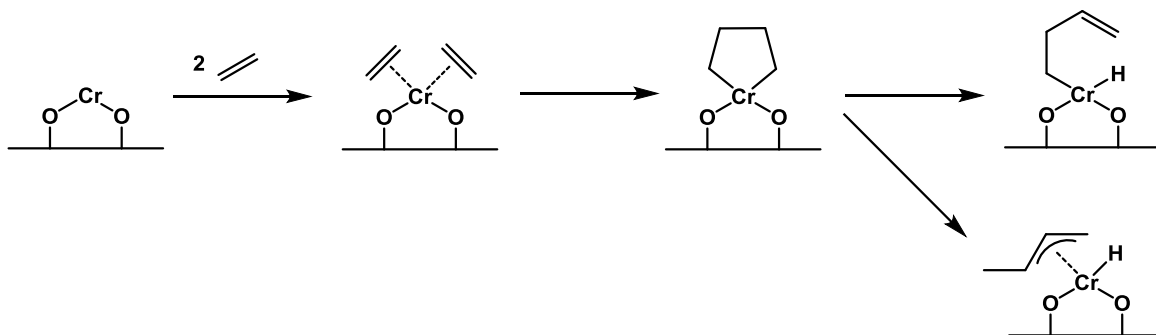
Scheme 3 Proposed initiation mechanism for ethylene polymerization on Phillips catalyst.

In addition, the mechanisms involving silanol groups to form alkyl chromium species have also been proposed (**Scheme 4**).^{35,36} It is presumed that the silanol group around the active site precursor gives hydrogen to chromium and ethylene insertion occurs or hydrogen of silanol group shifts to ethylene. However, it is hard to claim that this mechanism is actually progressed since a catalyst having less silanol groups by calcination shows higher activity.



Scheme 4 Proposed formation mechanism of alkylchromium species.

Metallic cycle mechanisms, in which two ethylene are coordinated to an active site precursor and chromacycle species is formed by oxidative cycloaddition reaction have also been proposed (**Scheme 5**).^{33,37} This mechanism does not require external hydrogen such as silanol groups.



Scheme 5 Proposed formation mechanism of chromacycle species.

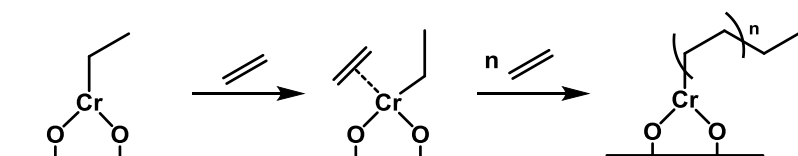
As described above, several reaction routes for generating an active site structure have been estimated, but the definitive proof of the active site structure has not been established and the true structure is unknown. In addition, it is believed that the molecular weight distribution of PE produced by Phillips catalyst is broad due to the mixture of various active site structures, and it can be said that it is difficult to regard only one structure as a catalyst active site.

Propagation reaction

As mentioned above, it has not been able to clarify the mechanism of active site structure formation from the active site precursor in Phillips catalyst, so there are various opinions on growth reaction. The proposed growth reaction mechanisms are summarized as follows.

Cossee-Arlman mechanism

Cossee-Arlman mechanism is a mechanism by which PE is formed by ethylene coordination/insertion repeated in alkyl chromium (**Scheme 6**).³⁸ This mechanism is similar to the mechanism proposed by Cossee *et al.* in Ziegler-Natta catalyst.³⁹⁻⁴⁰ In addition, Espelid *et al.* clarified that the activation energy of alkyl-chromium (III) species insertion reaction of ethylene is lower than that of the other mechanisms.⁴¹ Although the Cossee-Arlman mechanism is the most natural mechanism as a growth reaction mechanism in this way, the problem is that the mechanism of generation of the active site structure is not clarified.

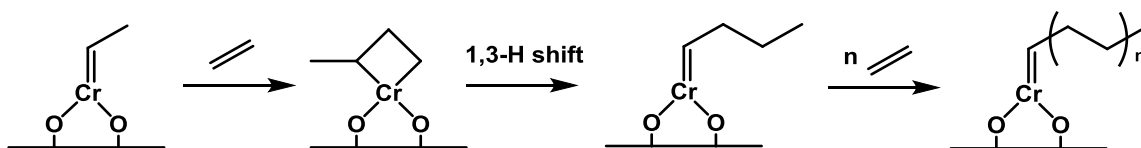


Scheme 6 Propagation reaction of alkylchromium species by Cossee-Arlman mechanism.

Green-Rooney mechanism (carbene mechanism)

The Green-Rooney mechanism regenerates alkylidene chromium species by 1,3-hydride shift after alkylidene chromium species and ethylene reacts with each other to form a chromacycle (**Scheme 7**).³³ In other words, it is the mechanism by which PE grows by repeating carbene metalacycle. This mechanism is similar to the mechanism proposed by Rooney *et al.* in the polymerization of stereoselective α -olefins by Ziegler-Natta catalyst.⁴² Ghiotti *et al.* carried out infrared spectroscopy in a Phillips catalyst to determine the presence of carbene species.⁴³ However, McDaniel *et al.* revealed that scrambling of hydrogen atoms did not occur during polymerization with

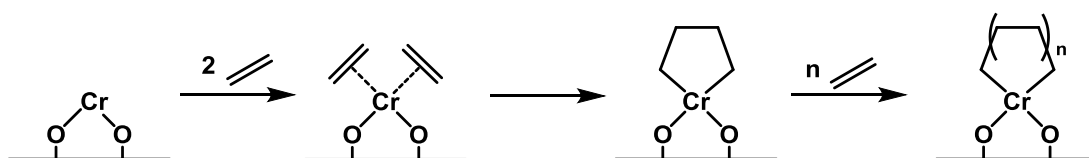
deuterated ethylene and this result denied the mechanism.⁴⁴



Scheme 7 Propagation reaction of alkylidene chromium species by Green-Rooney mechanism.

Metallacycle mechanism

In metallacycle mechanism, PE is grown by repeating the reaction of ethylene insertion into the chromacycle species formed by the oxidative cycloaddition reaction of ethylene (**Scheme 8**).⁴⁵ Groppo *et al.* have proposed spectroscopically that chromacyclopentane is produced during the polymerization of ethylene.³⁷



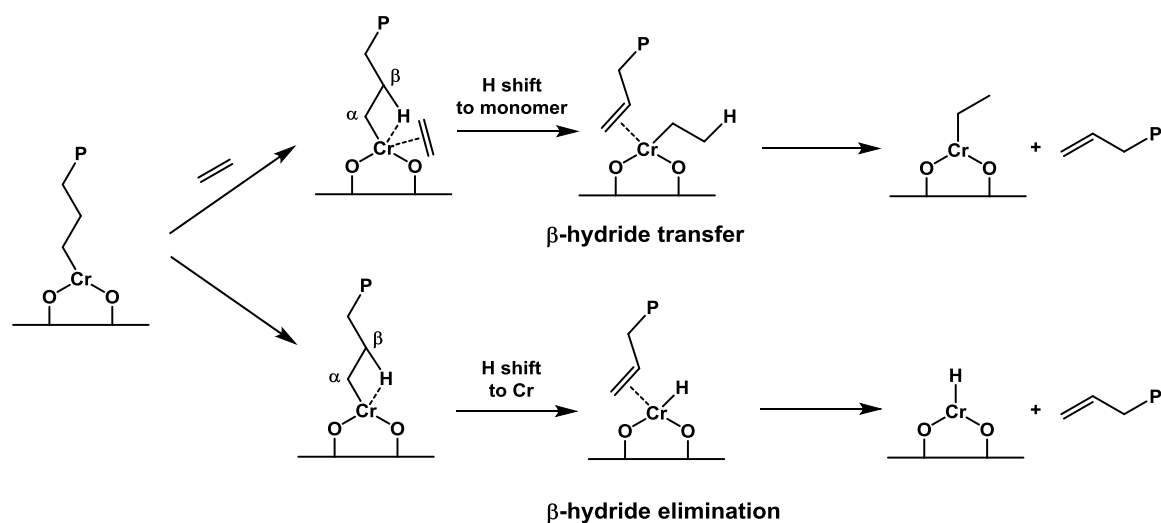
Scheme 8 Propagation reaction of chromacycle species by metallacycle mechanism.

As described above, some active site structures in the growth reaction have been proved experimentally. However, the formation mechanism of the active site structure from the precursor has not been elucidated. In addition, it is difficult to explain with just one mechanism due to various active site structures exist on silica surfaces.

Chain transfer reaction

Formationally, the chain transfer reaction is considered to happen through a

transfer of β -hydride to ethylene, or β -hydrogen elimination as shown in **Scheme 9**. Bolm and Saito *et al.* claimed that the chain transfer reaction to ethylene is mainly taking place from the kinetic analysis of the polymerization reaction.⁴⁶ Although β -hydride transfer by chain transfer reaction to ethylene occurs depending on the ethylene concentration in the former case, the molecular weight of produced PE does not depend on the ethylene concentration since the growth reaction has a linear proportional relation to the ethylene concentration. On the other hand, since the latter β -hydride elimination does not depend on the ethylene concentration, the molecular weight of PE produced is proportional to the ethylene concentration. It is thought that the β -hydride transfer to ethylene preferentially progresses because the molecular weight of PE produced in Phillips catalyst is not proportional to ethylene.



Scheme 9 Mechanism of chain transfer reactions in Phillips catalyst.

The molecular weight of PE is controlled by adjusting of temperature since the chain transfer reaction is promoted by increasing of temperature. However the precise control is difficult for Phillips catalyst due to the molecular weight distribution of the produced PE does not greatly shift. It is known that Ziegler-Natta catalyst and

metallocene catalyst have very high hydrogen response and are liable to cause a chain transfer reaction, but not for Phillips catalysts. That is why it is difficult to control molecular weight in Phillips ethylene polymerization.

Metallocene catalyst

Kaminsky and Shinn found that a titanocene catalyst combined with methylaluminoxane (MAO) system shows high activity for olefin polymerization.^{47,48} Since the metallocene catalyst has a clear single molecular structure, it is thought that it becomes a single site catalyst which consists of only one type of active species, and elucidation of the mechanism of olefin polymerization and design of catalyst are facilitated based on this advantage. Also, the molecular weight distribution of the polymer obtained with the metallocene catalyst is very narrow. It also shows high activity in copolymerization of α -olefin, and the resulting copolymer has a feature that the molecular weight distribution and the composition distribution are remarkably narrow. Based on these features, the metallocene catalyst is a suitable catalyst for the synthesis linear low density PE (LLDPE) containing many short chain branches, and LLDPE synthesized by metallocene catalyst has transparency, strength, low temperature heat sealability and so on. It is used as a polymer suitable for film applications.

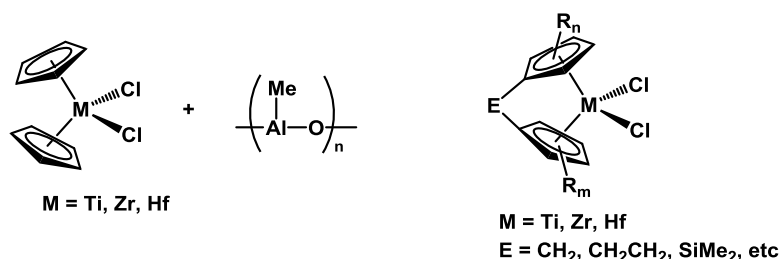
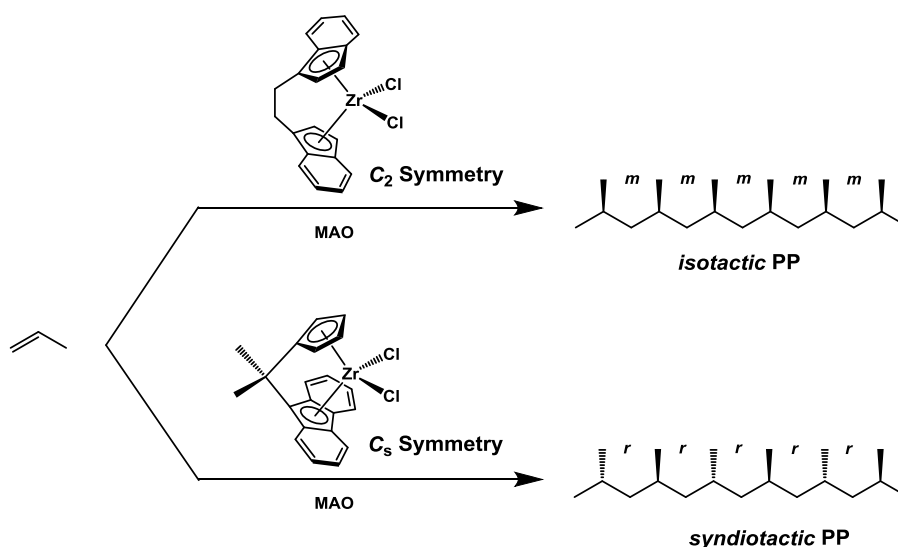


Figure 3 Typical metallocene catalyst and MAO system (left) and catalyst design concept (right).

The metallocene catalyst is designed by the choice of the central metal species, bridging portion (E) and the substituent (R_n , R_m) at the two cyclopentadienyl groups. Catalyst performance depends on the balance of bite angle adjustment of the ligand and steric hindrance due to substituent by the design of the bridge portion. Furthermore, it is known that isotactic PP and syndiotactic PP can be obtained by C_2 symmetry catalyst (*rac*-Et(Ind)₂ZrCl₂) and C_s symmetric catalyst (^{*i*}Pr(Flu)(Cp)ZrCl₂), respectively (Scheme 10).^{49,50}



Scheme 10 Different symmetry metallocene catalysts and the effect on a stereoregularity of polypropylene.

Post-metallocene catalyst

Constrained geometry catalyst

Dow Chemical and Exxon Chemical developed constrained geometry catalyst (CGC).⁵¹⁻⁵⁷ The bite angle of the complex can be adjusted by controlling the linkage of the cyclopentadienyl group and the amide. Since the coordination site of the monomer is wide, the activity is high and bulky α -olefin can also be inserted. Therefore, it is

possible to introduce a macromonomer having a vinyl group end and obtain PE having long chain branches using the CGC catalyst.

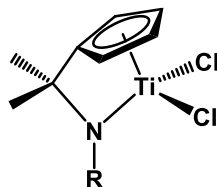


Figure 4 Typical catalyst structure of CGC.

Brookhart catalyst

While many studies for olefin polymerization using early transition metal complexes have been systematically progressed, it took time for the late transition metal catalyst. The reason is that the early transition metal alkyl complex reacts smoothly with the monomer without decomposition, whereas β -hydrogen elimination undergoes in the late transition metal complex. Thus, the late transition metal complex has been used as an oligomer forming catalyst such as SHOP (Shell Higher Olefin Process).⁵⁸⁻⁶⁰ Brookhart *et al.* reported that palladium and nickel with bulky diimine ligands exhibit activity for olefin polymerization (**Figure 5**).⁶¹⁻⁶³ It is believed that chain transfer reaction is suppressed by introducing bulky substituents on the diimine ligand. On the other hand, it is known that reversible β -hydrogen elimination readily proceeds and causes an isomerization reaction, so that a polymer having a highly branched structure can be obtained. It is also revealed that polymerization with polar monomers proceeds using the Brookhart catalyst whereas it can be a poison in the early transition metal catalyst due to the high affinity to oxygen.

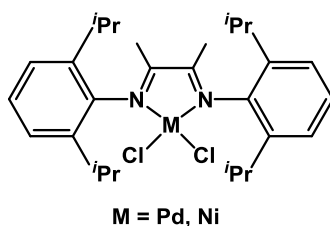
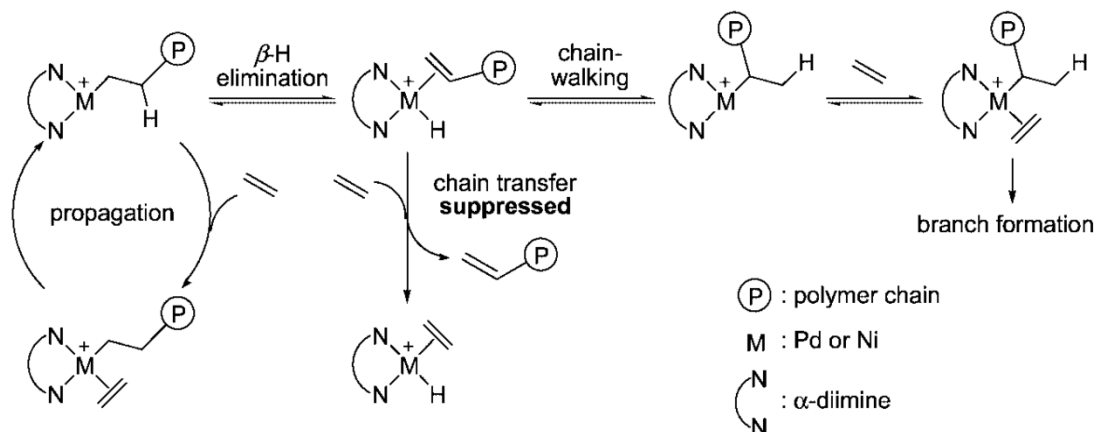


Figure 5 Typical catalyst structure of α -diamine complex.

An early transition metal complex provides a linear polymer in olefin polymerization and a catalyst that achieves high stereoregularity has also been developed. On the contrary, a late transition metal complex provides a highly branched polymer and the stereoregularity is low. In the α -olefin copolymerization, 1,2-insertion reaction mainly undergoes and the polymer grows linearly with an early transition metal complex, while a late transition metal complex induces various insertion reactions such as 1- ω insertion. This phenomenon is called chain walking and a highly branched polymer is obtained (**Scheme 11**).^{61,62, 64-68}



Scheme 11 Mechanism of branched polymer formation (chain walking) by Pd or Ni α -diamine complex.

Phenoxy-Imine catalyst

Fujita *et al.* found that titanium or zirconium complexes with bisphenoxyimine ligands called FI catalysts have high olefin polymerization activity.⁶⁹⁻⁷⁴ It can produce polymers having different molecular weight from thousands to millions by the choice of ligand structure and an activator. It has also been reported that some FI catalysts show living polymerization.

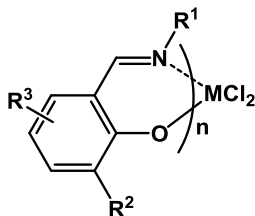


Figure 6 Typical catalyst structure of FI catalyst.

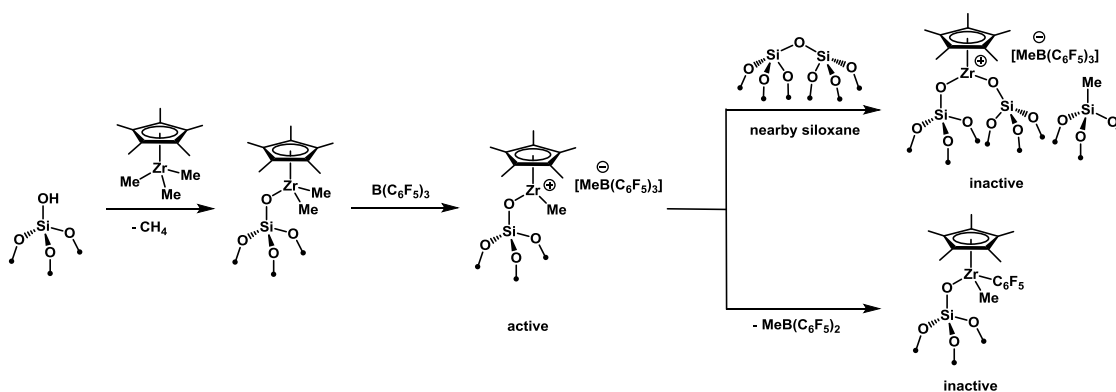
1.3 Approaches Using Heterogeneous and Homogeneous Catalysts

Surface organometallic chemistry approach

In the solid catalyst, it is difficult to evaluate the relationship between an active site structure and its performance since multiple active sites exist at different ratio. Surface organometallic chemistry (SOMC) is a powerful approach that utilizes organometallic complexes grafted on solid supports and investigates its characteristics.⁷⁵⁻⁸⁴ The objective is to clarify the structure-performance relationship (SPR) and understand the mechanism of catalytic reaction using catalyst defined at a molecular level.

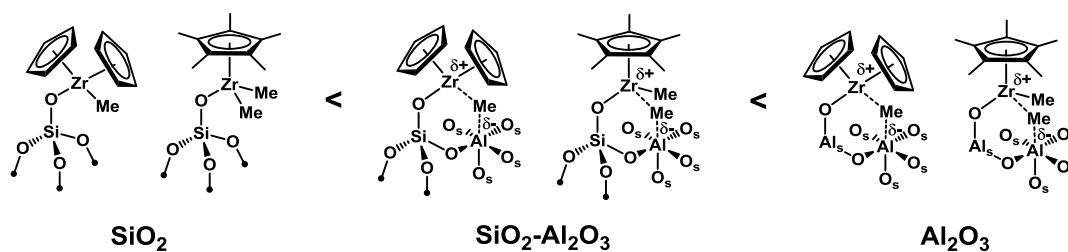
Single site models by grafting early transition metal complexes on solid supports

Grafting metallocene or other molecular catalyst onto inorganic supports such as silica has been investigated because a control of the polymer morphology produced by single site catalysts is difficult. However, it is known that the intrinsic high activity of the metallocene catalyst is easily lost by the supporting. Silica supported metallocene catalysts require cocatalysts to form catalytically active sites. For example, Cp^{*}ZrMe₃ grafted on silica support catalyst shows low activity in ethylene polymerization, however B(C₆F₅)₄ forms cationic species [(≡SiO)ZrCp^{*}Me][MeB(C₆F₅)₄], which is active (**Scheme 12**).⁸⁵ When MAO is utilized as a cocatalyst, cationic species are similarly formed and exhibit polymerization activity. However, these active species are unstable under polymerization condition and easily form inactive sites. For instance, [(≡SiO)ZrCp^{*}Me][MeB(C₆F₅)₃] decomposes by the following two process.^{86,87} Alkyl transfer to silica surface and transfer of C₆F₅ from [MeB(C₆F₅)₃] generate [(≡SiO)₂ZrCp^{*}][MeB(C₆F₅)₃] and (≡SiO)ZrCp^{*}C₆F₅Me that are inactive. These decompositions are also confirmed in conventional homogeneous catalysts.⁸⁸



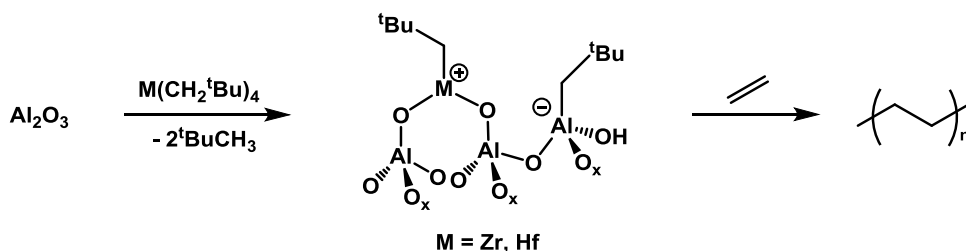
Scheme 12 Activation and deactivation of Cp^*ZrMe_3 grafted on silica support catalyst.

The catalyst performance depends on the supports and polymerization conditions. When Lewis acidic support such as silica-alumina ($\text{SiO}_2\text{-Al}_2\text{O}_3$) or alumina (Al_2O_3) are employed for Cp^*ZrMe_3 or $\text{Cp}^*_2\text{ZrMe}_2$, Zr species became partially cationic by methyl group transfer to aluminum vacant site and enhance the activities. Likewise, the order of the activity follows $\text{SiO}_2 < \text{SiO}_2\text{-Al}_2\text{O}_3 < \text{Al}_2\text{O}_3$ (**Scheme 13**).



Scheme 13 $\text{Cp}^*_2\text{ZrMe}_2$ and Cp^*ZrMe_3 grafted on different supports.

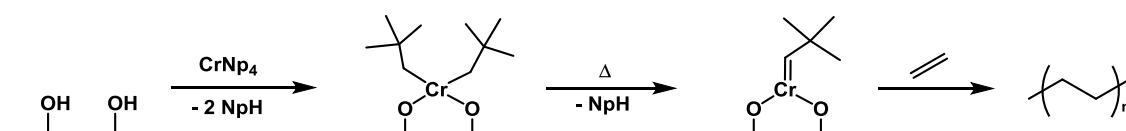
Alkyl complexes $[\text{M}(\text{CH}_2^t\text{Bu})_4]$ ($\text{M} = \text{Zr}, \text{Hf}$) on Al_2O_3 support also provide well-defined sites $[(\equiv\text{AlO})_2\text{M}(\text{CH}_2^t\text{Bu})^+]\text{-}[\text{Al}_s\text{CH}_2^t\text{Bu}^-]$ and they showed good activity for ethylene polymerization without co-catalyst (**Scheme 14**).^{89,90}



Scheme 14 $M(\text{CH}_2^t\text{Bu})_4$ supported on Al_2O_3 for ethylene polymerization.

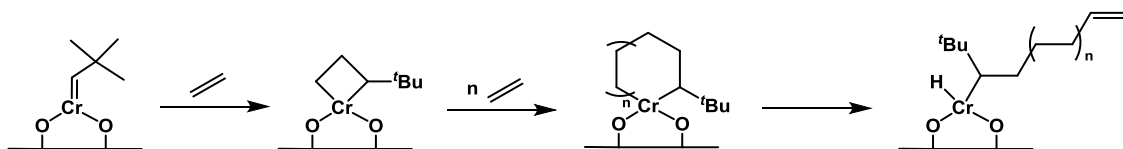
Single site models for Phillips catalyst

Scott *et al.* prepared a dialkyl Cr (IV) site catalyst by grafting CrNp_4 (Np = neopentyl) complex on silica support using chemical vapor deposition (**Scheme 15**).⁹¹⁻⁹⁷ This catalyst showed no activity at low ethylene pressure (ca. 60 Torr). However, a neopentyl was removed by heating at 70°C and the catalyst showed high polymerization activity even at low ethylene pressure. They clarified that alkylidene Cr (IV) species are formed by the elimination of neopentyl from the dialkyl Cr (IV) species and it shows polymerization activity using various analytical methods.



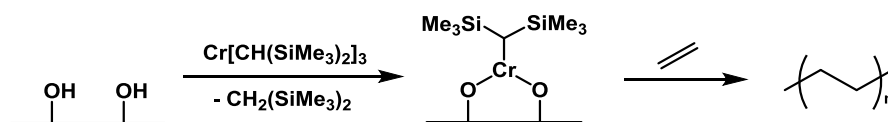
Scheme 15 CrNp_4 grafted on silica catalyst and its active site structure.

As a result, it was proposed that the polymerization is progressed by alkylidene-metallacycle mechanism. From the kinetic experiment using ethylene- d_4 , it is also considered that Cr-alkyl-hydride species by β -hydride elimination is formed and the chain growth proceeds.^{94,98}



Scheme 16 Formation of alkylidene-chromacycle species and alkyl-hydride Cr species.

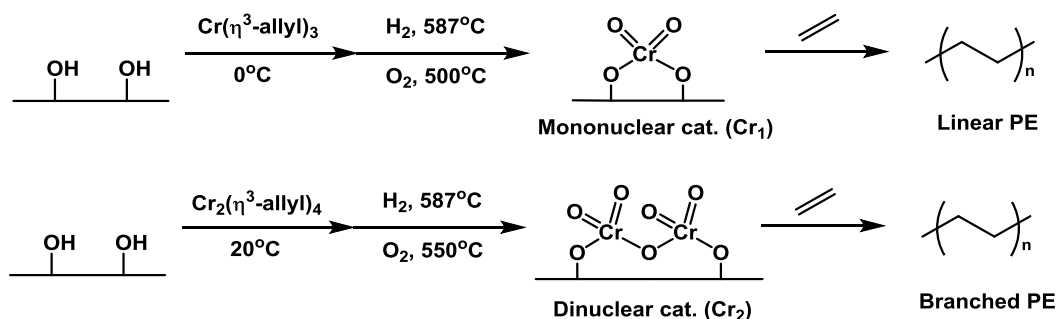
Monoi *et al.* prepared a monoalkyl Cr (III) site using $\text{Cr}[\text{CH}(\text{SiMe}_3)_2]_3$ and performed ethylene polymerization (**Scheme 17**).⁹⁹ This catalyst showed 6 times higher activity compared with normal Phillips catalyst and it did not require co-catalyst. They presumed monoalkyl Cr (III) species is active species. However, it can not be considered that the active site structure is completely single in this catalyst system because the produced PE had a broad molecular weight distribution and a branched structure as with ordinary Phillips catalysts.



Scheme 17 $\text{Cr}[\text{CH}(\text{SiMe}_3)_2]_3$ grafted on silica catalyst.

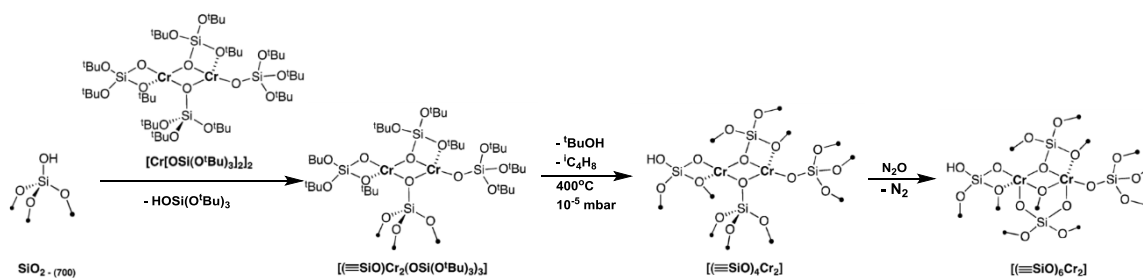
They also reported that a $\text{Cr}[\text{N}(\text{SiMe}_3)_2]_3$ grafted on silica with aluminoxane shows activity for ethylene polymerization and the property of this catalyst depends on the calcination temperature.¹⁰⁰ It was confirmed that high molecular weight PE is formed at low calcination temperature (200-400°C), and high selective trimerization reaction to produce 1-hexene proceeds at high calcination temperature (600°C). This result suggests that the difference in the silanol structure on the silica surface has an influence on the catalytic properties.

Tonosaki *et al.* prepared mono- and binuclear chromates using $\text{Cr}(\eta^3\text{-allyl})_3$ and $\text{Cr}_2(\eta^3\text{-allyl})_4$ and ethylene polymerization were conducted with them (**Scheme 18**).¹⁰¹ It was revealed that PE having a less branched structure is formed at a mononuclear site and PE having a more branched structure is produced at a binuclear structure. They considered that the formation of a crosslinked structure of alkylidene chromium species on the binuclear structure promotes to produce propylene during polymerization from the DFT calculation.

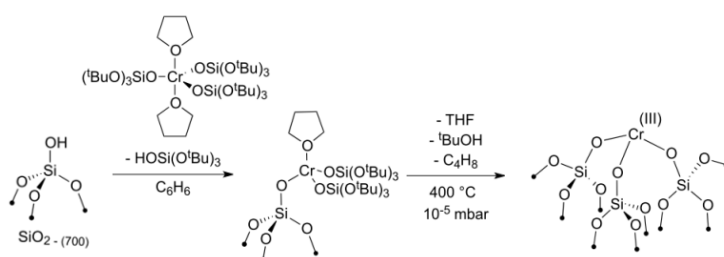


Scheme 18 $\text{Cr}(\eta^3\text{-allyl})_3$ and $\text{Cr}_2(\eta^3\text{-allyl})_4$ grafted on silica catalysts.

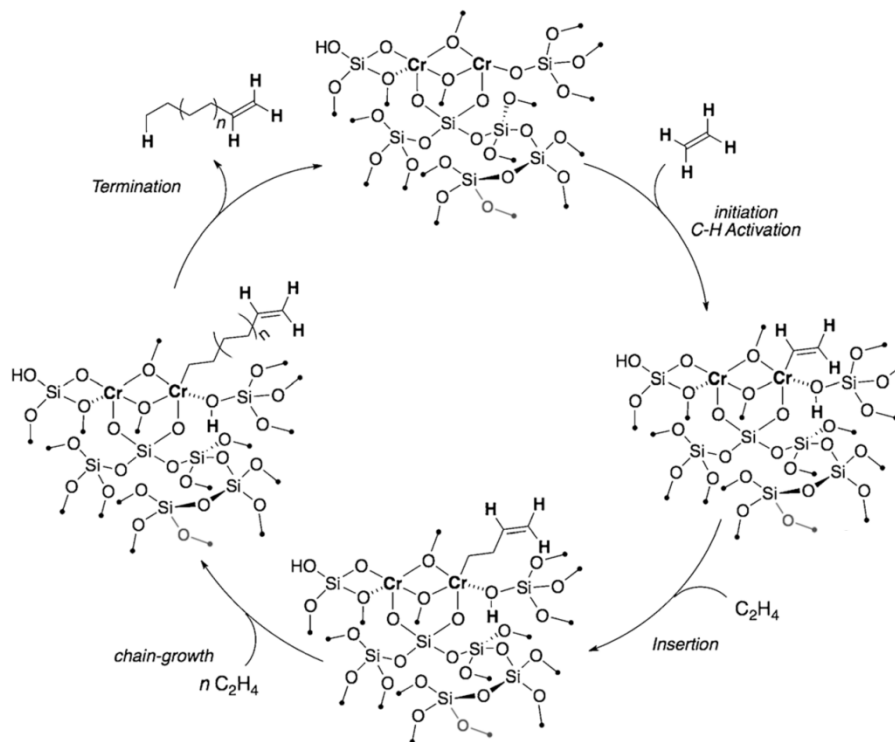
Copéret *et al.* prepared well defined Cr(II) and Cr(III) species on silica using Cr dimer $\{\text{Cr}[\text{OSi}(\text{O}^t\text{Bu})_3]_2\}_2$ (**Scheme 19**) and mononuclear Cr(III) species using $\text{Cr}[\text{OSi}(\text{O}^t\text{Bu})_3]_3 \cdot 2\text{THF}$ (**Scheme 20**).¹⁰²⁻¹⁰⁶ Whereas Cr(II) species was inactive for ethylene polymerization, Cr(III) site showed higher activity. Furthermore, they proposed that heterolytic C–H bond activation of ethylene is a key step in initiation mechanism from isotope labeling experiments and DFT calculations (**Scheme 21**).



Scheme 19 $\{\text{Cr}[\text{OSi}(\text{O}^t\text{Bu})_3]_2\}_2$ grafted on silica catalyst.



Scheme 20 $\text{Cr}[\text{OSi}(\text{O}^t\text{Bu})_3]_3 \cdot 2\text{THF}$ grafted on silica catalyst.



Scheme 21 Proposed C-H bond activation mechanism in ethylene polymerization.

Model Molecular Catalyst Approaches

Siloxane compound is a generic term for compounds having a siloxane (Si-O-Si) bond as a framework. Among them, siloxane consisting of a T structure ($\text{RSiO}_{3/2}$) has 1.5 oxygen atoms (*sesqui* in Latin) in the unit structure and is called silsesquioxane.¹⁰⁷ Silsesquioxane has several structures such as a cage or ladder structure and random structure (**Figure 7**). Especially cage type silsesquioxane is classified to a fully condensed cage type and an incompletely condensed cage type and they are called polyhedral oligomeric silsesquioxane (POSS). Although the abbreviation POSS was originally used only for completely condensed cage type silsesquioxane, recently incompletely condensed cage type silsesquioxane has been used in various fields, so the both silsesquioxanes are called as POSS nowadays.

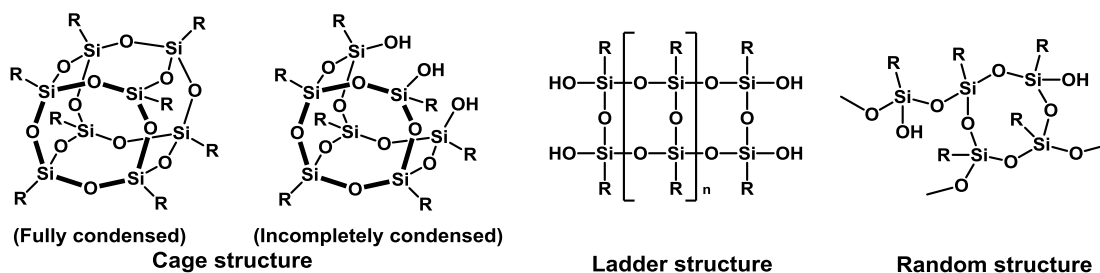


Figure 7 Various silsesquioxane compounds and their structures.

The incompletely condensed cage silsesquioxane has a reactive silanol group and this makes it attractive for various modifications. The synthesis of incompletely condensed silsesquioxane has been reported from the 1960's. For example, Brown *et al.* report that $(c\text{-C}_6\text{H}_5)_7\text{Si}_7\text{O}_9(\text{OH})_3$ can be obtained by hydrolysis and dehydration condensation of $c\text{-C}_6\text{H}_5\text{SiCl}_3$ in acetone-water system.¹⁰⁸ However, the application of incompletely condensed cage type silsesquioxane had not progressed for a long time because the synthesis required an extremely long time like several months and the yield

was quite low. Meanwhile, Feher *et al.* synthesized similar incompletely condensed cage type silsesquioxane in one week using acid or base catalyst and an efficient synthesis method was successfully established.¹⁰⁹ From the X-ray crystal structure analysis, it was shown that the OH group of $R_7Si_7O_9(OH)_3$ is structurally similar to the silanol on the silica surface of the β -cristobalite crystal having the (111) face. Furthermore, the incompletely condensed cage type silsesquioxane and the silanol group structure on the silica surface seem to closely resemble as shown in **Figure 8**. From IR measurement and pKa examination, it is clarified that the silanol groups of different POSS possess similar properties isolated, vicinal and geminal silanol group of silica surfaces.¹¹⁰⁻¹¹²

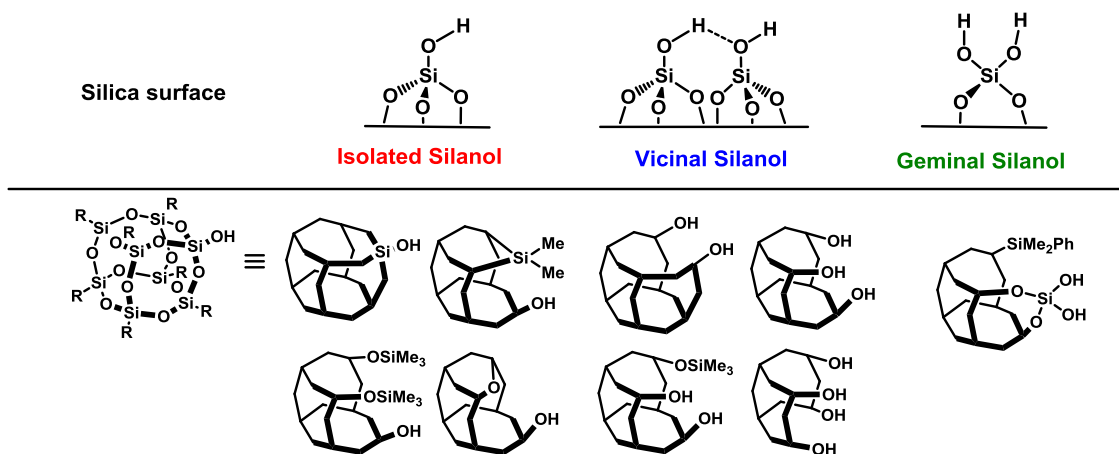


Figure 8 Silsesquioxane compounds as a model of surface silanol groups of silica.

Silica is utilized as a prevalent support in catalyst chemistry such as olefin polymerization catalyst, olefin metathesis catalyst, cross coupling catalyst and so on. Complexes of POSS with transition metals have been reported a lot since they are regarded as a model molecule of silica supported catalysts.¹¹³⁻¹¹⁵ Regarding the olefin polymerization catalyst, synthesis of model catalysts of silica supported Ziegler-Natta

catalyst, metallocene catalyst, Phillips catalyst and vanadium catalyst have been reported with their polymerization performance.

For example, Liu *et al.* synthesized $[(c\text{-C}_6\text{H}_{11})_7\text{Si}_7\text{O}_{12}\text{MgTiCl}_3]_n$ ($n = 1, 2$) as a model molecule of Ziegler-Natta catalyst and reported that it shows ethylene polymerization activity using AlEt_3 as an activator (**Figure 9**).¹¹⁶ It was shown that this catalyst system produced PE having a more or less broad molecular weight distribution ($M_w = 140000$, $M_w/M_n = 5.5$).

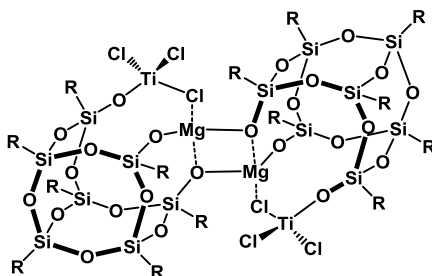


Figure 9 Structure of $[(c\text{-C}_6\text{H}_{11})_7\text{Si}_7\text{O}_{12}\text{MgTiCl}_3]_n$ as Ziegler-Natta model catalyst.

There are also several reports for model molecules of silica supported metallocene catalysts. Duchateau *et al.* synthesized $\text{Cp}''[(c\text{-C}_5\text{H}_9)_7\text{Si}_8\text{O}_{13}]\text{TiCl}_2$ ($\text{Cp}'' = 1,3\text{-C}_5\text{H}_3(\text{SiMe}_3)_2$) and $\text{Cp}''[(c\text{-C}_5\text{H}_9)_7\text{Si}_8\text{O}_{13}]_2\text{-TiCl}$ and ethylene polymerization was performed using MAO as an activator (**Figure 10**).¹¹⁷⁻¹¹⁹ The both catalyst exhibited similarly low activity because of the titanium-siloxy bond was cleaved by excess amount of MAO having a strong Lewis acidity. On the other hand, $\text{Cp}''[(c\text{-C}_5\text{H}_9)_7\text{Si}_8\text{O}_{13}]\text{Ti}(\text{CH}_2\text{Ph})_2$ which is an alkyl complex activated by $\text{B}(\text{C}_6\text{F}_5)_3$ produced PE with narrow molecular weight distribution ($M_w = 260000$, $M_w/M_n = 3.3$) at high activity. Moreover, it also showed activity for copolymerization with 1-hexene and provided narrow distribution polymer ($M_w = 3000$, $M_w/M_n = 2.0$). From these results, they suggested that this catalyst system works as a single site catalyst. Also they proved

that $[\text{PhCH}_2\text{B}(\text{C}_6\text{F}_5)_3]$ species existed in the reaction of $\text{Cp}''[(c\text{-C}_5\text{H}_9)_7\text{Si}_8\text{O}_{13}]\text{Ti}(\text{CH}_2\text{Ph})_2$ with $\text{B}(\text{C}_6\text{F}_5)_3$ by ^{19}F NMR measurement and considered the titanium cationic species worked as an active site. Thus, they clarified the influence of MAO and $\text{B}(\text{C}_6\text{F}_5)_3$ at a molecular level.

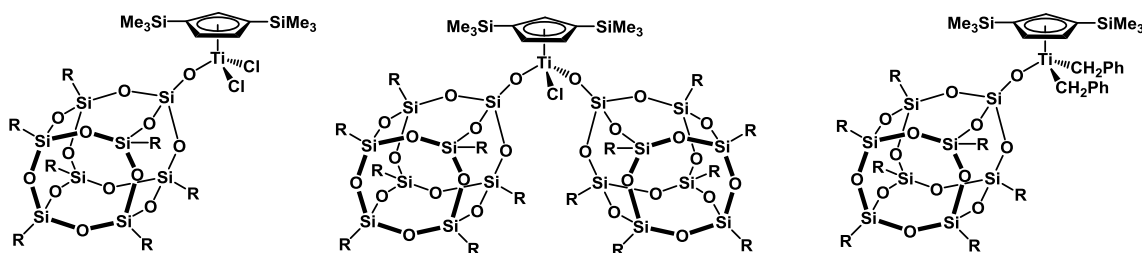
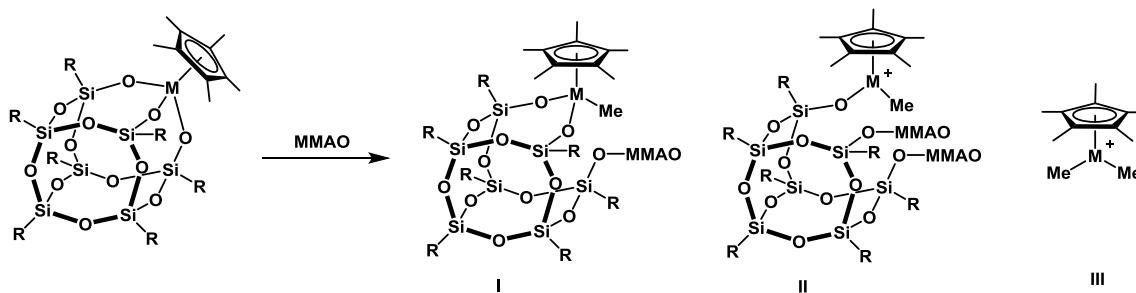


Figure 10 Structure of $\text{Cp}''[(c\text{-C}_5\text{H}_9)_7\text{Si}_8\text{O}_{13}]\text{TiCl}_2$ ($\text{Cp}'' = 1,3\text{-C}_5\text{H}_3(\text{SiMe}_3)_2$), $\text{Cp}''[(c\text{-C}_5\text{H}_9)_7\text{Si}_8\text{O}_{13}]_2\text{TiCl}$ and $\text{Cp}''[(c\text{-C}_5\text{H}_9)_7\text{Si}_8\text{O}_{13}]\text{Ti}(\text{CH}_2\text{Ph})_2$.

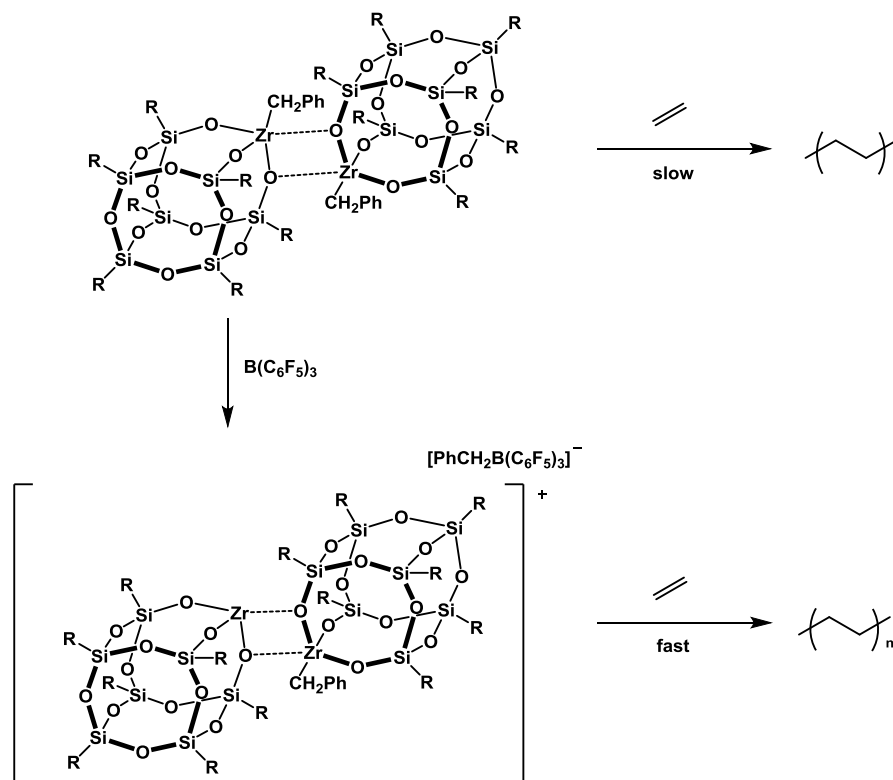
Do *et al.* reported that the metal-siloxy bond cleavage of $[(c\text{-C}_5\text{H}_9)_7\text{Si}_7\text{O}_{12}]\text{MCp}^*$ by MMAO depends on temperature (**Scheme 22**).¹²⁰ They proposed that complex II and III were formed and they afforded PE with a bimodal molecular weight distribution at 0°C and only complex III that was dissociated from POSS existed and produced a monomodal PE at high temperature.



Scheme 22 Reaction of $[(c\text{-C}_5\text{H}_9)_7\text{Si}_7\text{O}_{12}]\text{MCp}^*$ with MMAO.

Alkyl zirconium and hydride zirconium based on silica and aluminosilicate

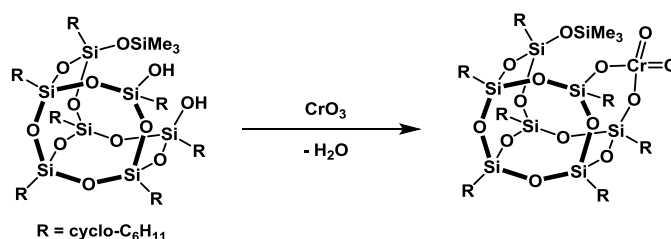
catalysts (ZrR_4/SiO_2 and ZrR_4/Al_2O_3) for olefin polymerization have been reported by Basset group^{76,121-128} and Ittel group^{129,130}. Duchateau *et al.* synthesized model molecular analogues of these catalysts using $Zr(CH_2Ph)_4$ with $(c-C_5H_9)_7Si_7O_{11}(OH)_3$.¹¹⁸ From NMR and X-ray analysis, it was found that the obtained complex exists as a dimer $\{[(c-C_5H_9)_7Si_7O_{12}]ZrCH_2Ph\}_2$. Although the catalyst showed low ethylene polymerization activity (10 kg-PE/mol-Zr-h), the activity improved to 2400 kg-PE/mol-Zr-h when it was activated by $B(C_6F_5)_3$ and a narrow molecular weight distribution PE ($M_w = 6600$, $M_w/M_n = 2.3$) was generated (**Scheme 23**).



Scheme 23 Difference of ethylene polymerization activity for $\{[(c-C_5H_9)_7Si_7O_{12}]ZrCH_2Ph\}_2$ with $B(C_6F_5)_3$.

Feher *et al.* synthesized $(c-C_6H_{11})_7Si_7O_{11}(OSiMe_3)CrO_2$ by the reaction of $(c-C_6H_{11})_7Si_7O_9(OH)_2(OSiMe_3)$ with chromium oxide and ethylene polymerization was

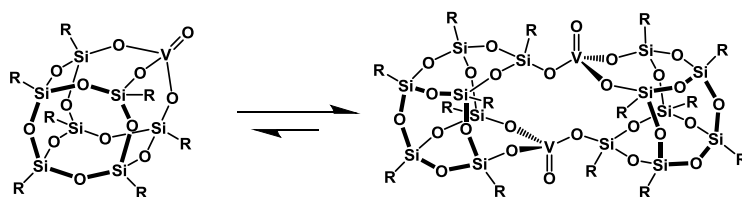
carried out with AlMe_3 (2-10 equiv.) at room temperature and 1 atm ethylene pressure (Scheme 24).¹³¹ The maximum polymerization activity was 2.3 kg-PE/mol-Cr·h and narrower molecular weight distribution PE than original Phillips catalyst was obtained. However, this study was carried out around the time when an efficient synthesis method of POSS began to be established. Its main purpose is synthesis and investigation of the polymerization activity. The obtained PE structure and active site structure were not sufficiently addressed and this is only the study related to a molecular analogue of Phillips catalyst based on POSS.



Scheme 24 Synthesis of $(c\text{-C}_6\text{H}_{11})_7\text{Si}_7\text{O}_{11}(\text{OSiMe}_3)\text{CrO}_2$.

It is known that silica-supported vanadium catalyst also shows activity for α -olefin polymerization. Feher *et al.* synthesized $(c\text{-C}_6\text{H}_{11})_7\text{Si}_7\text{O}_{12}\text{V}=\text{O}$ by a reaction of $(c\text{-C}_6\text{H}_{11})_7\text{Si}_7\text{O}_{11}(\text{OH})_3$ with $(n\text{-PrO})_3\text{VO}$, $(\text{Me}_3\text{SiCH}_2)_3\text{VO}$ or VOCl_3 in high yield. The dimer $[(c\text{-C}_6\text{H}_{11})_7\text{Si}_7\text{O}_{12}\text{V}=\text{O}]_2$ was also isolated by recrystallization from CH_2Cl_2 solution of pure $(c\text{-C}_6\text{H}_{11})_7\text{Si}_7\text{O}_{12}\text{V}=\text{O}$ (Scheme 25).¹³²⁻¹³⁴ They reported that the dimer $[(c\text{-C}_6\text{H}_{11})_7\text{Si}_7\text{O}_{12}\text{V}=\text{O}]_2$ is favored in an enthalpic reason, but $(c\text{-C}_6\text{H}_{11})_7\text{Si}_7\text{O}_{12}\text{V}=\text{O}$ exists as major species at low concentrations and/or at a room temperature over 25°C . In ethylene polymerization using AlMe_3 , it produced PE with a narrow molecular weight distribution ($M_w = 48000$, $M_w/M_n = 2.3$). It was indicated that the catalyst was truly of single site. Different olefin polymerization and copolymerization were also investigated.

The activity for propylene was rather low and provided low molecular weight atactic PP (M_w 104). In the copolymerization of propylene (neat) and ethylene (1%), small amounts of polymer containing 5-10% propylene was obtained. On the other hand, it showed activity for the 1,3-butadiene homopolymerization, mainly affording *trans*-polybutadiene.



Scheme 25 POSS-supported vanadium catalyst $(c\text{-C}_6\text{H}_{11})_7\text{Si}_7\text{O}_{12}\text{V}=\text{O}$ and its dimerization.

They also investigated the reaction of $[(c\text{-C}_6\text{H}_{11})_7\text{Si}_7\text{O}_{12}\text{V}=\text{O}]_n$ ($n = 1, 2$) and $\text{Al}(\text{CH}_2\text{SiMe}_3)_3$ at low temperature and analyzed it by NMR measurements. It was found that POSS-supported vanadium complex was alkylated by $\text{Al}(\text{CH}_2\text{SiMe}_3)_3$ and formed the $(c\text{-C}_6\text{H}_{11})_7\text{Si}_7\text{O}_{11}[\text{OAl}(\text{CH}_2\text{SiMe}_3)_2]\text{V}(=\text{O})(\text{CH}_2\text{SiMe}_3)$ at $-50\text{ }^\circ\text{C}$. Moreover, a new peak was observed at $-10\text{ }^\circ\text{C}$, and it was considered that the $(c\text{-C}_6\text{H}_{11})_7\text{Si}_7\text{O}_{11}[(\text{OAl}(\text{CH}_2\text{SiMe}_3)]\text{V}(=\text{O})(\text{CH}_2\text{SiMe}_3)_2$ was formed. When ethylene was introduced into this complex solution, PE with a broad molecular weight distribution ($M_w = 128500$, $M_w/M_n = 5.7$) was generated. There has been no other example that identified the reaction intermediate of POSS-supported complex and an activator. While it sounds useful for elucidating the polymerization mechanism at a molecular level.

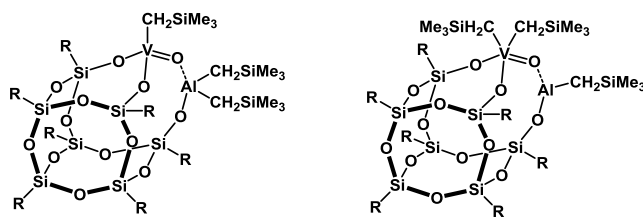


Figure 11 Reaction product of $[(c\text{-C}_6\text{H}_{11})_7\text{Si}_7\text{O}_{12}\text{V}=\text{O}]_n$ ($n = 1, 2$) and $\text{Al}(\text{CH}_2\text{SiMe}_3)_3$.

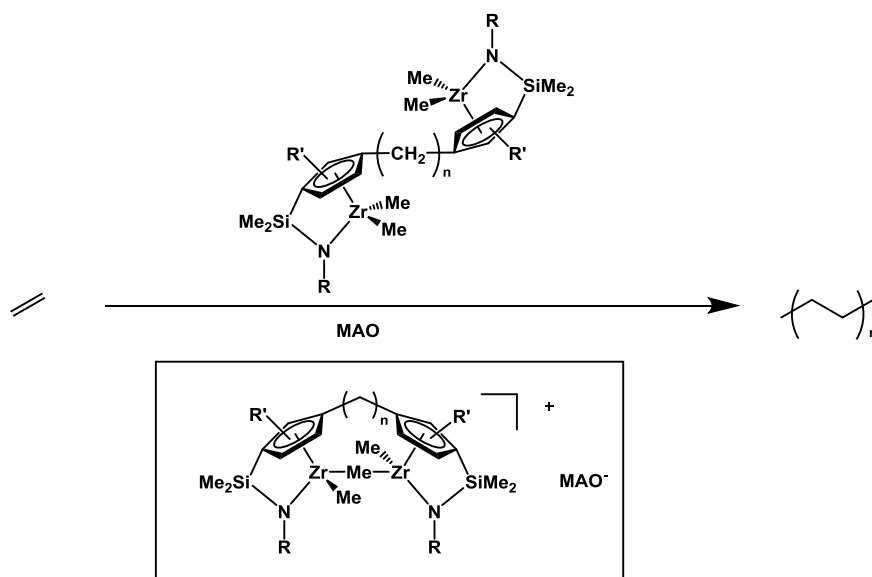
As described above, various POSS-supported catalysts have been studied as a model molecule of silica-supported olefin polymerization catalyst and they are helpful for controlling and understanding the coordination environment of catalytic active sites at a molecular level.

1.4 Bridging Catalysts in Olefin Polymerization

Recently, multimetallic catalyst is extensively studied to create a unique polymer which can not be synthesized by a monometallic catalyst. Such a catalyst system is expected to withdraw a new catalytic reaction by the cooperative effect due to the interaction between active centers.¹³⁵⁻¹³⁸

Application to homobimetallic polymerization catalyst

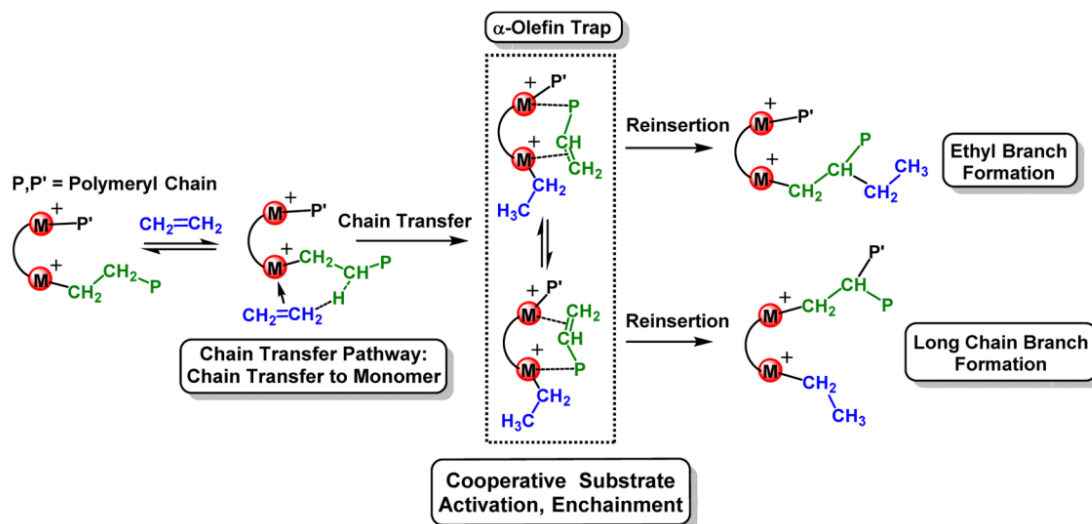
Marks *et al.* synthesized C_n -CGCZr₂ ($n = 1$ or 2) catalyst that linked CGC-type Zr complexes through a methylene bridge (**Scheme 26**).¹³⁹⁻¹⁴² In ethylene polymerization activated with MAO, it provided 600 times higher M_w PE than the monometallic analogue. It was presumed that the chain transfer reaction was suppressed because of the formation of μ -Me complex confirmed by ¹H NMR measurement.



Scheme 26 Ethylene polymerization using C_n -CGCZr₂ catalyst.

Moreover, the bimetallic catalyst produced highly branched polyethylene than monometallic catalyst. It was indicated that chain transfer to monomer followed by

α -olefin re-insertion to propagation site (**Scheme 27**).^{139,140,143} C2-CGCZr2 activated by bifunctional borate reagent $[\text{Ph}_3\text{C}]_2[1,4-(\text{C}_6\text{F}_5)_3\text{BC}_6\text{F}_4\text{B}(\text{C}_6\text{F}_5)_3]$ produced 1.4 times higher M_w and 4.8 times more branched polymer compared with $[\text{Ph}_3\text{C}][\text{B}(\text{C}_6\text{F}_5)_4]$.



Scheme 27 Proposed mechanism of cooperative effect for branch formation by bimetallic CGC catalyst.

The binuclear hafnium catalyst (Catalyst B in **Figure 12**) which has Hf...Hf distance 6.16 Å (in solid state) produced PE of 5.7 times higher M_w than its monometallic analogue (Catalyst A).¹⁴⁴⁻¹⁴⁵ Moreover, in copolymerization of ethylene and 1-octene, it produced 2.4 times higher M_w and 1.9 times more branched polymer. The authors mentioned that the efficient insertion of 1-octene occurred by intermolecular chain shuttling. In addition, they revealed that Catalyst C which has a larger Hf...Hf distance (8.06 Å) produced similar polyethylene and co-polymer with the monometallic catalyst. Therefore, it was suggested that the distance between metal centers affects the expression of cooperative effect even in binuclear complexes having similar structures.

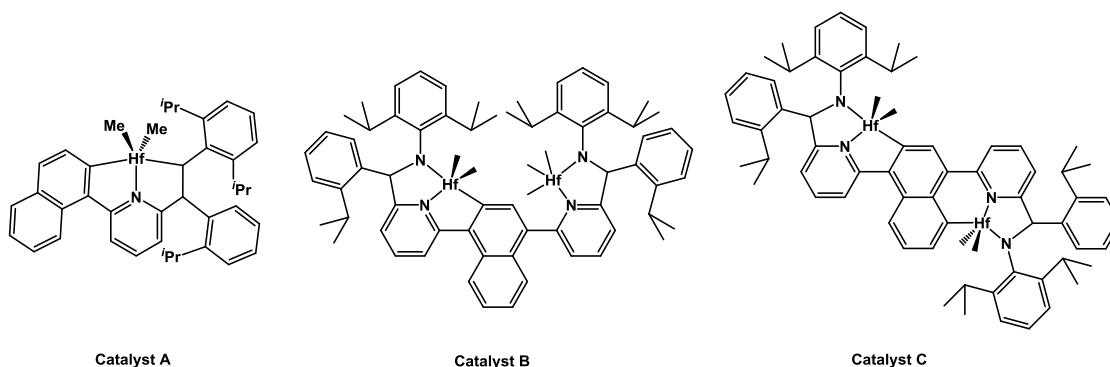


Figure 12 Mono- and bimetallic hafnium polymerization catalysts

Application to heterobimetallic polymerization catalyst

Heterobimetallic catalyst named CGCTiZr which is covalently linked CGCZr and CGCTi can create high molecular weight ($M_w = 779$ kg/mol) with high activity (520 kg-PE \cdot mol $^{-1}$ atm $^{-1}$ h $^{-1}$).¹⁴⁶ The number of branches (\geq C6) increased with increasing temperature while the others such as monometallic catalysts (CGCTi and CGCZr) or their mixture (CGCTi + CGCZr) could not enhance the branching. This fact indicated that the Ti site efficiently captured the oligomers produced by the neighboring Zr site into the propagating polymer chain. The branch formation proposed as an evidence for intermolecular cooperative effect (**Figure 13**).

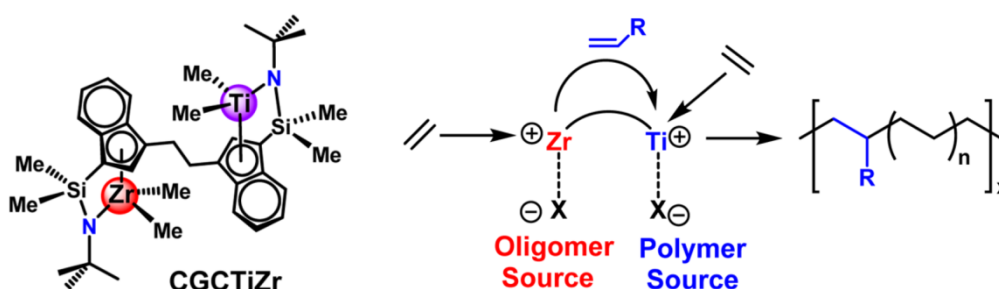


Figure 13 Proposed mechanism of cooperative effect at heterobimetallic catalyst (CGCTiZr).

Moreover, Marks *et. al.* synthesized heterobimetallic catalyst CGCTi-SNSCr which is a combination of CGCTi-type complex for polymerization and SNSCr complex for selective ethylene trimerization, and compared its performance with a mixture of the two monometallic catalysts (**Figure 14**).^{147,148} In addition, they also investigated the effect of the methylene chain numbers as a linkage. It was found that the bimetallic catalyst provides highly branched polyethylene than tandem catalyst system and the branch frequency increased with decreasing the number of methylene chain linkage. Thus, they demonstrated that the distance between Ti and Cr site is crucial to enhance the cooperative effect.

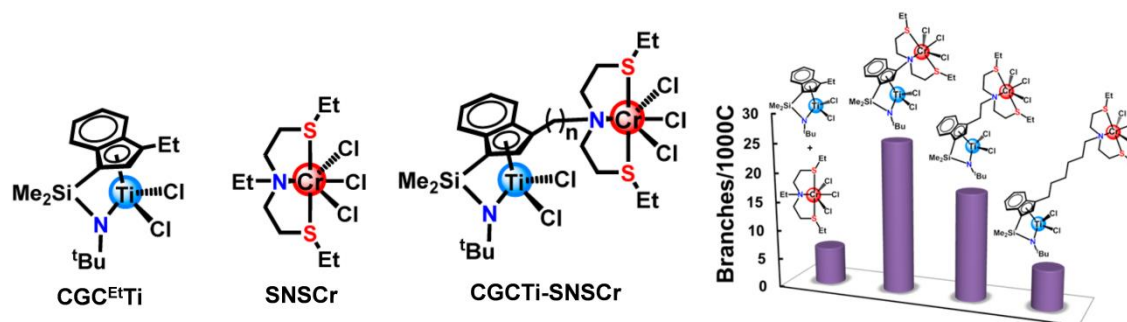


Figure 14 Structures of heterobimetallic catalyst CGCTi-SNSCr and the monometallic analogues CGCTi, SNSCr (left) and branch amount in the produced PEs (right).

1.5 Purpose of the Present Research

As described above, both solid catalysts and molecular catalysts have been developed in the field of olefin polymerization catalysts. In the solid catalyst, it is difficult to clarify the SPR and reaction mechanism because various chemical and physical structural factors ranging from atoms to the particle size scale exist and its performance emerges as a sum of a large number of catalytic active sites. Evaluation of the nature of well-defined active sites by the SOMC approach has advanced, but complete understanding is not easy. On the other hand, the molecular catalyst is powerful not only to understand the reaction mechanism but also to design the catalyst function since a single structure endows a clear relationship with the produced polymer structure. However, catalytic multifunctionalization by multinuclear complexation or loading on a solid support is required to obtain a unique polymer structure and there are problems such as restriction on synthesis of ligands and unevenness of active site structure. Molecular catalysts that mimic traced chemical structure of solid catalyst or precise enable function accumulation in a single molecule are strongly required to fill the gap between the solid and molecular catalysts. In this dissertation, the purpose is to establish catalyst combining the concepts of solid and molecular catalyst through the study of molecular catalyst that mimics solid catalyst structure with a systematic design and polymer-supported catalyst possessing well defined active site structures and multifunctionality.

In Chapter 2, Phillips type model molecular catalysts were synthesized and its catalytic properties were investigated. Trifunctional POSS [e.g. $(t\text{Bu})_7\text{Si}_7\text{O}_9(\text{OH})_3$] was employed to support Cr species on homogeneous coordination environment at a molecular level. At the same time, different functional groups were introduced to the

remaining silanol group of POSS-supported catalyst for designing the ligand environment around Cr species. The influence of the introduced functional groups by chemical modification on the silica surface was also evaluated. In Chapter 3, a series of POSS-supported chromium catalyst was used with various alkyl aluminum (AlEt_3 , Al^iBu_3 , Al^nOt_3) and $\text{Ph}_3\text{CB}(\text{C}_6\text{F}_5)_4$ and the influences on the catalyst performance were investigated. In Chapter 4, multiple catalytic active sites with different functions were accumulated using polymer chain support that is soluble in organic solvent and has uniform structure. The polymer support was synthesized by ring-opening metathesis polymerization of norbornene using Grubbs catalyst. Two types of active sites with different catalyst performances were introduced and the influence on the produced PE was investigated.

Reference

- [1] K. Ziegler, E. Holzkamp, H. Breil, H. Martin, *Angew. Chem. Int. Ed.* 1955, **67**, 541.
- [2] K. Ziegler, H. Breil, H. Martin, E. Holzkamp, German Patent 1953, **973**, 626.
- [3] G. Natta, P. Pino, P. Corradini, F. Danusso, E. Mantica, G. Mazzanti, G. Moraglio, *J. Am. Chem. Soc.* 1955, **77**, 1708.
- [4] G. Natta, *Angew. Chem. Int. Ed.* 1956, **68**, 393.
- [5] E. P. Moore Jr., *Polypropylene Handbook*; Hanser: Munich, 1986.
- [6] J. P. Hogan, R. L. Banks, U.S. Patent 2,825,721, 1958.
- [7] M. P. McDaniel, *Adv. Catal.* 1985, **33**, 47.
- [8] M. P. McDaniel, *Adv. Catal.*, 2010, **53**, 123.
- [9] Z. Liu, X. He, R. Cheng, M. S. Eisen, M. Terano, S. L. Scott, B. Liu, *Adv. Polym. Sci.* 2013, **257**, 135.
- [10] E. Groppo, C. Lamberti, S. Bordiga, G. Spoto, A. Zecchina, *Chem. Rev.* 2005, **105**, 115.
- [11] A. Zecchina, E. Garrone, G. Ghiotti, C. Morterra, E. Borello, *J. Phys. Chem.* 1975, **79**, 966.
- [12] B. M. Weckhuysen, L. M. De Ridder, R. A. Schoonheydt, *J. Phys. Chem.* 1993, **97**, 4756.
- [13] J. M. Jehng, I. E. Wachs, B. M. Weckhuysen, R. A. Schoonheydt, *J. Chem. Soc., Faraday Trans.* 1993, **97**, 4756.
- [14] B. M. Weckhuysen, I. E. Wachs, R. A. Schoonheydt, *Chem. Rev.* 1996, **96**, 3327.
- [15] D. S. Kim, J. M. Tatibouet, I. E. Wachs, *J. Catal.* 1992, **136**, 209.
- [16] D. S. Kim, I. E. Wachs, *J. Catal.* 1993, **142**, 166.
- [17] J. M. Jehng, I. E. Wachs, B. M. Weckhuysen, R. A. Schoonheydt, *J. Chem. Soc.*,

Faraday Trans. 1995, **91**, 953.

[18] Y. Wang, Q. Zhang, Q. Guo, T. Chen, H. Wan, Y. Ohishi, T. Shishido, K. Takehira, *Chem. Lett.* 2002, **31**, 1152.

[19] Y. Wang, Y. Ohishi, T. Shishido, Q. Zhang, W. Yang, Q. Guo, H. Wan, K. Takehira, *J. Catal.* 2003, **220**, 347.

[20] C. Moisii, E. W. Deguns, A. Lita, S. D. Callahan, L. J. van de Burgt, D. Magana, A. E. Stiegman, *Chem. Mater.* 2006, **18**, 3965.

[21] B. M. Weckhuysen, L. M. De Ridder, P. J. Grobet, R. A. Schoonheydt, *J. Phys. Chem.* 1995, **99**, 320.

[22] J. A. Chudek, G. Hunter, G. W. McQuire, C. H. Rochester, T. F. S. Smith, *J. Chem. Soc., Faraday Trans.* 1996, **92**, 453.

[23] B. Liu, M. Terano, *J. Mol. Catal. A: Chem.* 2001, **172**, 227.

[24] B. Liu, Y. Fang, M. Terano, *J. Mol. Catal. A: Chem.* 2004, **219**, 165.

[25] Y. Fang, B. Liu, M. Terano, *J. Mol. Catal. A: Chem.* 2005, **131**, 279.

[26] B. Liu, H. Nakatani, M. Terano, *J. Mol. Catal. A: Chem.* 2002, **184**, 387.

[27] P. G. D. Croce, F. Aubriet, P. Bertrand, P. Rouxhet, P. Grange, *Stud. Surf. Sci. Catal.* 2002, **143**, 823.

[28] B. M. Weckhuysen, R. A. Schoonheydt, J.-M. Jehng, I. E. Wachs, S. J. Cho, R. Ryoo, S. Kijlstra, E. Poels, *J. Chem. Soc., Faraday Trans.* 1995, **91**, 3245.

[29] R. Merryfield, M. P. McDaniel, G. Parks, *J. Catal.* 1982, **77**, 348.

[30] L. M. Baker, W. L. Carrick, *J. Org. Chem.* 1968, **33**, 616.

[31] L. M. Baker, W. L. Carrick, *J. Org. Chem.* 1970, **35**, 774.

[32] A. Zecchina, E. Groppo, A. Damin, C. Pestimino, *Top. Organomet. Chem.* 2005, **16**,

1.

- [33] G. Ghiotti, E. Garrone, A. Zecchina, *J. Mol. Catal.* 1988, **46**, 61.
- [34] M. Kantcheva, I. G. Dalla Lana, J. A. Szymura, *J. Catal.* 1995, **154**, 329.
- [35] C. Groeneveld, P. P. M. M. Wittgen, H. P. M. Swinnen, A. Wernsen, G. C. A. Schuit, *J. Catal.* 1983, **83**, 346.
- [36] W. K. Jozwiak, I. G. Dalla Lana, R. Fiederow, *J. Catal.* 1990, **121**, 183.
- [37] E. Groppo, C. Lamberti, S. Bordiga, G. Spoto, A. Zecchina, *J. Catal.* 2006, **240**, 172.
- [38] M. P. McDaniel, *Ind. Eng. Chem. Res.* 1998, **27**, 1559.
- [39] P. J. Cossee, *J. Catal.* 1964, **3**, 80.
- [40] P. J. Cossee, E. J. Arman, *J. Catal.* 1964, **3**, 99.
- [41] Ø. Espelid, K. J. Børve, *J. Catal.* 2000, **195**, 125.
- [42] K. J. Ivin, J. J. Rooney, C. D. Stewart, M. L. H. Green, J. R. Mahtab, *J. Chem. Soc., Chem. Commun.* 1978, 604.
- [43] G. Ghiotti, E. Garrone, S. Coluccia, C. Morterra, A. Zecchina, *J. Chem. Soc., Chem. Commun.* 1979, 1032.
- [44] M. P. McDaniel, D. M. Cantor, *J. Polym. Sci., Polym. Chem. Ed.* 1983, **21**, 1217.
- [45] G. Ghiotti, E. Garrone, A. Zecchina, *J. Mol. Catal.* 1991, **65**, 73.
- [46] R. Blom, A. Follestad, O. Noel, *J. Mol. Catal.* 1994, **91**, 237.
- [47] H. Sinn, W. Kaminsky, *Adv. Organomet. Chem.* 1980, **18**, 99.
- [48] H. Sinn, W. Kaminsky, H. J. Vollmer, R. Woldt, *Angew. Chem., Int. Ed.* 1980, **19**, 390.
- [49] G. W. Coates, *Chem. Rev.* 2000, **100**, 1223.
- [50] L. Resconi, L. Cavallo, A. Fait, F. Piemontesi, *Chem. Rev.* 2000, **100**, 1253.
- [51] J. A. M. Canich, U.S. Patent 5,026,798, 1991.

- [52] J. A. M. Canich, G. F. Licciardi, U.S. Patent 5,057,475, 1991.
- [53] J. A. M. Canich, Eur. Pat. Appl. 0 420 436 A1, 1991.
- [54] J. C. Stevens, F. J. Timmers, D. R. Wilson, G. F. Schmidt, P. N. Nickias, R. K. Rosen, G. W. Knight, S.-y. Lai, Eur. Pat. Appl. 0 416 815 A2, 1991.
- [55] J. C. Stevens, D. R. Neithamer, Eur. Pat. Appl. 0 418 044 A2, 1991.
- [56] H. H. Brintzinger, R. Fischer, Mulhaupt, B. Rieger, R. M. Waymouth, *Angew. Chem. Int. Ed. Engl.* 1995, **34**, 1143.
- [57] A. L. McKnight, R. M. Waymouth, *Chem. Rev.* 1998, **98**, 2587.
- [58] W. Keim, F. H. Kowaldt, R. Goddard, C. Krüger, *Angew. Chem. Int. Ed.* 1978, **17**, 466.
- [59] W. Keim, *Angew. Chem. Int. Ed.* 2013, **52**, 12492.
- [60] J. Skupinska, *Chem. Rev.* 1991, **91**, 613.
- [61] L. K. Johnson, C. K. Killian, M. S. Brookhart, *J. Am. Chem. Soc.* 1995, **117**, 6414.
- [62] L. K. Johnson, S. Mecking, M. S. Brookhart, *J. Am. Chem. Soc.* 1995, **118**, 267.
- [63] C. M. Killian, D. J. Tempel, L. K. Johnson, M. S. Brookhart, *J. Am. Chem. Soc.* 1996, **118**, 11664.
- [64] V. M. Möhring, G. Fink, *Angew. Chem. Int. Ed.* 1985, **24**, 1001.
- [65] R. Schubbe, K. Angermund, G. Fink, R. Goddard, *Macromol. Chem. Phys.* 1995, **196**, 467.
- [66] S. Mecking, L. K. Johnson, L. Wang, M. Brookhart, *J. Am. Chem. Soc.* 1998, **120**, 888.
- [67] Z. Guan, P. M. Cotts, E. F. McCord, S. J. McLain, *Science* 1999, **283**, 2059.
- [68] A. Nakamura, S. Ito, K. Nozaki, *Chem. Rev.* 2009, **109**, 5215.
- [69] T. Fujita, Y. Tohi, M. Mitani, S. Matsui, J. Saito, M. Nitabaru, K. Sugi, H. Makio, Y.

Tsutsui, 1998, EP-0874005.

[70] S. Matsui, T. Fujita, *Catal. Today* 2001, **66**, 63.

[71] N. Matsukawa, S. Matsui, M. Mitani, J. Saito, K. Tsuru, N. Kashiwa, T. Fujita, *J. Mol. Catal. A: Chem.* 2002, **179**, 11.

[72] H. Makio, N. Kashiwa, T. Fujita, *Adv. Synth. Catal.* 2002, **344**, 477.

[73] R. Furuyama, J. Saito, S. Ishii, M. Mitani, Y. Tohi, H. Makio, N. Matsukawa, H. Tanaka, T. Fujita, *J. Mol. Catal. A: Chem.* 2003, **200**, 31.

[74] H. Makio, H. Terao, A. Iwashita, T. Fujita, *Chem. Rev.* 2011, **111**, 2363.

[75] Modern Surface Organometallic Chemistry, J.-M. Basset, R. Psaro, D. Roberto, R. Ugo, Eds., Wiley-VCH Verlag GmbH & Co. KGaA: Weinheim, Germany, 2009.

[76] J.-M. Basset, F. Lefebvre, C. Santini, *Coord. Chem. Rev.* 1998, **178-180** 1703.

[77] C. Copéret, M. Chabanas, R. P. Saint-Arroman, J.-M. Basset, *Angew. Chem. Int. Ed.* 2003, **42**, 156.

[78] S. L. Wegener, T. J. Marks, P. C. Stair, *Acc. Chem. Res.* 2012, **45**, 206.

[79] P. Serna, B. C. Gates, *Acc. Chem. Res.* 2014, **47**, 2612.

[80] M. M. Stalzer, M. Delferro, T. J. Marks, *Catal. Lett.* 2015, **145**, 3.

[81] J. D. A. Pelletier, J.-M. Basset, *Acc. Chem. Res.* 2016, **49**, 664.

[82] C. Copéret, A. Comas-Vives, M. P. Conley, D. P. Estes, A. Fedorov, V. Mougél, H. Nagae, F. Núñez-Zarur, P. A. Zhizhko, *Chem. Rev.* 2016, **116**, 323.

[83] C. Copéret, A. Fedorov, P. A. Zhizhko, *Catal. Lett.* 2017, **147**, 2247.

[84] C. Copéret, F. Allouche, K. W. Chan, M. P. Conley, M. F. Delley, A. Fedorov, I. B. Moroz, V. Mougél, M. Pucino, K. Searles, K. Yamamoto, P. A. Zhizhko, *Angew. Chem. Int. Ed.* 2018, **57**, 6398.

[85] M. Jezequel, V. Dufaud, M. J. Ruiz-Garcia, F. Carrillo-Hermosilla, U. Neugebauer,

- G. P. Niccolai, F. Lefebvre, F. Bayard, J. Corker, S. Fiddy, J. Evans, J.-P. Broyer, J. Malinge, J.-M. Basset, *J. Am. Chem. Soc.* 2001, **123**, 3520.
- [86] N. Popoff, R. M. Gauvin, A. D. Mallmann, M. Taoufik, *Organometallics* 2012, **31**, 4763.
- [87] N. Millot, C. C. Santini, A. Baudouin, J.-M. Basset, *Chem. Commun.* 2003, 2034.
- [88] E. Y.-X. Chen, T. J. Marks, *Chem. Rev.* 2000, **100**, 1391.
- [89] J. Joubert, F. Delbecq, P. Sautet, E. L. Roux, M. Taoufik, C. Thieuleux, F. Blanc, C. Copéret, J. Thivolle-Cazat, J.-M. Basset, *J. Am. Chem. Soc.* 2006, **128**, 9157.
- [90] M. Delgado, C. C. Santini, F. Delbecq, R. Wischert, B. L. Guennic, G. Tosin, R. Spitz, J.-M. Basset, P. Sautet, *J. Phys. Chem. C* 2010, **114**, 18516.
- [91] J. Amor Nait Ajjou, S. L. Scott, *Organometallics* 1997, **16**, 86.
- [92] J. Amor Nait Ajjou, S. L. Scott, V. Paquet, *J. Am. Chem. Soc.* 1998, **120**, 415.
- [93] J. Amor Nait Ajjou, G. L. Rice, S. L. Scott, *J. Am. Chem. Soc.* 1998, **120**, 13436.
- [94] J. Amor Nait Ajjou, S. L. Scott, *J. Am. Chem. Soc.* 2000, **122**, 8968.
- [95] J. Amor Nait Ajjou, Structure and Reactivity of Silica-Supported Chromium(IV) Complexes. Ph.D. Thesis, University of Ottawa, Ottawa, Canada, 2000.
- [96] S. L. Scott, J. Amor Nait Ajjou, *Chem. Eng. Sci.* 2001, **56**, 4155.
- [97] S. L. Scott, A. Fu, L. A. MacAdams, *Inorg. Chim. Acta* 2008, **361**, 3315.
- [98] T. Agapie, S. J. Schofer, J. A. Labinger, J. E. Bercaw, *J. Am. Chem. Soc.* 2004, **126**, 1304.
- [99] Ikeda, H.; Monoi, T. *J. Polym. Sci., A: Polym. Chem.* 2002, **41**, 413.
- [100] Monoi, T.; Sasaki, Y. *J. Mol. Catal. A: Chem.* 2002, **187**, 135.
- [101] K. Tonosaki, T. Taniike, M. Terano, *Macromol. React. Eng.* 2011, **5**, 332.
- [102] M. P. Conley, M. F. Delley, G. Siddiqi, G. Lapadula, S. Norsic, V. Monteil, O. V.

- Safonova, C. Copéret, *Angew. Chem. Int. Ed.* 2014, **53**, 1872.
- [103] M. F. Delley, M. P. Conley, C. Copéret, *Catal. Lett.* 2014, **144**, 805.
- [104] M. F. Delley, F. Núñez-Zarur, M. P. Conley, A. Comas-Vives, G. Siddiqi, S. Norsic, V. Monteil, O. V. Safonova, C. Copéret, *Proc. Natl. Acad. Sci. U.S.A.* 2014, **111**, 11624.
- [105] M. F. Delley, F. Nuñez-Zarura, M. P. Conley, A. Comas-Vives, G. Siddiqi, S. Norsic, V. Monteil, O. V. Safonova, C. Copéret, *Proc. Natl. Acad. Sci. U.S.A.* 2015, **112**, E4162.
- [106] M. P. Conley, M. F. Delley, F. Núñez-Zarur, A. Comas-Vives, C. Copéret, *Inorg. Chem.* 2015, **54**, 5065.
- [107] T. Pullukat, R. E. Hoff, *Catal. Rev.-Sci. Eng.* 1999, **41**, 389.
- [108] J. F. Brown, L. H. Vogt, *J. Am. Chem. Soc.* 1965, **87**, 4313.
- [109] F. J. Feher, T. A. Budzichowski, R. L. Blanski, K. J. Weller, J. W. Ziller, *Organometallics* 1991, **10**, 2526.
- [110] F. J. Feher, T. A. Budzichowskib, *Polyhedron* 1995, **14**, 3229.
- [111] T. W. Dijkstra, R. Duchateau, R. A. van Santen, A. Meetsma, G. P. A. Yap, *J. Am. Chem. Soc.* 2002, **124**, 9856.
- [112] S. Krijnen, R. J. Harmsen, H. C. L. Abbenhuis, J. H. C. Van Hooff, R. A. Van Santen, *Chem. Commun.* 1999, 501.
- [113] R. Duchateau, *Chem. Rev.* 2002, **102**, 3525.
- [114] E. A. Quadrelli, J.-M. Basset, *Coord. Chem. Rev.* 2010, **254**, 707.
- [115] H. C. L. Abbenhuis, *Chem. Eur. J.* 2000, **6**, 25.
- [116] J.-C. Liu, *Chem. Commun.* 1996, 1109.
- [117] R. Duchateau, H. C. L. Abbenhuis, R. A. van Santen, S. K.-H. Thiele, M. F. H.

- van Tol, *Organometallics* 1998, **17**, 5222.
- [118] R. Duchateau, H. C. L. Abbenhuis, R. A. van Santen, A. Meetsma, S. K.-H. Thiele, M. F. H. van Tol, *Organometallics* 1998, **17**, 5663.
- [119] R. Duchateau, U. Cremer, R. J. Harmsen, S. I. Mohamud, H. C. L. Abbenhuis, R. A. van Santen, A. Meetsma, S. A. K.-H. Thiele, M. F. H. van Tol, M. Kranenburg, *Organometallics* 1999, **18**, 5447.
- [120] Y. Kim, Y. Han, M. H. Lee, S. W. Yoon, K. H. Choi, B. G. Song, Y. Do, *Macromol. Rapid Commun.* 2001, **22**, 573.
- [121] C. Lecuyer, F. Quignard, A. Choplin, D. Olivier, J.-M. Basset, *Angew. Chem., Int. Ed. Engl.* 1991, **30**, 1660.
- [122] F. Quignard, C. Lecuyer, C. Bougault, F. Lefebvre, A. Choplin, D. Olivier, J.-M. Basset, *Inorg. Chem.* 1992, **31**, 928.
- [123] S. Scott, J.-M. Basset, G. P. Niccolai, C. C. Santini, J.-P. Candy, C. Lecuyer, F. Quignard, A. Choplin, *New J. Chem.* 1994, **18**, 115.
- [124] A. Choplin, F. Quignard, *Coord. Chem. Rev.* 1998, **178-180**, 1679.
- [125] H. Schneider, G. T. Puchta, F. A. R. Kaul, G. Raudaschl-Sieber, F. Lefebvre, G. Saggio, D. Mihailios, W. A. Herrmann, J.-M. Basset, *J. Mol. Catal. A: Chem.* 2001, **170**, 127.
- [126] V. Vidal, A. Théolier, J. Thucolle-Cavat, J.-M. Basset, J. Corker, *J. Am. Chem. Soc.* 1996, **118**, 4595.
- [127] C. Rosier, G. P. Niccolai, J.-M. Basset, *J. Am. Chem. Soc.* 1997, **119**, 12408.
- [128] F. Lefebvre, J. Thivolle-Gazet, Dufaud, V. G. P. Niccolai, J.-M. Basset, *Appl. Catal. A: Gen.* 1999, **182**, 1.
- [129] S. D. Ittel, *J. Macromol. Sci., Chem.* 1990, **A27**, 1133.

- [130] S. D. Ittel, L. T. J. Nelson, *Polym. Prepr.* 1994, **35**, 665.
- [131] F. J. Feher, R. L. Blanski, *J. Chem. Soc., Chem. Commun.* 1990, 1614.
- [132] F. J. Feher, J. F. Walzer, *Inorg. Chem.* 1991, **30**, 1689.
- [133] F. J. Feher, J. F. Walzer, R. L. Blanski, *J. Am. Chem. Soc.* 1991, **113**, 3618.
- [134] F. J. Feher, R. L. Blanski, *J. Am. Chem. Soc.* 1992, **114**, 5886.
- [135] H. Li, T. J. Marks, *Proc. Natl. Acad. Sci. U.S.A.* 2006, **103**, 15295.
- [136] M. Delferro, T. J. Marks, *Chem. Rev.* 2011, **111**, 2450.
- [137] J. P. McInnis, M. Delferro, T. J. Marks, *Acc. Chem. Res.* 2014, **47**, 2545.
- [138] H. Suo, G. A. Solan, Y. Maa, W.-H. Sun, *Coord. Chem. Rev.* 2018, **372**, 101.
- [139] L. Li, M. V. Metz, H. Li, M.-C. Chen, T. J. Marks, L. Liable-Sands, A. L. Rheingold, *J. Am. Chem. Soc.* 2002, **124**, 12725.
- [140] H. Li, L. Li, T. J. Marks, *Angew. Chem. Int. Ed.* 2004, **43**, 4937.
- [141] H. Li, C. L. Stern, T. J. Marks, *Macromolecules* 2005, **38**, 9015.
- [142] A. Motta, I. L. Fragala, T. J. Marks, *J. Am. Chem. Soc.* 2009, **131**, 3974.
- [143] M. R. Salata, T. J. Marks, *Macromolecules* 2009, **42**, 1920.
- [144] Y. Gao, A. R. Mouat, A. Motta, A. Macchioni, C. Zuccaccia, M. Delferro, T. J. Marks, *ACS Catal.* 2015, **5**, 5272.
- [145] Y. Gao, X. Chen, J. Zhang, J. Chen, T. L. Lohr, T. J. Marks, *Macromolecules* 2018, **51**, 2401.
- [146] J. Wang, H. Li, N. Guo, L. Li, C. L. Stern, T. J. Marks, *Organometallics* 2004, **23**, 5112.
- [147] S. Liu, A. Motta, M. Delferro, T. J. Marks, *J. Am. Chem. Soc.* 2013, **135**, 8830.
- [148] S. Liu, A. Motta, A. R. Mouat, M. Delferro, T. J. Marks, *J. Am. Chem. Soc.* 2014, **136**, 10460.

Chapter 2

Synthesis of Silsesquioxane-Supported Chromium Catalysts as a Homogeneous Analogue to Phillips Catalyst

2.1 Introduction

Rational design of a catalyst requires the understanding of the correspondence between an active-site structure and its catalysis, which is extremely challenging for solid catalysts owing to heterogeneities of solid surfaces and complications in structures. In light of this, a model catalyst system with a simplified and/or uniform structure can be a powerful tool to clarify the said structure–performance relationship (SPR). In particular, a molecular analogue to a solid catalyst is an ideal system, in which the structure of an active site can be explicitly defined on the basis of the metal–ligand combination to tune the catalysis.

A Phillips polymerization catalyst is one of the most important industrial olefin polymerization catalysts, roughly accounting for one-third of industrial polyethylene production.^{1,2} It facilitates a unique grade of high-density polyethylene featured with a broad molecular weight distribution as well as short- and long-chain branches.^{1,2} Interestingly, the Phillips catalyst generates these unique structures as a consequence of homopolymerization of ethylene and in spite of the fact that a pro-catalyst comprises only hexavalent Cr species supported on a multi-grained SiO₂ support. In other words, it has been believed that supported Cr species are highly heterogeneous, at least in their functions, to allow the coexistence of multiple active sites that are respectively responsible for the production of short to long polyethylene chains as well as the *in situ* generation of α -olefins with various lengths (oligomer to macromonomer).¹⁻³

In order to address the SPR of the Phillips catalyst, enormous efforts have been devoted. For instance, Zecchina, Groppo and their coworkers have made a great contribution in addressing the identity of surface Cr species mainly by spectroscopic techniques.⁴⁻⁸ They identified three types of Cr species (Cr_A^{II}, Cr_B^{II}, and Cr_C^{II})

co-existing on the surfaces of pre-activated Phillips catalysts and demonstrated that the Cr_A^{II} and Cr_B^{II} sites are both active in ethylene polymerization, whereas the Cr_C^{II} sites are inactive.

Surface organometallic chemistry has been powerful to realize a specific molecular structure of Cr species on SiO_2 surfaces. Representatively, dialkyl-Cr(IV), monoalkyl-Cr(III), and mononuclear and dinuclear chromate structures were respectively introduced on SiO_2 surfaces using appropriate organochromium compounds. Scott *et al.* reported that dialkyl-Cr(IV) species were converted into alkylidene species upon heating, while the propagation was promoted at alkylalkenyl species.⁹⁻¹² According to Monoi *et al.*, monoalkyl-Cr(III) species has given by far the highest activity in ethylene polymerization without any induction time.¹³ Tonosaki *et al.* reported the influence of Cr nuclearity on branching.¹⁴ Copéret *et al.* suggested that heterolytic C–H bond activation on Cr(III) species is a key step in the initial ethylene polymerization reaction.¹⁵⁻¹⁹ These model catalysts have greatly advanced the understanding of surface chemistry of the Phillips catalyst by providing a clear definition in the oxidation and alkylation states, and the nuclearity of Cr species. On the other hand, even with uniform Cr structures, these catalysts still afforded polyethylene having a broad molecular weight distribution and sometimes branched. This fact implies that the heterogeneity of Cr species may largely arise from the heterogeneity of silanol groups to be grafted to Cr species.

Demmelmaier *et al.* reported a significant impact of the O–Cr–O angle of the chromasiloxane ring on the activation.²⁰ Tonosaki *et al.* reported that not only the angle of the chromasiloxane ring but also the coordination position of the silanol or siloxane groups is important to regulate the balance between the chain growth and termination,

i.e. molecular weight.²¹ These recent reports are also consistent with historically known facts that the calcination temperature of SiO₂ exerts great influences on the activity and molecular weight distribution^{2,22} and that the replacement or modification of a support material led to great modification in the molecular weight distribution (MWDs).^{2,23–25}

For alleviating the heterogeneity of silanol groups, the utilization of molecular model catalysts sounds attractive. For instance, molecular catalysts with two siloxy ligands bonded to the Cr center such as (Ph₃SiO)₂CrO₂,²⁶ Cr[{OSiPh₂(μ-Na·(THF)₂)}₂O]₂,²⁷ [Cr(=O)₂{(OSiPh₂)₂O}]₂,²⁸ and [(Ph₃SiO)Cr·(THF)]₂(μ-OSiPh₃)₂²⁹ have been studied as model catalysts. Polyhedral oligomeric silsesquioxanes (POSS) having cage-like molecular structures and reactive hydroxyl groups have offered an attractive homogeneous model of SiO₂ surfaces.^{30,31} To the best of our knowledge, [(*c*-C₆H₁₁)₇Si₇O₁₁(OSiMe₃)]CrO₂ reported by Feher *et al.* is the sole example of a POSSsupported Phillips-type catalyst.³²

In this chapter, a series of POSSsupported Phillips-type catalysts by grafting monoalkyl-Cr(III) species to R₇Si₇O₉(OH)₂(OSiMe₂R') (R = ^{*i*}Bu, R' = Me, Ph, C₆H₄(OMe-2), C₆H₄(PPh₂-2)) were synthesized and studied the influence of the active site structure on the ethylene polymerization performance and compared with solid catalyst.

2.2 Experimental

General procedures

All experiments were carried out under a nitrogen atmosphere using Schlenk techniques. Hexane, heptane and diethylether were distilled from sodium benzophenone ketyl and stored under nitrogen. Anhydrous tetrahydrofuran (THF) and toluene were used as received from Kanto Kagaku Co. Ltd. Triethylamine was distilled from calcium hydride and stored under nitrogen. *ortho*-Substituted arylchlorodimethylsilane compounds such as $\text{ClMe}_2\text{SiC}_6\text{H}_4(\text{OMe}-2)$, $\text{ClMe}_2\text{SiC}_6\text{H}_4(\text{NMe}_2-2)$ and $\text{ClMe}_2\text{SiC}_6\text{H}_4(\text{PPh}_2-2)$ were synthesized according to literature procedures.^{33–36} $\text{Cr}[\text{CH}(\text{SiMe}_3)_2]_3$ was also synthesized according to a literature report³⁷ and was donated by Japan Polyethylene Corporation. Triethylaluminum (TEA) and tri-*iso*-butylaluminum (TIBA) were donated by Tosoh Finechem Co. ^1H , $^{13}\text{C}\{^1\text{H}\}$, $^{29}\text{Si}\{^1\text{H}\}$ and $^{31}\text{P}\{^1\text{H}\}$ NMR spectra were recorded on a Bruker BioSpin AVANCE III 400 FT-NMR spectrometer. Chemical shifts were referenced to internal (^1H , ^{13}C , ^{29}Si) or external standards (^{31}P). IR spectra were recorded on a JASCO FT-IR 6100 spectrometer. Highresolution mass spectra were recorded on a Bruker Daltonics FT-ICR MS Solarix. UV-Vis spectroscopy (JASCO V670 UV-VIS-NIR spectrometer) was utilized to characterize the state of chromium species of POSS-supported catalysts, and to determine the chromium loading of SiO_2 -supported catalysts. For the latter, *ca.* 30 mg of a solid catalyst was stirred in a solution of 5.0 ml of 5 M NaOH (aq.) and 2.0 ml of 30% H_2O_2 at 80 °C for 5 h. The mixture was appropriately diluted with deionized water and the chromium concentration was determined based on the absorbance by CrO_4^{2-} at $\lambda_{\text{max}} = 373$ nm. Gel permeation chromatography (GPC) measurements were performed on a Waters ALC/GPC 150C with polystyrene gel columns (Shodex AD806

M/S) at 140 °C using *ortho*-dichlorobenzene as an eluent. The primary structure of PE was determined by $^{13}\text{C}\{^1\text{H}\}$ NMR using a Bruker BioSpin AVANCE III 400 FT-NMR spectrometer equipped with a $^{13}\text{C}/^1\text{H}$ Dual NMR 10 mm Cryo Probe at 120 °C. A polymer sample was dissolved in a 20/80 (v/v) mixture of bromobenzene- d_5 and *ortho*-dichlorobenzene.

POSS synthesis

$(^i\text{Bu})_7\text{Si}_7\text{O}_9(\text{OH})_2(\text{OSiMe}_3)$ (**1a**). Me_3SiCl (368 μl , 2.90 mmol) was added dropwise to a solution of $(^i\text{Bu})_7\text{Si}_7\text{O}_9(\text{OH})_3$ (2.00 g, 2.53 mmol) and trimethylamine (3.5 ml, 25 mmol) in THF (40 ml). The reaction mixture was stirred overnight at room temperature. $\text{Et}_3\text{N}\cdot\text{HCl}$ as a byproduct was removed by filtration and the solvent was evaporated under reduced pressure. The resultant solid was purified through recrystallization in hexane. Yield: 1.46 g (1.69 mmol, 67%). ^1H NMR (400 MHz, benzene- d_6 , r.t.): δ 0.27 (s, 9H, OSiMe_3), 0.76-0.88 [m, 14H, $\text{CH}_2\text{CH}(\text{CH}_3)_2$], 1.02-1.13 [m, 42H, $\text{CH}_2\text{CH}(\text{CH}_3)_2$], 2.02-2.17 [m, 7H, $\text{CH}_2\text{CH}(\text{CH}_3)_2$], 4.71 (br, 2H, OH). $^{13}\text{C}\{^1\text{H}\}$ NMR (100 MHz, benzene- d_6 , r.t.): δ 1.72 (OSiMe_3), 22.96, 23.11, 23.23, 23.63, 24.84 [$\text{CH}_2\text{CH}(\text{CH}_3)_2$], 24.43, 24.65 [$\text{CH}_2\text{CH}(\text{CH}_3)_2$], 25.87, 25.94, 25.98, 26.02, 26.08 [$\text{CH}_2\text{CH}(\text{CH}_3)_2$]. $^{29}\text{Si}\{^1\text{H}\}$ NMR (79.6 MHz, benzene- d_6 , r.t.): δ 12.58 (s, OSiMe_3), -56.39, -65.94, -66.06, -66.12, -67.51 (s, 2:1:1:1:2). IR (KBr): 3300 (br), 2955 (s), 2904 (m), 2871 (m), 1467 (m), 1402 (w), 1384 (w), 1366 (m), 1333 (m), 1253 (w), 1230 (s), 1115 (vs), 955 (w), 876 (s), 843 (s), 741 (m) cm^{-1} . HRMS (MALDI-FT-ICR) m/z : $[\text{M} + \text{Na}]^+$ calcd for $\text{C}_{31}\text{H}_{74}\text{O}_{12}\text{Si}_8$: 885.3227, found: 885.3223.

$(^i\text{Bu})_7\text{Si}_7\text{O}_9(\text{OH})_2(\text{OSiMe}_2\text{Ph})$ (**1b**). **1b** was synthesized according to the same procedure with **1a** except for the usage of PhMe_2SiCl (482 μl , 2.91 mmol) in place of

Me₃SiCl. Yield: 1.24 g (1.34 mmol, 53%). ¹H NMR (400 MHz, benzene-*d*₆, r.t.): δ 0.52 (s, 6H, OSiMe₂Ph), 0.72-0.89 [m, 14H, CH₂CH(CH₃)₂], 1.02-1.18 [m, 42H, CH₂CH(CH₃)₂], 1.97-2.18 [m, 7H, CH₂CH(CH₃)₂], 4.23 (br, 2H, OH), 7.20 (t, 1H, OSiMe₂Ph, *J* = 8.0 Hz), 7.28 (t, 2H, OSiMe₂Ph, *J* = 8.0 Hz), 7.70 (d, 2H, OSiMe₂Ph, *J* = 8.0 Hz). ¹³C{¹H} NMR (100 MHz, benzene-*d*₆, r.t.): δ 0.50 (OSiMe₂Ph), 22.97, 23.08, 23.24, 23.70, 24.84 [CH₂CH(CH₃)₂], 24.40, 24.45, 24.59 [CH₂CH(CH₃)₂], 25.88, 25.93, 35.97, 26.05, 26.07 [CH₂CH(CH₃)₂], 128.37, 130.08, 133.67, 139.17 (OSiMe₂Ph). ²⁹Si{¹H} NMR (79.6 MHz, benzene-*d*₆, r.t.): δ 1.30 (s, OSiMe₂Ph), -56.84, -66.13, -66.18, -66.57, -67.70 (s, 2:1:1:1:2). IR (KBr): 3318 (br), 3071 (w), 2954 (s), 2927 (m), 2905 (m), 2871 (m), 1467 (m), 1402 (w), 1366 (m), 1333 (m), 1255 (w), 1230 (s), 1186 (vs), 878 (s), 837 (s), 742 (s), 698 (m) cm⁻¹. HRMS (MALDI-FT-ICR) *m/z*: [M + Na]⁺ calcd for C₃₆H₇₆O₁₂Si₈: 947.3383, found: 947.3374.

(^{*i*}Bu)₇Si₇O₉(OH)₂[OSiMe₂C₆H₄(OMe-2)] (**1c**). **1c** was synthesized according to the same procedure with **1a** except for the usage of C₆H₄(OMe-2)Me₂SiCl (560 μl, 2.91 mmol) in place of Me₃SiCl. Yield: 1.63 g (1.71 mmol, 68%). ¹H NMR (400 MHz, benzene-*d*₆, r.t.): δ 0.67 [s, 6H, OSiMe₂C₆H₄(OMe-2)], 0.76-0.88 [m, 14H, CH₂CH(CH₃)₂], 1.04-1.15 [m, 42H, CH₂CH(CH₃)₂], 2.01-2.17 [m, 7H, CH₂CH(CH₃)₂], 3.33 [s, 3H, OSiMe₂C₆H₄(OMe-2)], 4.48 (br, 2H, OH), 6.49 [d, 1H, OSiMe₂C₆H₄(OMe-2), *J* = 8.0 Hz}, 7.05 [t, 1H, OSiMe₂C₆H₄(OMe-2), *J* = 8.0 Hz], 7.20 [t, 1H, OSiMe₂C₆H₄(OMe-2), *J* = 8.0 Hz], 7.82 [d, 1H, OSiMe₂C₆H₄(OMe-2), *J* = 8.0 Hz]. ¹³C{¹H} NMR (100 MHz, benzene-*d*₆, r.t.): δ 1.41 [s, OSiMe₂C₆H₄(OMe-2)], 23.00, 23.11, 23.29, 23.75, 24.84 [s, CH₂CH(CH₃)₂], 24.41, 24.48, 24.62 [s, CH₂CH(CH₃)₂], 25.89, 25.94, 25.98, 26.07, 26.12 [s, CH₂CH(CH₃)₂], 54.78 [s, OSiMe₂C₆H₄(OMe-2)], 110.22, 121.13, 126.77, 131.94, 135.50, 164.43 [s,

OSiMe₂C₆H₄(OMe-2)]. ²⁹Si{¹H} NMR (79.6 MHz, benzene-*d*₆, r.t.): δ 0.82 [s, OSiMe₂C₆H₄(OMe-2)], -56.85, -66.06, -66.10, -66.54, -67.72 (s, 2:1:1:1:2). IR (KBr): 3323 (br), 3066 (w), 2954 (s), 2905 (m), 2871 (m), 1590 (m), 1574 (m), 1465 (m), 1430 (w), 1402 (w), 1366 (m), 1333 (m), 1229 (s), 1108 (vs), 872 (w), 836 (s), 789 (s), 741 (s) cm⁻¹. HRMS (MALDI-FT-ICR) m/z: [M + Na]⁺ calcd for C₃₇H₇₈O₁₃Si₈: 977.3489, found: 977.3480.

(^{*i*}Bu)₇Si₇O₉(OH)₂[OSiMe₂C₆H₄(PPh₂-2)] (**1d**). **1d** was synthesized according to the same procedure with **1a** except for the usage of C₆H₄(PPh₂-2)Me₂SiCl (1.03 g, 2.91 mmol) in place of Me₃SiCl. Yield: 1.80 g (1.62 mmol, 64%). ¹H NMR (400 MHz, benzene-*d*₆, r.t.): δ 0.75-0.98 [m, 20H, OSiMe₂C₆H₄(PPh₂-2) and CH₂CH(CH₃)₂], 1.01-1.18 [m, 42H, CH₂CH(CH₃)₂], 1.98-2.20 [m, 7H, CH₂CH(CH₃)₂], 4.78 (br, 2H, OH), 6.98-7.10 [m, 7H, OSiMe₂C₆H₄(PPh₂-2)], 7.30-7.42 [m, 6H, OSiMe₂C₆H₄(PPh₂-2)], 8.10 [d, 1H, OSiMe₂C₆H₄(PPh₂-2), *J* = 8.0 Hz]. ¹³C{¹H} NMR (100 MHz, benzene-*d*₆, r.t.): δ 3.84 [d, OSiMe₂C₆H₄(PPh₂-2), *J* = 11 Hz], 23.01, 23.13, 23.34, 23.80, 25.80 [CH₂CH(CH₃)₂], 24.44, 24.51, 24.61 [CH₂CH(CH₃)₂], 25.91, 25.96, 26.07, 26.11, 26.14 [CH₂CH(CH₃)₂], 128.67, 128.77, 128.84, 129.10, 130.23, 133.68 (d, *J* = 18 Hz), 135.21 (d, *J* = 16 Hz), 135.78, 138.04 (d, *J* = 10 Hz), 142.56 (d, *J* = 18 Hz) [OSiMe₂C₆H₄(PPh₂-2)]. ²⁹Si{¹H} NMR (benzene-*d*₆, r.t.): δ 0.79 {d, OSiMe₂C₆H₄(PPh₂-2), *J* = 10.3 Hz}, -56.87, -66.08, -66.11, -66.75, -67.72 (s, 2:1:1:1:2). ³¹P{¹H} NMR (116 MHz, benzene-*d*₆, r.t.): δ -6.84 (s, PPh₂). IR (KBr): 3365 (br), 3054 (w), 2954 (s), 2927 (m), 2904 (m), 2871 (m), 1466 (m), 1435 (w), 1402 (w), 1380 (w), 1366 (m), 1333 (m), 1229 (s), 1105 (vs), 836 (s), 741 (s), 695 (m), 607 (w) cm⁻¹. HRMS (ESI-FT-ICR) m/z: [M + H]⁺ calcd for C₄₈H₈₆O₁₂PSi₈: 1109.4013, found: 1109.4013.

POSS-supported catalyst synthesis

$[(^i\text{Bu})_7\text{Si}_7\text{O}_{11}(\text{OSiMe}_3)]\text{CrCH}(\text{SiMe}_3)_2$ (**2a**). $\text{Cr}[\text{CH}(\text{SiMe}_3)_2]_3$ (212 mg, 0.40 mmol) was added to a solution of **1a** (345 mg, 0.40 mmol) in hexane (20 ml). The mixture was stirred at reflux for 6 h, followed by the removal of the solvent under vacuum. The obtained product was used in the ethylene polymerization without further purification. Yield: 420 mg (0.39 mmol, 98%). $^{29}\text{Si}\{^1\text{H}\}$ NMR (79.6 MHz, benzene- d_6 , r.t.): δ 9.34 (s, OSiMe₃), -54.15, -56.74, -65.12, -66.64, -67.18 (s, 1:2:1:2:1). IR (KBr): 2955 (s), 2906 (m), 2871 (m), 1467 (m), 1402 (w), 1384 (w), 1366 (m), 1333 (m), 1253 (w), 1229 (s), 1109 (vs), 1061 (vs), 956 (w), 842 (s), 742 (m) cm^{-1} . UV-vis (heptane): 428, 620 nm.

$[(^i\text{Bu})_7\text{Si}_7\text{O}_{11}(\text{OSiMe}_2\text{Ph})]\text{CrCH}(\text{SiMe}_3)_2$ (**2b**). **2b** was synthesized according to the same procedure with **2a** except for the usage of **1b** (370 mg, 0.40 mmol) in place of **1a**. Yield: 420 mg (0.37 mmol, 93%). $^{29}\text{Si}\{^1\text{H}\}$ NMR (79.6 MHz, benzene- d_6 , r.t.): δ -0.53 (s, OSiMe₂Ph), -54.16, -56.70, -65.10, -66.55, -66.89 (s, 1:2:1:2:1). IR (KBr): 3070 (w), 2955 (s), 2929 (m), 2907 (m), 2871 (m), 1467 (m), 1402 (w), 1366 (m), 1334 (m), 1258 (w), 1229 (s), 1106 (vs), 1062 (vs), 837 (s), 742 (s), 698 (m) cm^{-1} . UV-vis (heptane): 417, 613 nm.

$[(^i\text{Bu})_7\text{Si}_7\text{O}_{11}[\text{OSiMe}_2\text{C}_6\text{H}_4(\text{OMe}-2)]]\text{CrCH}(\text{SiMe}_3)_2$ (**2c**). **2c** was synthesized according to the same procedure with **2a** except for the usage of **1c** (382 mg, 0.40 mmol) in place of **1a**. Yield: 439 mg (0.38 mmol, 94%). $^{29}\text{Si}\{^1\text{H}\}$ NMR (79.6 MHz, benzene- d_6 , r.t.): δ -0.74 (s, OSiMe₂Ar), -54.16, -56.71, -65.10, -66.60, -67.04 (s, 1:2:1:2:1). IR (KBr): 3066 (w), 2954 (s), 2907 (m), 2871 (m), 1591 (m), 1575 (m), 1466 (m), 1430 (w), 1401 (w), 1366 (m), 1333 (m), 1229 (s), 1106 (vs), 1063(vs), 837 (s), 790 (s), 741 (s) cm^{-1} . UV-vis (heptane): 420, 616 nm.

$\{(\text{tBu})_7\text{Si}_7\text{O}_{11}[\text{OSiMe}_2\text{C}_6\text{H}_4(\text{PPh}_2\text{-}2)]\}\text{CrCH}(\text{SiMe}_3)_2$ (**2d**). **2d** was synthesized according to the same procedure with **2a** except for the usage of **1d** (443 mg, 0.40 mmol) in place of **1a** and the usage of toluene (20 ml) in place of hexane. Yield: 513 mg (0.39 mmol, 97%). $^{29}\text{Si}\{^1\text{H}\}$ NMR (79.6 MHz, benzene- d_6 , r.t.): δ -0.84 (dd, $J = 11.1$ Hz, 42.1 Hz, OSiMe₂Ar), -54.15, -56.66, -65.10, -66.56, -67.02 (s, 1:2:1:1:2). $^{31}\text{P}\{^1\text{H}\}$ NMR (116 MHz, benzene- d_6 , r.t.): δ -6.97 (s, PPh₂). IR (KBr): 3055 (w), 2954 (s), 2925 (m), 2903 (m), 2870 (m), 1466 (m), 1436 (w), 1402 (w), 1380 (w), 1366 (m), 1333 (m), 1250 (m), 1229 (s), 1104 (vs), 836 (s), 741 (s), 695 (m) cm⁻¹. UV-vis (heptane): 421, 618 nm.

SiO₂-supported catalyst preparation

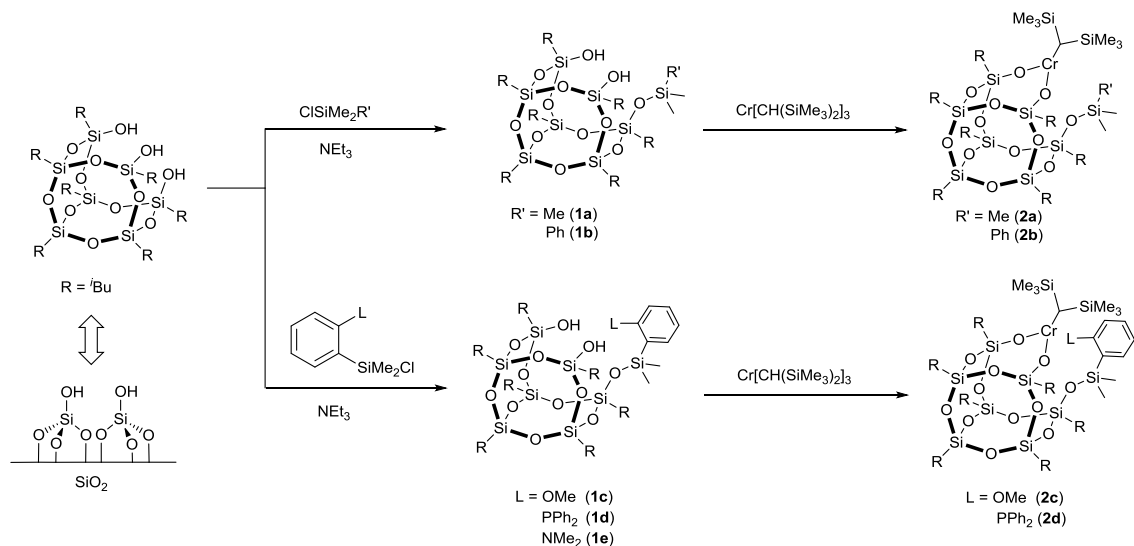
Preparation of functionalized silica-supported chromium catalysts SiO₂ of a polymerization grade (ES70X, 51 μm , 320 m² g⁻¹) was calcined at 400 °C under nitrogen for 6 h. SiO₂ (0.50 g) was suspended in THF (10 ml) containing trimethylamine (0.14 ml, 10 mmol). ClSiMe₂Ph, ClSiMe₂C₆H₄(OMe-2) or ClSiMe₂C₆H₄(PPh₂-2) (0.10 mmol) in THF solution (1.0 ml) was added to the slurry and stirred at room temperature overnight. Then, the slurry was repetitively washed with THF, MeOH and heptane. After vacuum drying, SiO₂ modified with -SiMe₂Ph, -SiMe₂C₆H₄(OMe-2) or -SiMe₂C₆H₄(PPh₂-2) was obtained (denoted as SiO₂-**b**, SiO₂-**c** and SiO₂-**d**, respectively). To the suspension of the modified SiO₂ in heptane (5.0 ml), Cr[CH(SiMe₃)₂]₃ (51 mg, 0.096 mmol, corresponding to 1.0 wt%) in heptane solution (2.0 ml) was added and then stirred at 40 °C for 2 h. The solid catalyst was washed with heptane 3 times and dried under vacuum.

Ethylene polymerization

Ethylene polymerization was conducted in heptane using a stainless steel stirred reactor. Heptane (200 ml) was added into the reactor, followed by heating to the polymerization temperature. The solvent was saturated with an ethylene monomer at 0.5 MPa for 30 min, and trialkylaluminium (0.20 mmol) and a catalyst (8.0 μmol in the case of the molecular catalysts, and 42 mg in the case of the solid catalysts) were added in this order. Ethylene pressure was kept at 0.5 MPa and the polymerization was performed for 1 h. The obtained polymer was recovered by filtration and analyzed by GPC and ^1H , $^{13}\text{C}\{^1\text{H}\}$ NMR.

2.3 Results and Discussion

Synthesis and characterization of POSS-supported chromium catalysts



Scheme 1 Synthesis route of POSS-supported chromium catalysts.

Demmelmaier *et al.* mentioned that 6-membered chromasiloxane can be activated by ethylene²⁰ but the activation of 8-membered chromasiloxane requires the aid of an alkylaluminum activator. The employed POSS, 1,3,5,7,9,11,14-heptaisobutyltricyclo[7.3.3.15,11]heptasiloxane-endo-3,7,14-triol [(^tBu)₇Si₇O₉(OH)₃], affords 8-membered chromasiloxane when the chromium center is immobilized in a bipodal manner. As was expected, the resultant catalyst was unable to be activated by ethylene only and required alkylaluminum also. Nonetheless, I have considered that POSS-supported chromium catalysts would provide some useful insights into the design of an active site environment as follows: arylchlorodimethylsilane derivatives were stoichiometrically reacted with one of the hydroxyl groups of POSS in the presence of trimethylamine (**1b–1e**). Different functional groups (methoxy (**1c**), diphenylphosphino (**1d**), and dimethylamino (**1e**))

were introduced through the substitution at the ortho position of the aryl group, which was obtained by a reaction between dichlorodimethylsilane and the corresponding aryllithium derivative. For comparison, trimethylsilane-modified POSS (**1a**) was also synthesized. To a functionalized POSS, $\text{Cr}[\text{CH}(\text{SiMe}_3)_2]_3$ was stoichiometrically grafted in a bipodal manner to afford a POSS-supported chromium catalyst (**Scheme 1**). It was reported that $\text{Cr}[\text{CH}(\text{SiMe}_3)_2]_3$ afforded a monoalkylated trivalent chromium species on SiO_2 surfaces, which is highly active in ethylene polymerization.¹³

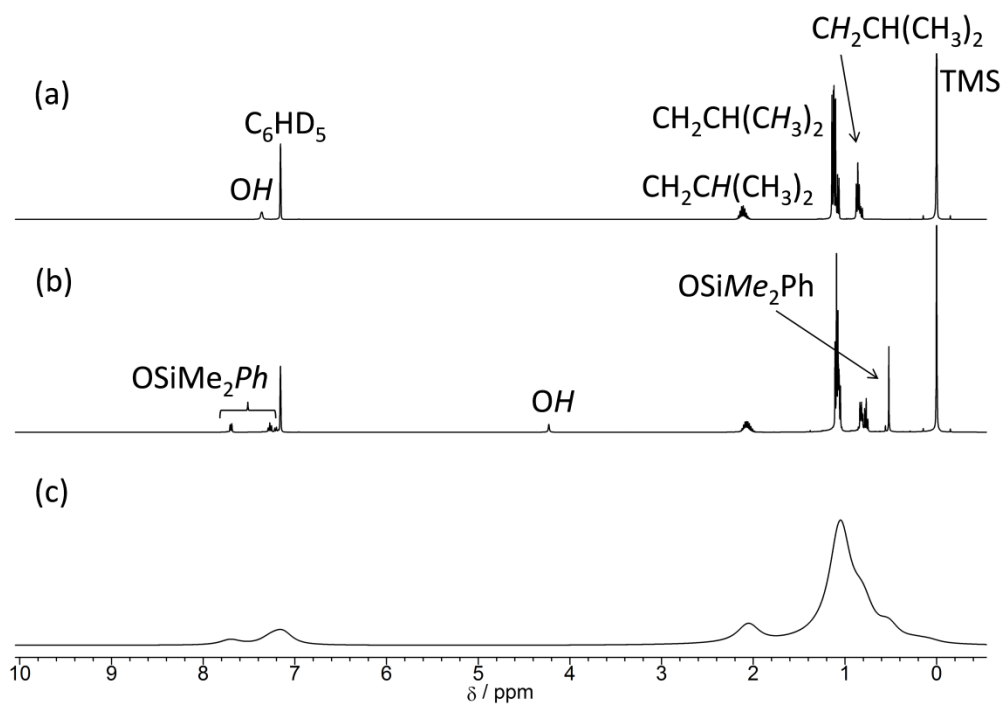


Figure 1 ^1H NMR spectra of (a) $(t\text{Bu})_7\text{Si}_7\text{O}_9(\text{OH})_3$, (b) **1b**, and (c) **2b** in benzene- d_6 .

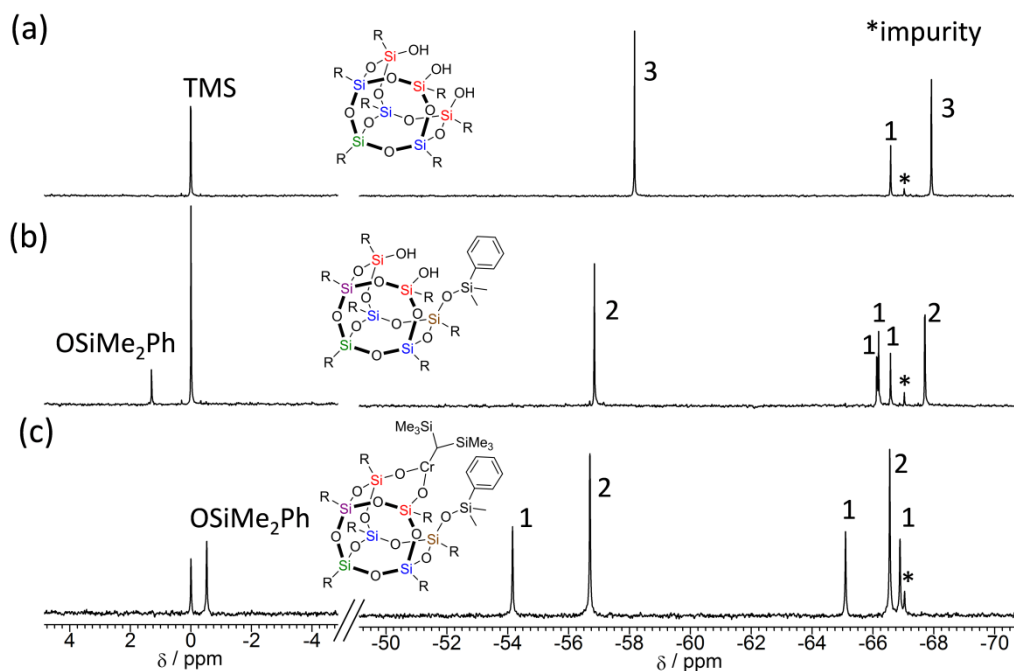


Figure 2 $^{29}\text{Si}\{^1\text{H}\}$ NMR spectra of (a) $(t\text{Bu})_7\text{Si}_7\text{O}_9(\text{OH})_3$, (b) **1b**, and (c) **2b** in benzene- d_6 . The numbers in the spectra represent the ratio of the peak areas for the POSS cage.

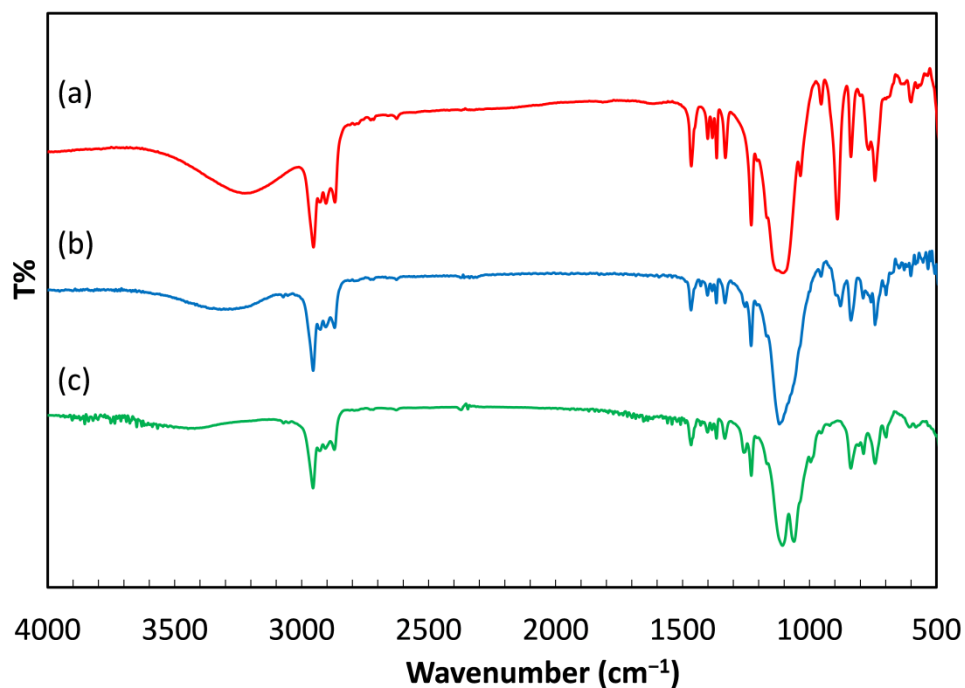


Figure 3 IR spectra of (a) $(t\text{Bu})_7\text{Si}_7\text{O}_9(\text{OH})_3$, (b) **1b**, and (c) **2b**.

The structures of the modified POSS and catalysts were determined by ^1H NMR, $^{29}\text{Si}\{^1\text{H}\}$ NMR, and IR spectra (**Figure 1–3**, respectively). For the sake of brevity, the results of synthesis and characterization are described only for dimethylphenylsilane-modified POSS and its catalysts (**1b** and **2b**). The results for the other derivatives were similar unless specially mentioned and reported in the appendix. In addition to the seven iso-butyl groups of POSS [$\text{CH}_2\text{CH}(\text{CH}_3)_2$; δ 0.72–0.89 (m, 14H), $\text{CH}_2\text{CH}(\text{CH}_3)_2$; δ 1.02–1.18 (m, 42H), $\text{CH}_2\text{CH}(\text{CH}_3)_2$; δ 1.97–2.18 (m, 7H)], one $-\text{OSiMe}_2\text{Ph}$ group [OSiMe_2Ph ; δ 0.52 (s, 6H), OSiMe_2Ph ; δ 7.20 (t, 1H), 7.28 (t, 2H), 7.70 (d, 2H)] and two hydroxyl groups [OH ; δ 4.23 (br, 2H)] were observed (**Figure 1a** and **b**) to confirm the replacement of only one of the three hydroxyl groups by the $-\text{OSiMe}_2\text{Ph}$ group. The $^{29}\text{Si}\{^1\text{H}\}$ NMR spectrum of the original POSS showed resonances at δ -56.17 , -66.58 , -67.92 ppm at a ratio of 3 : 1 : 3, corresponding to a C_{3v} symmetry (**Figure 2a**). The spectrum of the modified product **1b** showed six resonances: one for $-\text{OSiMe}_2\text{Ph}$ at δ 1.30, and five for the cage at δ -56.84 , -66.13 , -66.18 , -66.57 , -67.70 ppm (**Figure 2b**). The five resonances for the cage appeared at a ratio of 2 : 1 : 1 : 1 : 2, which indicated that the modification converted the cage symmetry from C_{3v} to C_s . Similar results were obtained for **1a–1d**, while **1e** could not be isolated from several by-products and was therefore not used in the catalyst preparation. The grafting of $\text{Cr}[\text{CH}(\text{SiMe}_3)_2]_3$ to **1a–1d** led to the production of black solid products. It was difficult to determine the exact structures based on ^1H NMR spectra, as the proton signals were broadened in the presence of paramagnetic Cr(III). However the broadening of the iso-butyl and $-\text{OSiMe}_2\text{Ph}$ signals itself implied that Cr(III) species was bonded to POSS (**Figure 1c**). In the $^{29}\text{Si}\{^1\text{H}\}$ NMR spectrum of **2b**, the peak for the $-\text{OSiMe}_2\text{Ph}$ group and those for the cage structure were shifted to δ

-0.53 ppm and δ -54.16 , -56.70 , -65.10 , -66.55 , -66.89 ppm at a ratio of 1 : 2 : 1 : 2 : 1, respectively. The $-\text{CH}(\text{SiMe}_3)_2$ group was hardly visible because of the shortest distance from paramagnetic Cr(III). Such strong disturbance was also detected for $\text{Cr}[\text{CH}(\text{SiMe}_3)_2]_3$. Nonetheless, it was strongly believed that the chromium species was successfully grafted to the POSS cage in a bipodal manner owing to the following reasons: (i) in $^{29}\text{Si}\{^1\text{H}\}$ NMR, the peaks for the cage structure were greatly shifted after the grafting reaction, while the cage symmetry was still kept at C_s (*i.e.* 1 : 2 : 1 : 2 : 1 ratio). Unipodal grafting as well as two POSS cages bridged by a single chromium center would result in C_1 symmetry. (ii) Hydroxyl groups were totally eliminated by the grafting reaction as can be seen in the IR spectra (**Figure 3**). (iii) When the POSS-supported catalyst was treated with aq. HCl, the moles of $\text{CH}_2(\text{SiMe}_3)_2$ liberated (measured by gas chromatography) corresponded to the moles of POSS used. In the UV/vis spectrum of **2b**, the absorbance related to the d–d transition of Cr(III) was observed at 417 and 613 nm, while $\text{Cr}[\text{CH}(\text{SiMe}_3)_2]_3$ exhibited the absorbance at 450 and 600 nm, suggesting that the chromium center maintained the oxidation state and symmetry. The other catalysts $[(^i\text{Bu})_7\text{Si}_7\text{O}_{11}(\text{OSiMe}_3)]\text{CrCH}(\text{SiMe}_3)_2$ (**2a**), $\{(^i\text{Bu})_7\text{Si}_7\text{O}_{11}[\text{OSiMe}_2\text{C}_6\text{H}_4(\text{OMe}-2)]\}\text{CrCH}(\text{SiMe}_3)_2$ (**2c**) and $\{(^i\text{Bu})_7\text{Si}_7\text{O}_{11}[\text{OSiMe}_2\text{C}_6\text{H}_4(\text{PPh}_2-2)]\}\text{CrCH}(\text{SiMe}_3)_2$ (**2d**) were obtained and characterized by the same procedures (in the appendix.).

Ethylene polymerization with POSS-supported chromium catalysts

Ethylene polymerization was carried out using the POSS-supported chromium catalysts and the catalyst activity at 60 °C is summarized in **Figure 4a**. It was found that all the POSS-supported catalysts exhibited a reasonable activity toward ethylene polymerization in the presence of tri-iso-butylaluminium (TIBA), while the activity was dependent on the modification introduced to the POSS cage. The activity of **2b** having a bulky substituent was slightly lower than that of **2a**. The substitution of functional groups at the *ortho* position of the aryl group induced a positive effect on the activity in spite of increased bulkiness. The drop in the activity of **2c** with the methoxy group was milder than that observed for **2b**, and the activity of **2d** having the diphenylphosphino group was even 1.5 times higher than that of **2a**. Next, the relationship between the catalytic activity and polymerization temperature was examined. As can be seen in **Figure 4b**, **2a** exhibited a monotonous increase of the activity along the polymerization temperature. On the other hand, the activity of **2b** reached the maximum at 50–60 °C, followed by a steep loss over 60 °C. The temperature dependence of the activity of **2c** and **2d** was quite similar to that of **2b** with the maxima located at 60 °C. The activity order followed **2d** \gg **2a**, **2c** > **2b** until 60 °C. Thus, it seems plausible that the introduction of functional groups having a lone pair near the chromium center does not result in simple steric hindrance, but somehow promotes the polymerization.

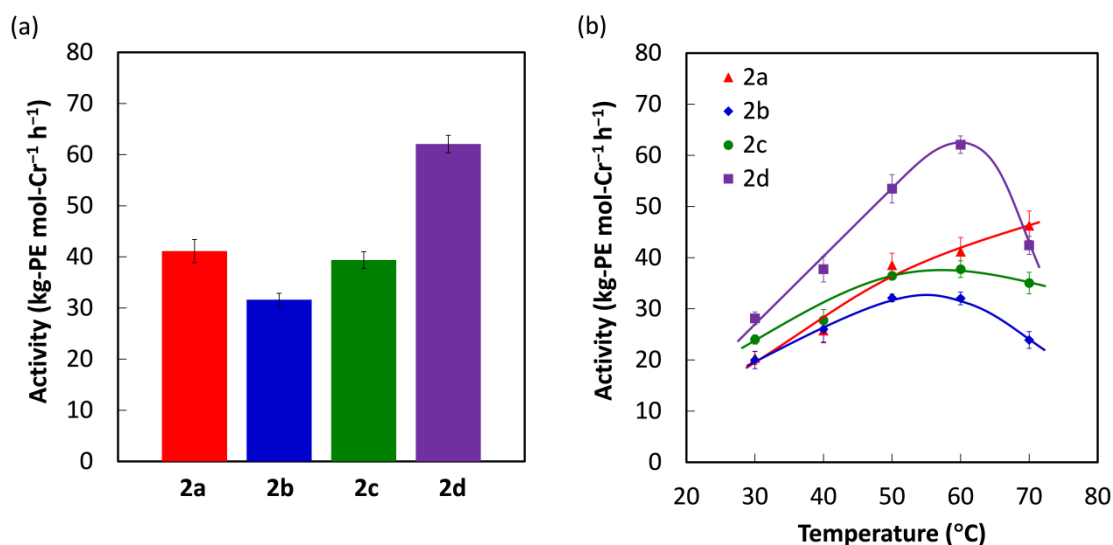


Figure 4 (a) Ethylene polymerization activity of **2a–2d** at 60 °C, (b) temperature dependence of the activity.

This idea was investigated by additional ethylene polymerization at 50 °C using **2a** in the presence of PPh₃ (1, 2, 5, 25, 100 equiv.) which was externally added (**Figure 5**). The addition of free PPh₃ never improved the activity of **2a**, and the obtained activity was much lower than that of **2d**. It was clear that free PPh₃ does not strongly interact with the chromium center and/or the activator so that it does not compete with ethylene coordination and/or activation. This result indicated that the positive consequence of the phosphino group on the activity is easily overcome by the entropic loss, so that it cannot be exploited without the fixation near the chromium center. In other words, the integration of functional groups through the hydroxyl groups of POSS (or silica) can tune the catalytic performance of chromium species in a way completely different from the addition of the functional groups as free molecules.

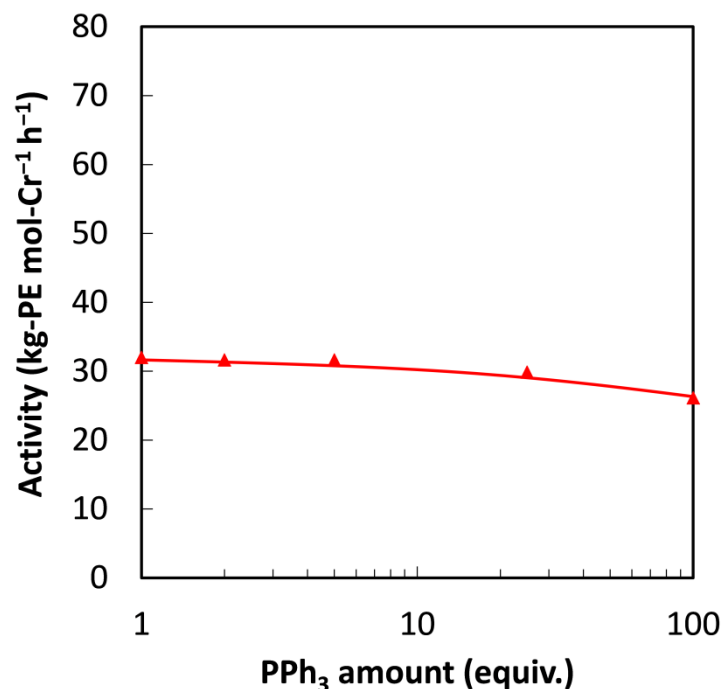


Figure 5 The effect of the addition of free PPh₃ molecules to **2a** at 50 °C.

The MWDs of PE produced at 50 °C using **2a–2d** are shown in **Figure 6a**. The catalysts **2a** and **2b** afforded PE with a very high molecular weight ($M_w = 1.8, 3.3 \times 10^6$). In spite of slight tailing on the low molecular weight side, their MWDs were much narrower than those of PE produced using typical Phillips catalysts. This must be a consequence of the uniform coordination environment around the chromium center, which was brought by the utilization of POSS. When a functional group having a lone pair was introduced at the ortho position of the aryl group, the catalysts (**2c** and **2d**) provided PE with a bimodal character. It is interesting to find that the MWD of PE was quite sensitive to the coordination environment of the chromium center using POSS-supported catalysts, and that specific functional groups could provide MWDs similarly broad to those obtained by using Phillips catalysts. The temperature

dependence of MWDs was investigated for **2b** and **2d** (Figure 6b and c). The MWD of PE was basically insensitive to the temperature for **2b**, even though the tailing was gradually enhanced at higher temperature. On the contrary, the MWD of PE was very sensitive to the temperature for **2d**: the fraction of the low molecular weight peak obviously increased at a higher temperature.

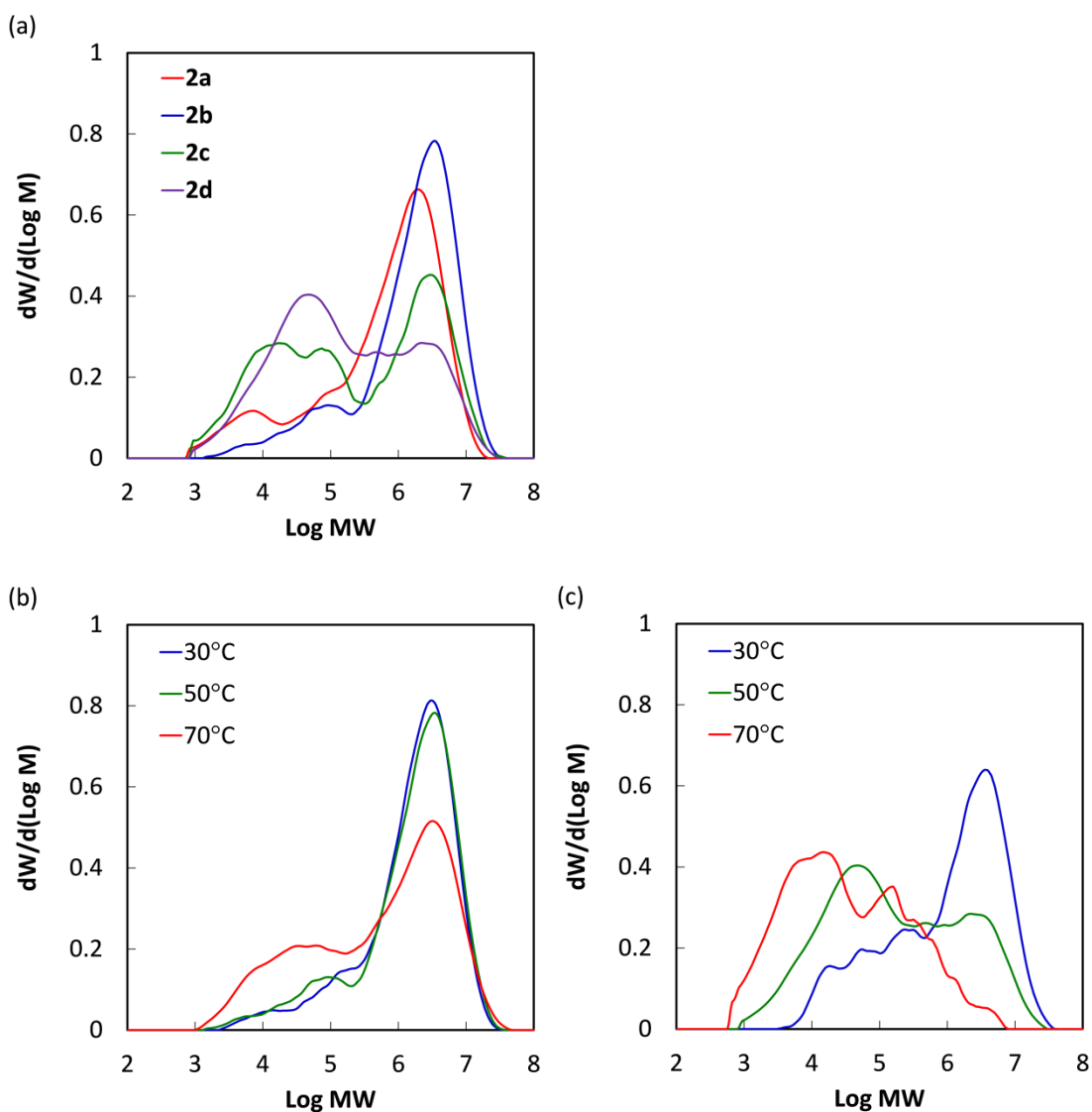


Figure 6 (a) Molecular weight distributions of the produced PE using **2a–2d** at 50 °C, and (b, c) their temperature dependence for **2b** and **2d**.

The primary structures of PE produced using **2b** and **2d** were characterized by ^1H and $^{13}\text{C}\{^1\text{H}\}$ NMR. The results are summarized in **Table 1**. In general, Phillips catalysts provide PE with short and long chain branches. In the case of POSS-supported catalysts, only methyl branches were detected irrespective of the POSS modification and the polymerization temperature. McDaniel *et al.* reported that long chain branching necessitates the spatial proximity of two active sites, respectively responsible for macromonomer formation and reinsertion.¹⁻³ It was reasonable that the chromium species isolatedly supported on POSS was unable to produce long chain branches. The methyl branches were plausibly formed by either the isomerization or reinsertion of in situ generated propylene.^{1-3,38}

Table 1 Primary structures of the produced PE^a

Entry	Cat.	Temp. (°C)	M_n^b ($\times 10^{-3}$)	M_w/M_n	Methyl branch ^c /1000C	Saturated end ^c /1000C	Vinyl end ^d /1000C	Chain transfer to alkylaluminum ^e (%)
1	2b	30	175	17	ND	<0.2	0.14	<18
2	2b	50	130	25	ND	0.3	0.20	20
3	2b	70	38	68	0.3	1.1	0.33	54
4	2d	30	120	25	ND	0.5	0.16	52
5	2d	50	23	55	0.2	1.2	0.36	54
6	2c	50	18	98	<0.2	1.0	0.26	59

^aTNOA at 25 equiv. was employed as an activator. ^bDetermined by GPC. ^cDetermined by $^{13}\text{C}\{^1\text{H}\}$ NMR. ^dDetermined by ^1H NMR. ^ePolymer chains can be terminated either by saturated end groups when transferred to alkylaluminum or by unsaturated end groups when transferred to the monomer. The former fraction was derived by $(A - B)/(A + B)$, where A and B are the amounts of saturated and unsaturated end groups, respectively.

In the case of ethylene polymerization using Phillips catalysts, the predominant mechanism of chain transfer occurs to the monomer,^{39,40} providing vinyl end groups. When an alkylaluminum activator is employed, the chain transfer to alkylaluminum is feasible,⁴¹ which results in the formation of saturated end groups. Considering that chain heads are always saturated groups, the amount of the saturated end groups is necessarily greater than that of the unsaturated end groups: the excess amount of the saturated end groups corresponds to the occurrence of chain transfer to alkylaluminum. In **Table 1**, the sum of the end groups had an anti-proportional correlation with the number-averaged molecular weight (M_n) of PE, while the type of end group, i.e. the chain transfer mechanism, largely depended on the POSS modification. For **2b**, if not the polymerization temperature was increased to 70 °C, the majority of chain transfer occurred to the monomer, producing a high molecular weight of PE with a narrow distribution. Whereas for **2d**, the chain transfer to alkylaluminum occupied 50–60% of the whole chain transfer irrespective of the polymerization temperature. A similar result was obtained for **2c** bearing a methoxy group at the aryl *ortho* position. These results were likely consistent with our consideration that a lone pair of the diphenylphosphino or methoxy group attracts alkylaluminum near the chromium center.

Extension to SiO₂-supported chromium catalysts The results obtained for POSS-supported chromium catalysts were extended to SiO₂-supported catalysts, in which three kinds of functionalized SiO₂ were prepared by modifying a part of surface hydroxyl groups using ClSiMe₂C₆H₅, ClSiMe₂C₆H₄(OMe-2) or ClSiMe₂C₆H₄(PPh₂-2) and the ethylene polymerization performances of the resultant catalysts (termed SiO₂-**b**, SiO₂-**c** and SiO₂-**d** analogous to **2b**, **2c** and **2d**) were evaluated. The results are summarized in **Figure 7**. In a quantitative sense, the activities of the SiO₂-supported

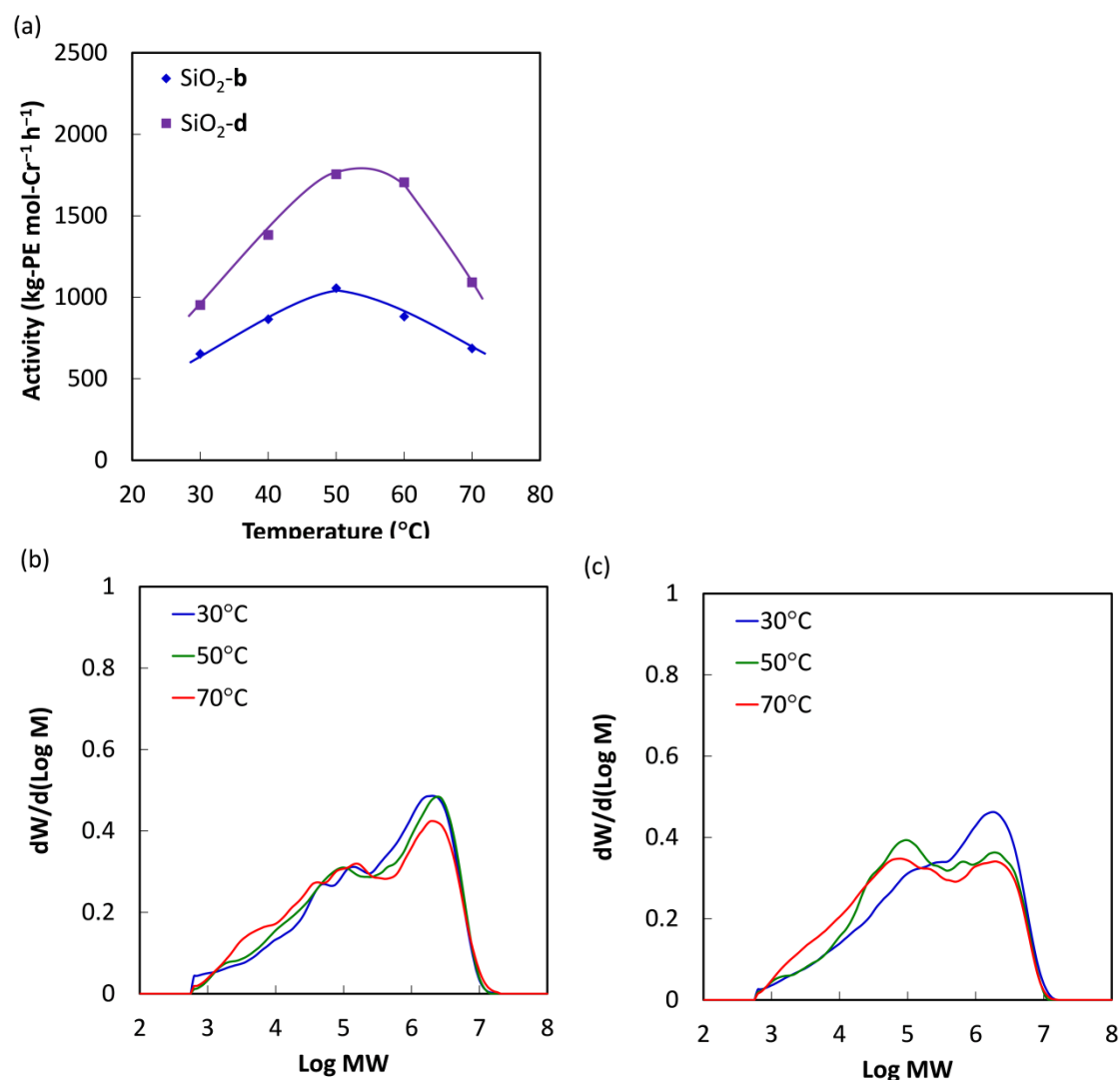


Figure 7 (a) Ethylene polymerization activity of SiO₂-supported chromium catalysts, and (b) molecular weight distributions of the produced PE for SiO₂-**b** and SiO₂-**d**.

catalysts were much higher than those of the corresponding POSS-supported catalysts, plausibly because of the formation of 6-membered chromasiloxane species on SiO₂ surfaces.²⁰ In contrast, qualitative results of the functionalization were similar between the SiO₂- and POSS-supported catalysts: the activity of the SiO₂-**d** catalyst bearing the diphenylphosphino group was about 2 times higher than that of the SiO₂-**b** catalyst, and the SiO₂-**d** catalyst reduced its high activity at 70 °C. Furthermore, the MWD of PE obtained using the SiO₂-**d** catalyst exhibited a clearer bimodal character, which was

sensitive to the polymerization temperature, all of these results were qualitatively similar to those obtained for **2d**. This fact suggested that the behavior of POSS-supported catalysts more or less resembles that of Phillips catalysts, and as evidenced here, a structure–performance relationship obtained for POSS-supported catalysts is applicable for the design of active sites in Phillips catalysts at least when an alkylaluminum activator is employed.^{1,2,42,43}

2.4 Conclusions

In order to minimize the heterogeneity of solid support surfaces and the resultant complication, I employed polyhedral oligomeric silsesquioxanes (POSS) to synthesize Phillips-type molecular catalysts for ethylene polymerization. Through the introduction of different functional groups to POSS, a variety of POSS-supported chromium catalysts with different active-site environments were obtained. Their ethylene polymerization performances indicated the significance of the active-site environment on the performance of the catalysts. In particular, the introduction of a diphenylphosphino group in the vicinity of the active site markedly enhanced the polymerization activity of the catalyst and the obtained polyethylene (PE) exhibited a clear bimodal character. It was considered that the lone pair of the diphenylphosphino group attracted alkylaluminum near the chromium center, which was not applicable for free triphenylphosphine molecules added in the polymerization. The results obtained using the POSS-supported catalysts were directly transferrable to SiO₂-supported catalysts, in which the introduction of diphenylphosphino groups on the SiO₂ surfaces delivered similar results with a dramatically enhanced activity. To this end, I have successfully shown a novel platform to study and improve the Phillips catalyst, which is based on the design of POSS-supported chromium catalysts.

2.5 References

- [1] M. P. McDaniel, *Adv. Catal.*, 1985, **33**, 47.
- [2] M. P. McDaniel, *Adv. Catal.*, 2010, **53**, 123.
- [3] M. P. McDaniel, D. C. Rohlfiing, and E. A. Benham, *Polym. React. Eng.*, 2003, **11**, 101.
- [4] E. Groppo, C. Lamberti, S. Bordiga, G. Spoto and A. Zecchina, *Chem. Rev.*, 2005, **105**, 115.
- [5] E. Groppo, K. Seenivasan and C. Barzan, *Catal. Sci. Technol.*, 2013, **3**, 858.
- [6] E. Groppo, C. Lamberti, G. Spoto, S. Bordiga, G. Magnacca and A. Zecchina, *J. Catal.*, 2005, **236**, 233.
- [7] E. Groppo, C. Lamberti, S. Bordiga, G. Spoto and A. Zecchina, *J. Catal.*, 2006, **240**, 172.
- [8] E. Groppo, A. Damin, C. O. Arean and A. Zecchina, *Chem. Eur. J.*, 2011, **17**, 11110.
- [9] J. Amor Nait Ajjou and S. L. Scott, *Organometallics*, 1997, **16**, 86.
- [10] J. Amor Nait Ajjou, S. L. Scott and V. Paquet, *J. Am. Chem. Soc.*, 1998, **120**, 415.
- [11] J. Amor Nait Ajjou, G. L. Rice and S. L. Scott, *J. Am. Chem. Soc.*, 1998, **120**, 13436.
- [12] J. Amor Nait Ajjou and S. L. Scott, *J. Am. Chem. Soc.*, 2000, **122**, 8968.
- [13] H. Ikeda, T. Monoi and Y. Sasaki, *J. Polym. Sci., Part A: Polym. Chem.*, 2003, **41**, 413.
- [14] K. Tonosaki, T. Taniike and M. Terano, *Macromol. React. Eng.*, 2011, **5**, 332.
- [15] M. P. Conley, M. F. Delley, G. Siddiqi, G. Lapadula, S. Norsic, V. Monteil, O. V. Safonova and C. Copéret, *Angew. Chem. Int. Ed.*, 2014, **53**, 1872.
- [16] M. F. Delley, M. P. Conley and C. Copéret, *Catal. Lett.*, 2014, **144**, 805.

- [17] M. F. Delley, F. Núñez-Zarur, M. P. Conley, A. Comas-Vives, G. Siddiqi, S. Norsic, V. Monteil, O. V. Safonova and C. Copéret, *Proc. Natl. Acad. Sci. U. S. A.*, 2014, **111**, 11624.
- [18] M. F. Delley, F. Nuñez-Zarura, M. P. Conley, A. Comas-Vives, G. Siddiqi, S. Norsic, V. Monteil, O. V. Safonova and C. Copéret, *Proc. Natl. Acad. Sci. U. S. A.*, 2015, **112**, E4162.
- [19] M. P. Conley, M. F. Delley, F. Núñez-Zarur, A. Comas-Vives and C. Copéret, *Inorg. Chem.*, 2015, **54**, 5065.
- [20] C. A. Demmelmaier, R. E. Whitea, J. A. van Bokhoven and S. L. Scott, *J. Catal.*, 2009, **262**, 44.
- [21] K. Tonosaki, T. Taniike and M. Terano, *J. Mol. Catal. A: Chem.*, 2011, **340**, 33.
- [22] P. J. DesLauriers and M. P. McDaniel, *J. Polym. Sci., Part A: Polym. Chem.*, 2007, **45**, 3135.
- [23] P. J. DesLauriers, M. P. McDaniel, D. C. Rohlfiing, R. K. Krishnaswamy, S. J. Secora, E. A. Benham, P. L. Maeger, A. R. Wolfe, A. M. Sukhadia and B. B. Beaulieu, *Polym. Eng. Sci.*, 2005, **45**, 1203.
- [24] P. J. DesLauriers, C. Tso, Y. Yu, D. L. Rohlfiing and M. P. McDaniel, *Appl. Catal. A: Gen.*, 2010, **388**, 102.
- [25] M. P. McDaniel, M. B. Welch and M. J. Dreiling, *J. Catal.*, 1983, **82**, 118.
- [26] L. M. Baker and W. L. Carrick, *J. Org. Chem.*, 1970, **35**, 774.
- [27] M. Motevalli, M. Sanganee, P. D. Savage, S. Shah and A. C. Sullivan, *J. Chem. Soc., Chem. Commun.*, 1993, 1132.
- [28] H. C. L. Abbenhuis, M. L. W. Vorstenbosch, R. A. van Santen, W. J. J. Smeets and A. L. Spek, *Inorg. Chem.*, 1997, **36**, 6431.

- [29] P. Qiu, R. Cheng, B. Liu, B. Tumanskii, R. J. Batrice, M. Botoshansky and M. S. Eisen, *Organometallics*, 2011, **30**, 2144.
- [30] R. Duchateau, *Chem. Rev.*, 2002, **102**, 3525.
- [31] E. A. Quadrelli and J.-M. Basset, *Coord. Chem. Rev.*, 2010, **254**, 707.
- [32] F. J. Feher and R. L. Blanski, *J. Chem. Soc., Chem. Commun.*, 1990, 1614.
- [33] M. Nabika, H. Katayama, T. Watanabe, H. Kawamura-Kuribayashi, K. Yanagi and A. Imai, *Organometallics*, 2009, **28**, 3785.
- [34] T. G. Wetzel and P. W. Roesky, *Organometallics*, 1998, **17**, 4009.
- [35] D. Quintard, M. Keller and B. Breit, *Synthesis*, 2004, **6**, 905.
- [36] T. Sanji, K. Naito, T. Kashiwabara and M. Tanaka, *Heteroat. Chem.*, 2012, **23**, 520.
- [37] H. Ikeda, T. Monoi, K. Ogata and H. Yasuda, *Macromol. Chem. Phys.*, 2001, **202**, 1806.
- [38] M. P. McDaniel, *Ind. Eng. Chem. Res.*, 1988, **27**, 1559.
- [39] R. Blom, A. Follestad and O. Noel, *J. Mol. Catal.*, 1994, **91**, 237.
- [40] T. Saito, M. Motegi, H. Furuhashi and S. Ueki, *Stud. Surf. Sci. Catal.*, 1999, **121**, 477.
- [41] W. Xia, B. Liu, Y. Fang, K. Hasebe, M. Terano, *J. Mol. Catal. A: Chem*, 2006, **256**, 301.
- [42] K. Hasebe and T. Nozaki, JP 2001294612.
- [43] K. J. Cann, M. Zhang, J. F. Cevallos-Candau, J. Moorhouse, M. G. Goode, D. P. Zilker and M. Apecetche, US 20110060111.

Appendix for Chapter 2

Contents

- A. NMR spectra of modified POSS (**1a-1d**)
- B. NMR spectra of POSS-supported chromium catalysts (**2a-2d**)
- C. UV/vis spectra of POSS- and SiO₂-supported chromium catalysts (**2a-2d**, SiO₂-**b-d**)
- D. Assignment and analytical method in NMR for polyethylene

A. NMR spectra of modified POSS (**1a-1d**)

(*t*-Bu)₇Si₇O₉(OH)₂(OSiMe₃) (**1a**)

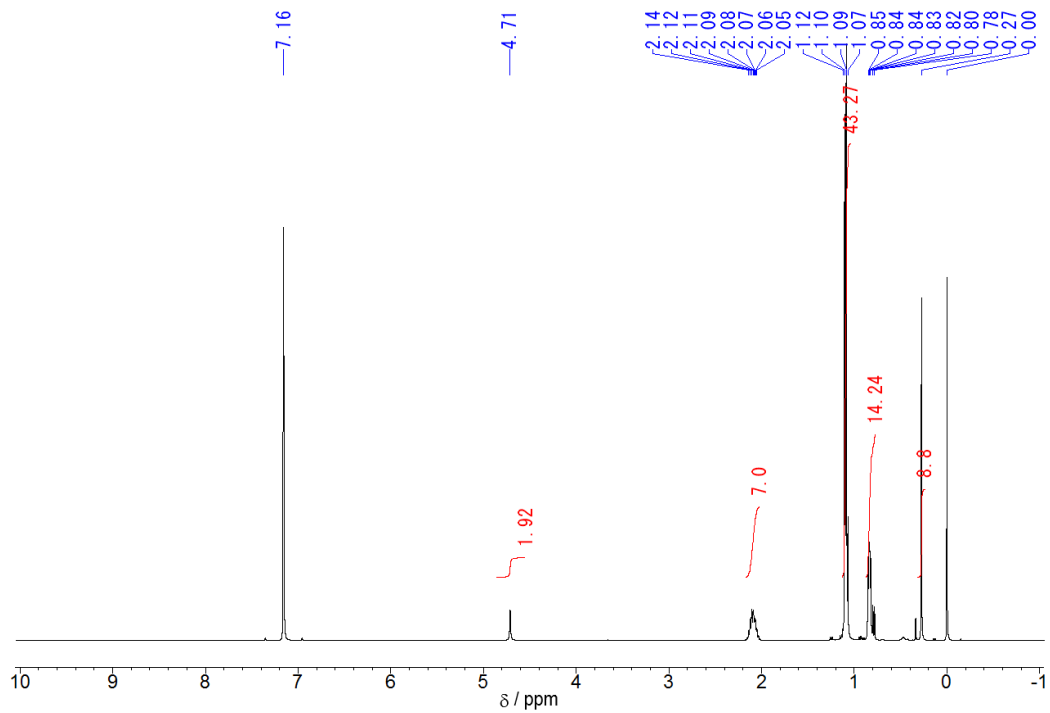


Figure A1 ¹H NMR spectrum of **1a** in benzene-*d*₆ at r.t. (400 MHz).

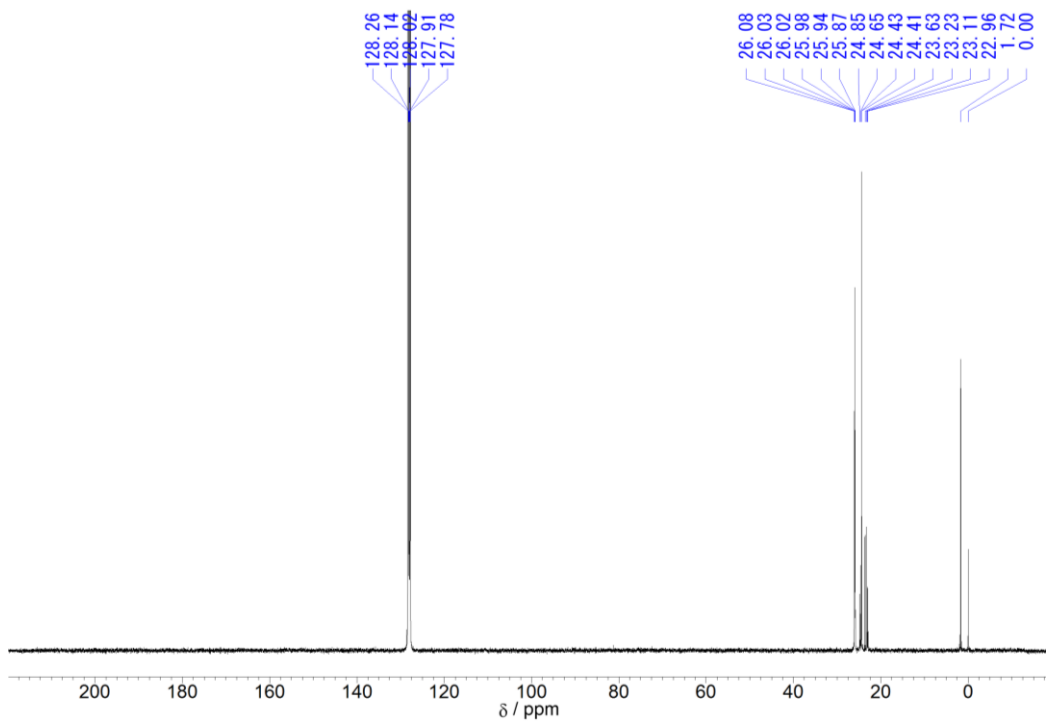


Figure A2 ¹³C{¹H} NMR spectrum of **1a** in benzene-*d*₆ at r.t. (100 MHz).

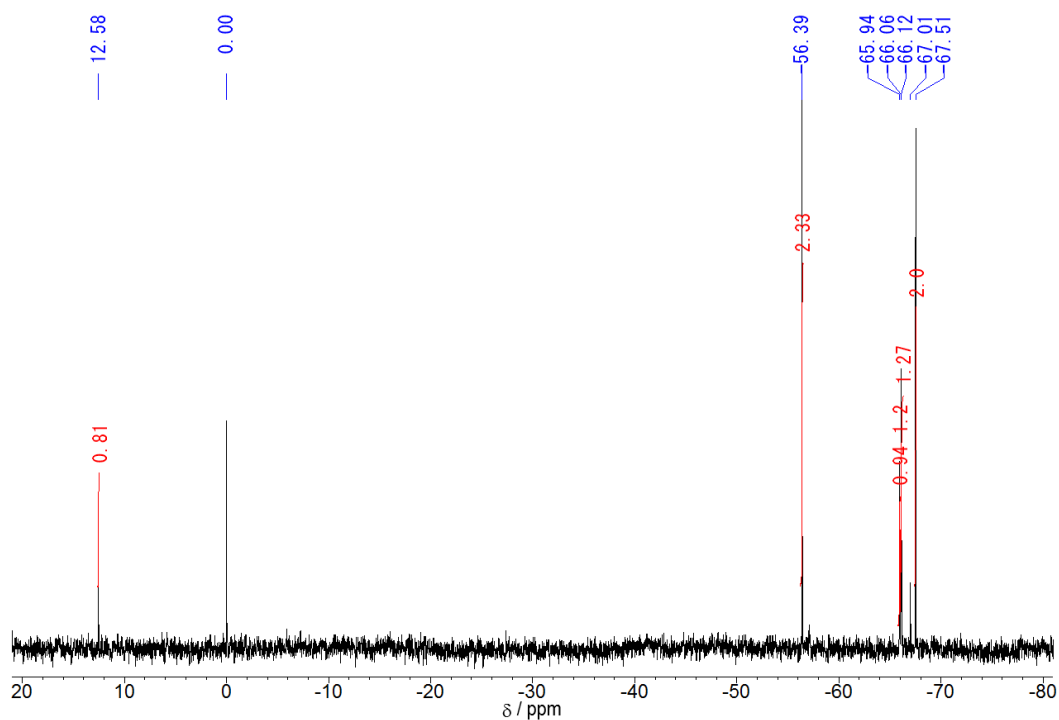


Figure A3 $^{29}\text{Si}\{^1\text{H}\}$ NMR spectrum of **1a** in benzene- d_6 at r.t. (79 MHz).

$(^t\text{Bu})_7\text{Si}_7\text{O}_9(\text{OH})_2(\text{OSiMe}_2\text{Ph})$ (**1b**)

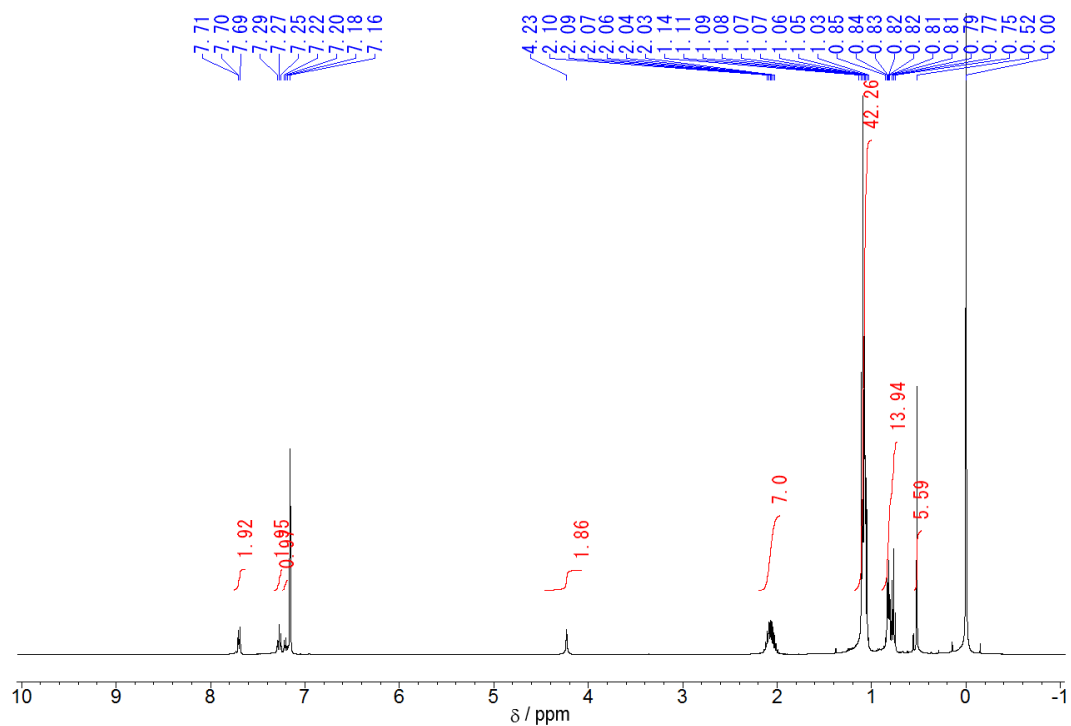


Figure A4 ^1H NMR spectrum of **1b** in benzene- d_6 at r.t. (400 MHz).

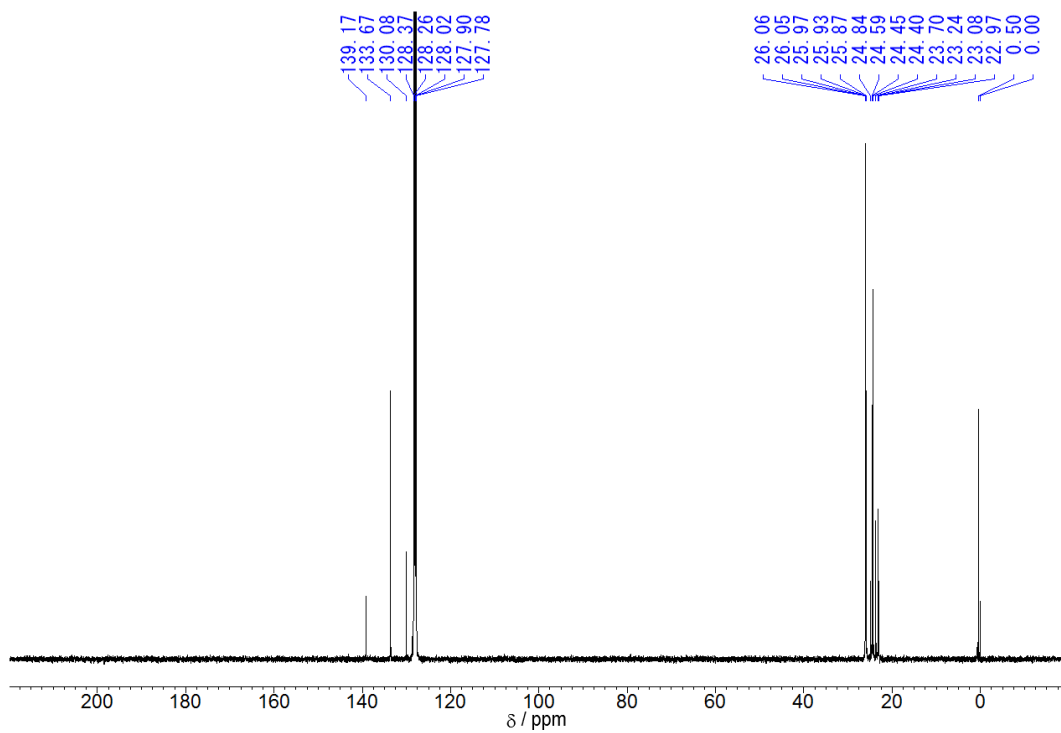


Figure A5 $^{13}\text{C}\{^1\text{H}\}$ NMR spectrum of **1b** in benzene- d_6 at r.t. (100 MHz).

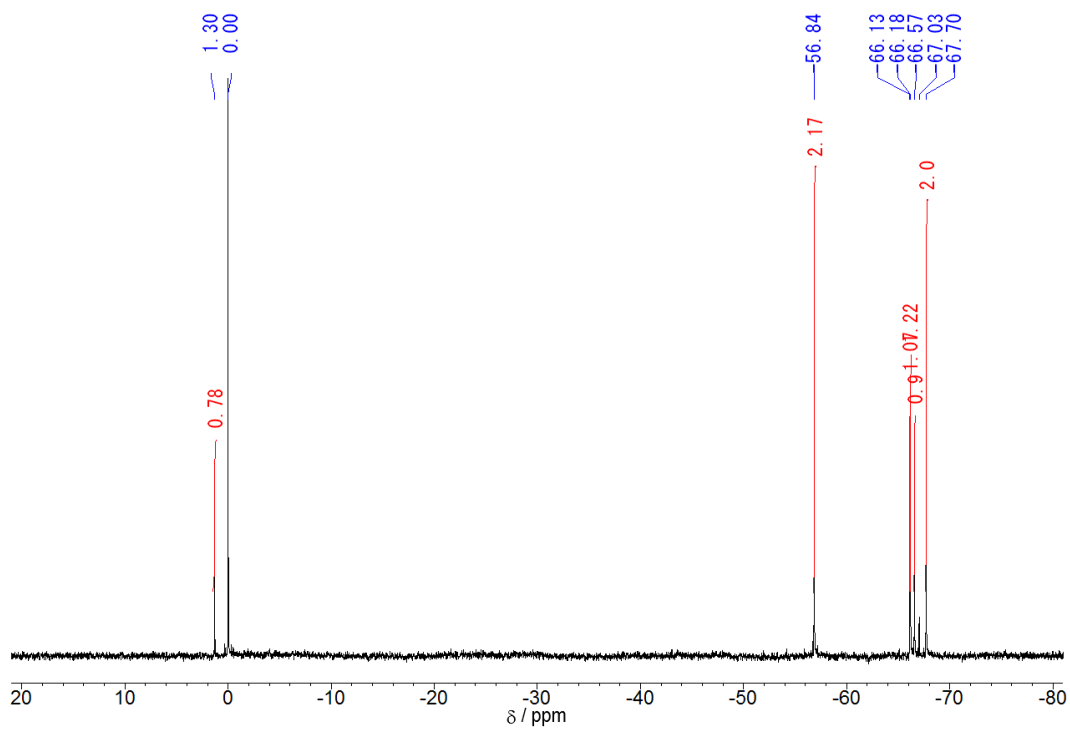


Figure A6 $^{29}\text{Si}\{^1\text{H}\}$ NMR spectrum of **1b** in benzene- d_6 at r.t. (79 MHz).

(^tBu)₇Si₇O₉(OH)₂[OSiMe₂C₆H₄(OMe-2)] (**1c**)

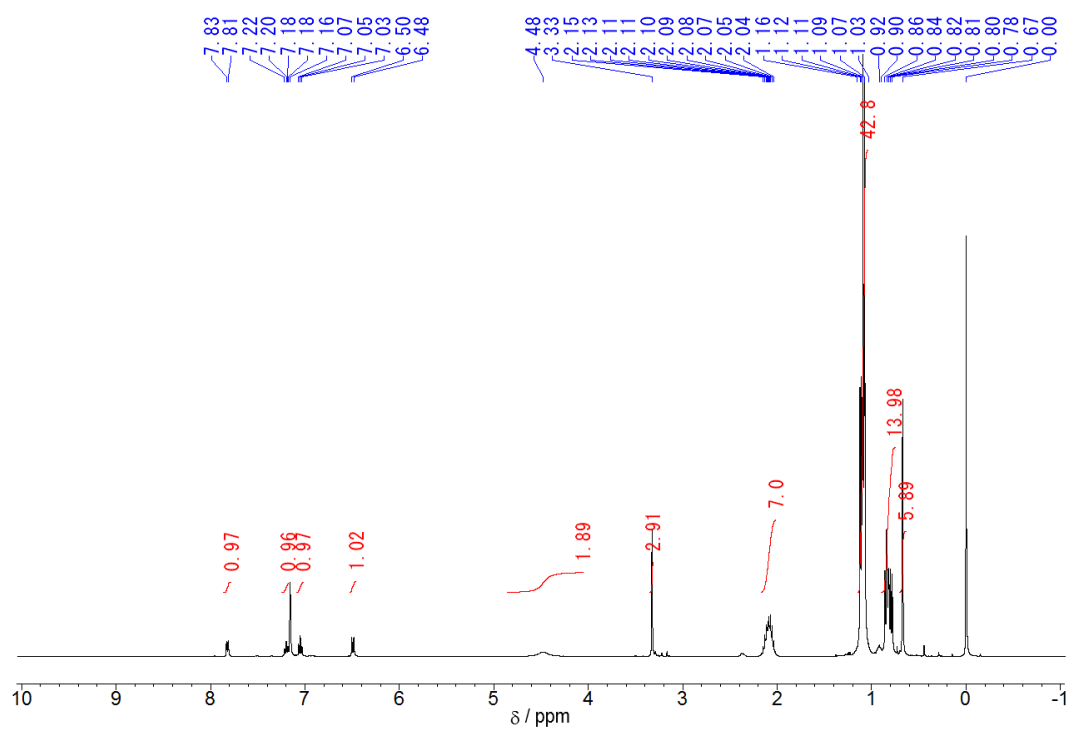


Figure A7 ¹H NMR spectrum of **1c** in benzene-*d*₆ at r.t. (400 MHz).

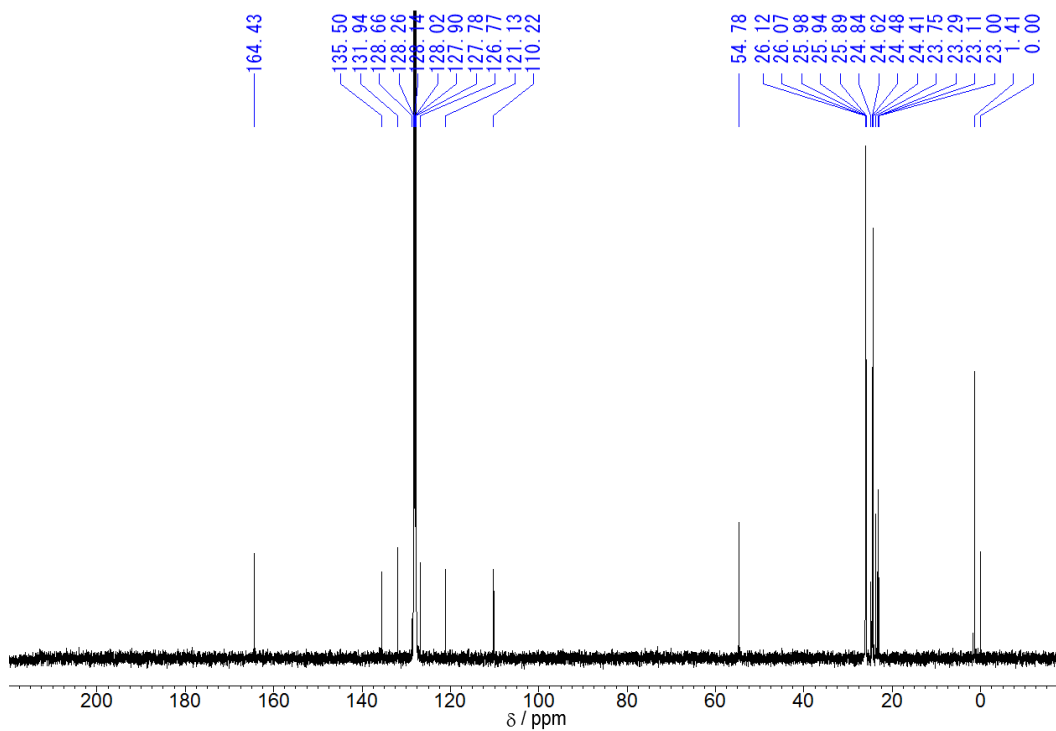


Figure A8 ¹³C{¹H} NMR spectrum of **1c** in benzene-*d*₆ at r.t. (100 MHz).

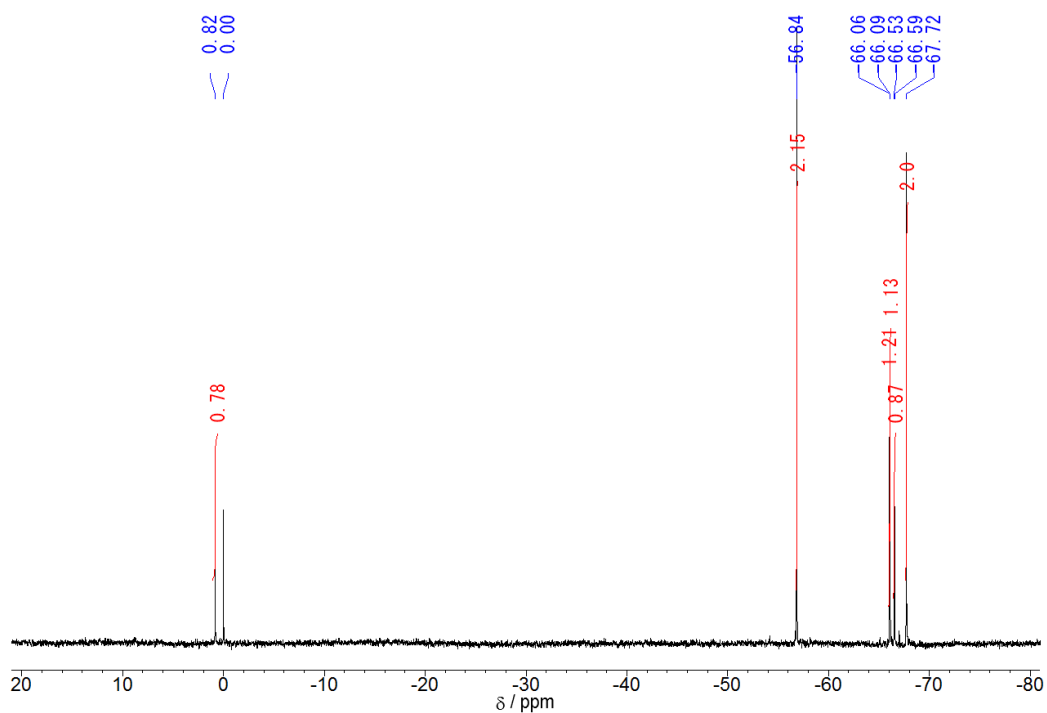


Figure A9 $^{29}\text{Si}\{^1\text{H}\}$ NMR spectrum of **1c** in benzene- d_6 at r.t. (79 MHz).

$(^t\text{Bu})_7\text{Si}_7\text{O}_9(\text{OH})_2[\text{OSiMe}_2\text{C}_6\text{H}_4(\text{PPh}_2-2)]$ (**1d**)

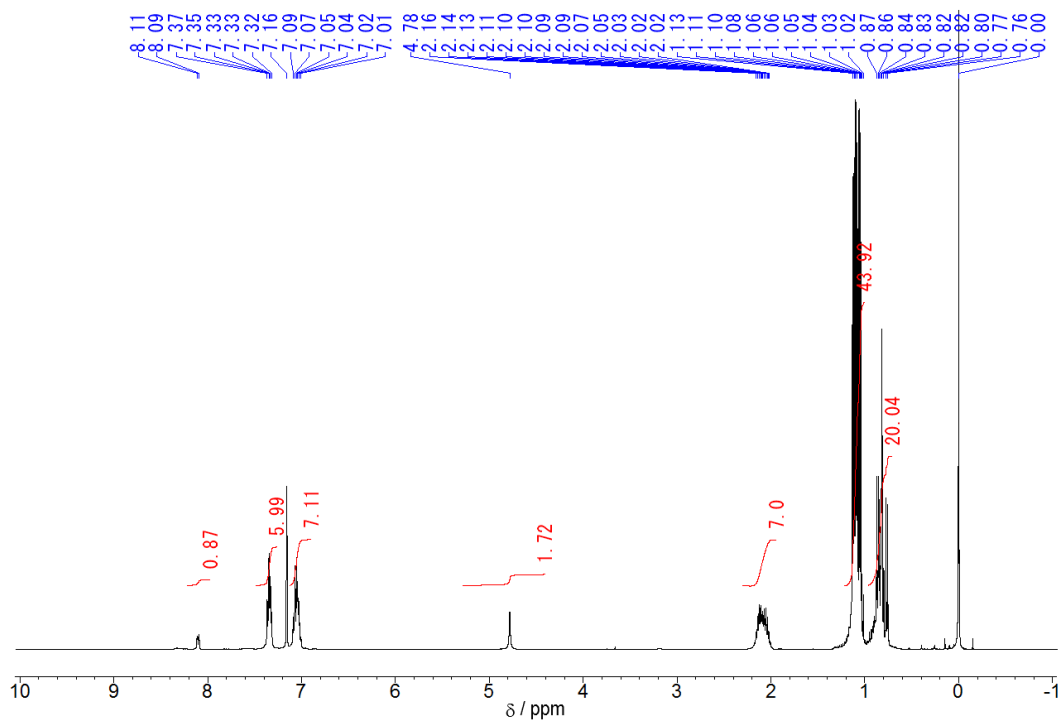


Figure A10 ^1H NMR spectrum of **1d** in benzene- d_6 at r.t. (400 MHz).

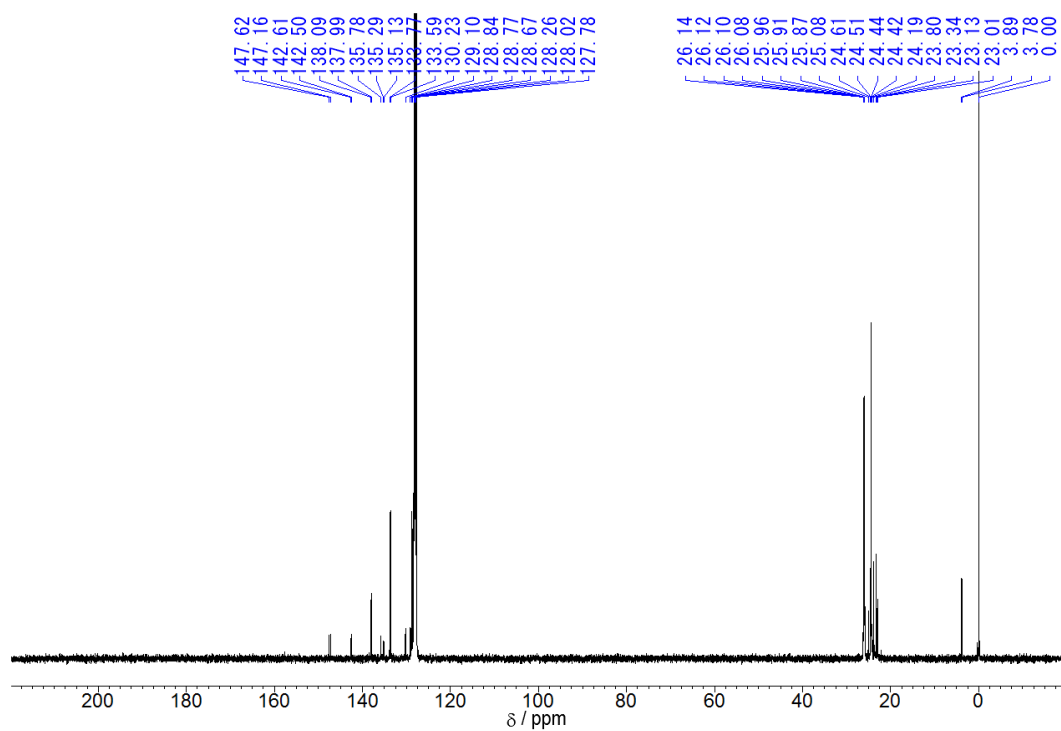


Figure A11 $^{13}\text{C}\{^1\text{H}\}$ NMR spectrum of **1d** in benzene- d_6 at r.t. (100 MHz).

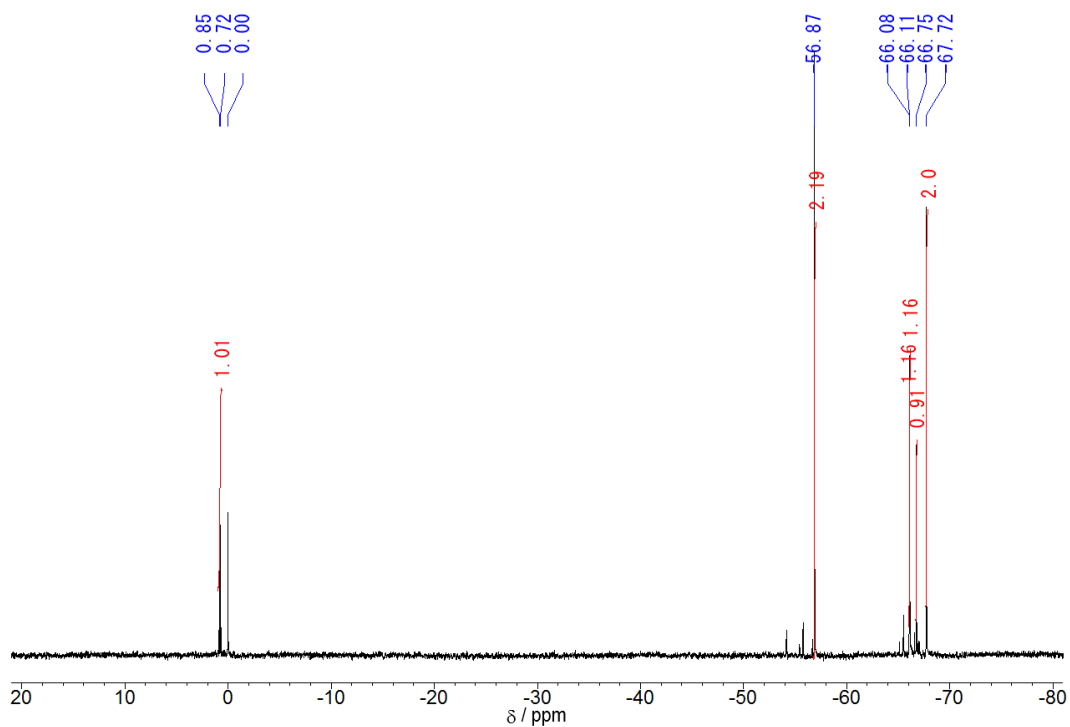


Figure A12 $^{29}\text{Si}\{^1\text{H}\}$ NMR spectrum of **1d** in benzene- d_6 at r.t. (79 MHz).

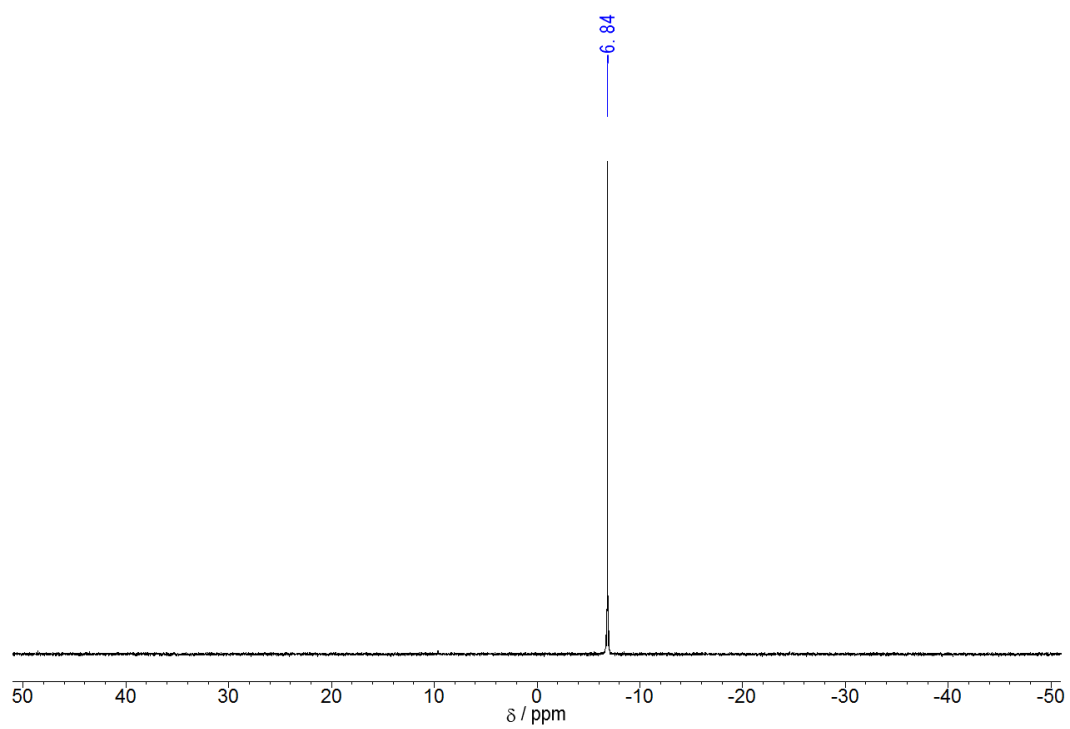


Figure A13 $^{31}\text{P}\{^1\text{H}\}$ NMR spectrum of **1d** in benzene- d_6 at r.t. (162 MHz).

B. NMR spectra of POSS supported chromium catalysts (**2a-2d**)

$[(^i\text{Bu})_7\text{Si}_7\text{O}_{11}(\text{OSiMe}_3)]\text{CrCH}(\text{SiMe}_3)_2$ (**2a**)

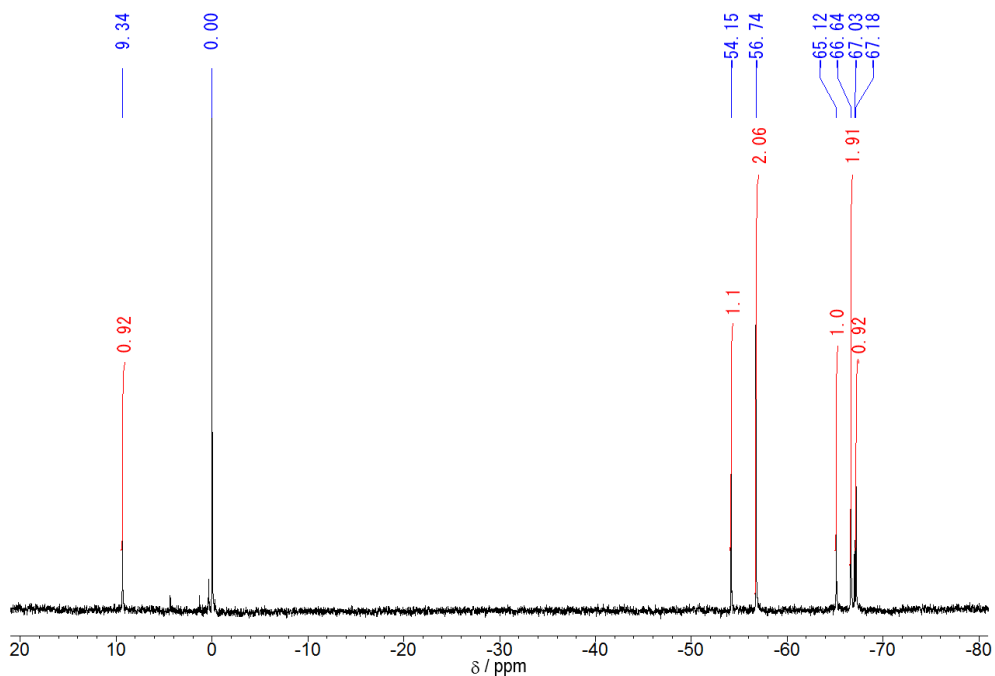


Figure A14 $^{29}\text{Si}\{^1\text{H}\}$ NMR spectrum of **2a** in benzene- d_6 at r.t. (79 MHz).

$(^i\text{Bu})_7\text{Si}_7\text{O}_{11}(\text{OSiMe}_2\text{Ph})\text{CrCH}(\text{SiMe}_3)_2$ (**2b**)

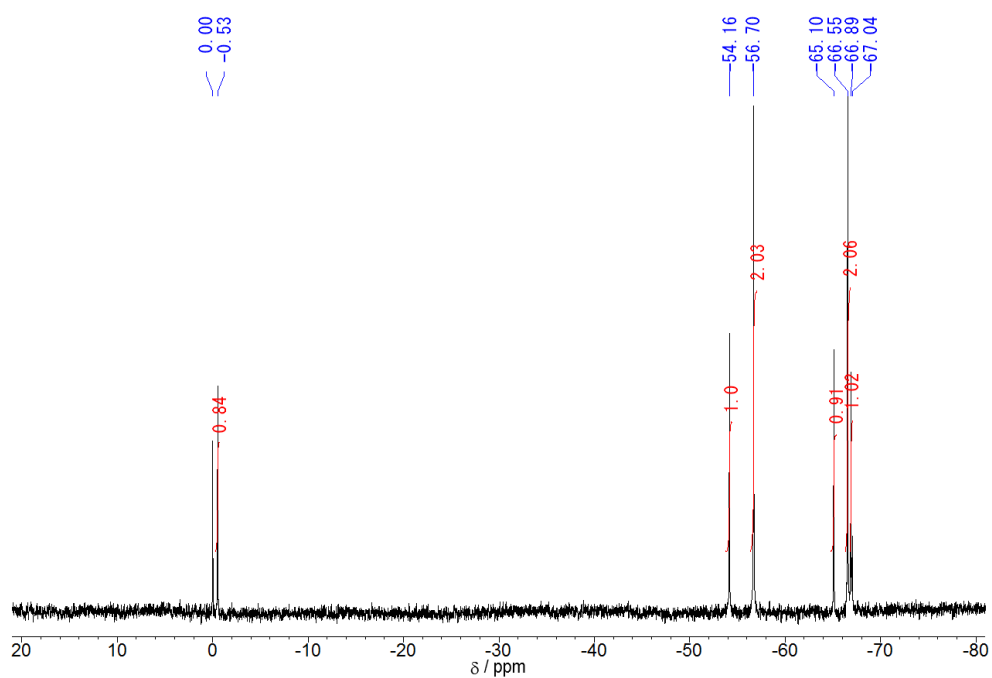


Figure A15 $^{29}\text{Si}\{^1\text{H}\}$ NMR spectrum of **2b** in benzene- d_6 at r.t. (79 MHz).

$\{(\text{iBu})_7\text{Si}_7\text{O}_{11}[\text{OSiMe}_2\text{C}_6\text{H}_4(\text{OMe}-2)]\}\text{CrCH}(\text{SiMe}_3)_2$ (**2c**)

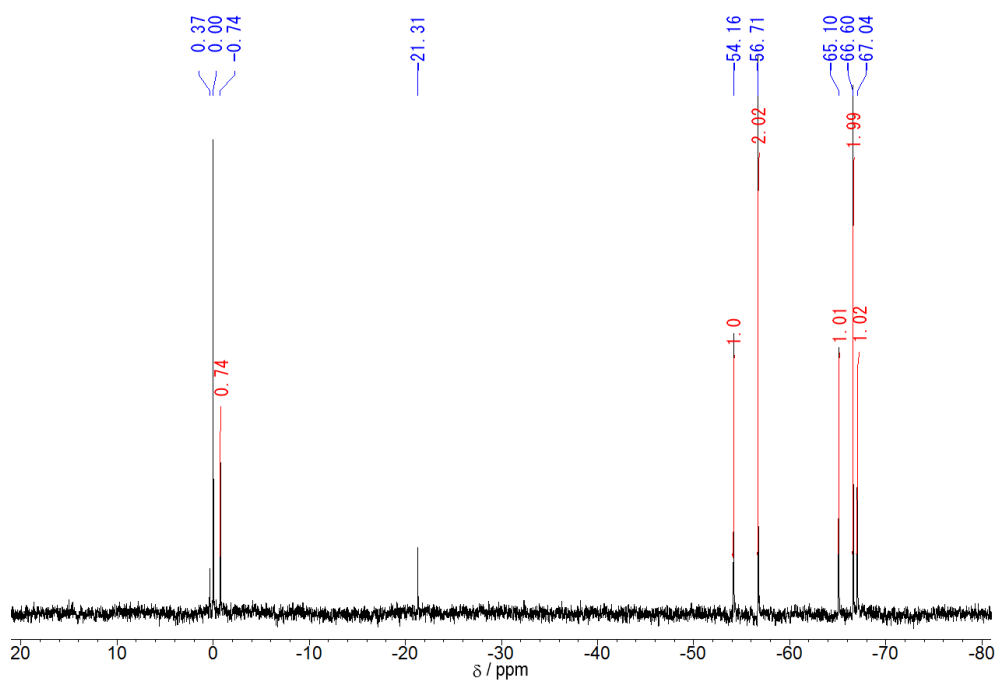


Figure A16 $^{29}\text{Si}\{^1\text{H}\}$ NMR spectrum of **2c** in benzene- d_6 at r.t. (79 MHz).

$\{(\text{iBu})_7\text{Si}_7\text{O}_{11}[\text{OSiMe}_2\text{C}_6\text{H}_4(\text{PPh}_2-2)]\}\text{CrCH}(\text{SiMe}_3)_2$ (**2d**)

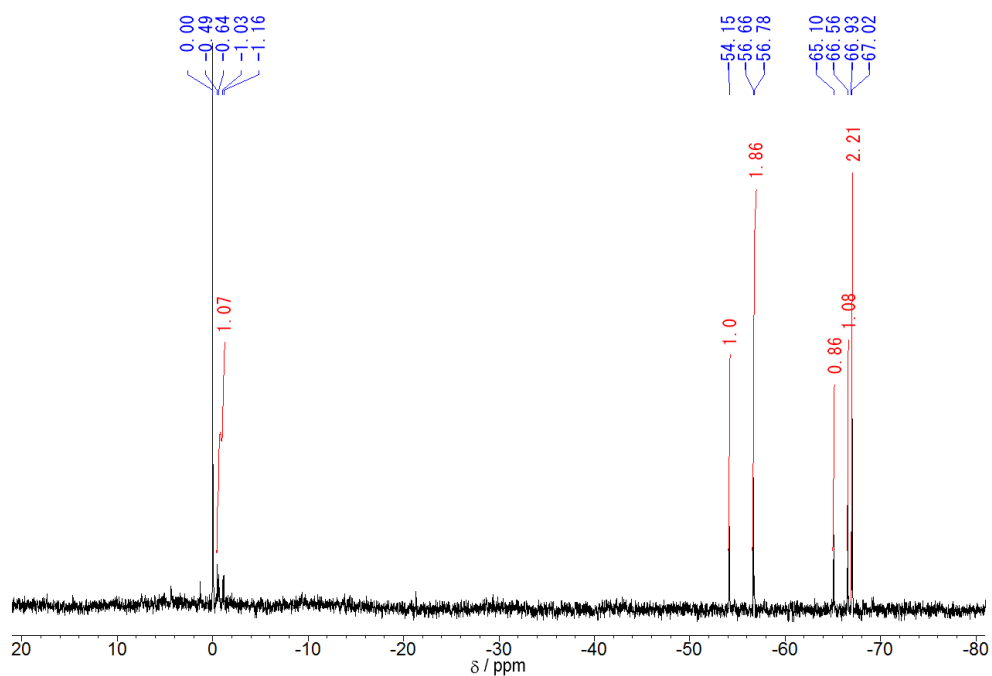


Figure A17 $^{29}\text{Si}\{^1\text{H}\}$ NMR spectrum of **2d** in benzene- d_6 at r.t. (79 MHz).

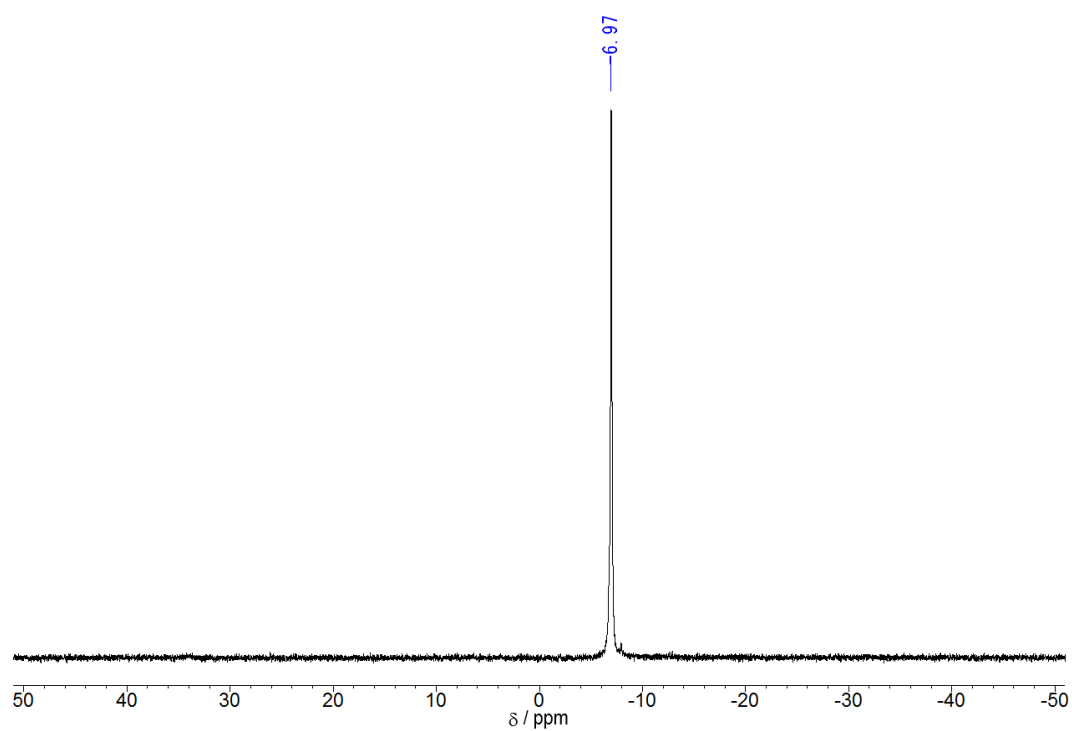


Figure A18 ^{31}P NMR spectrum of **2d** in benzene- d_6 at r.t. (162 MHz).

C. UV/vis spectra measurement

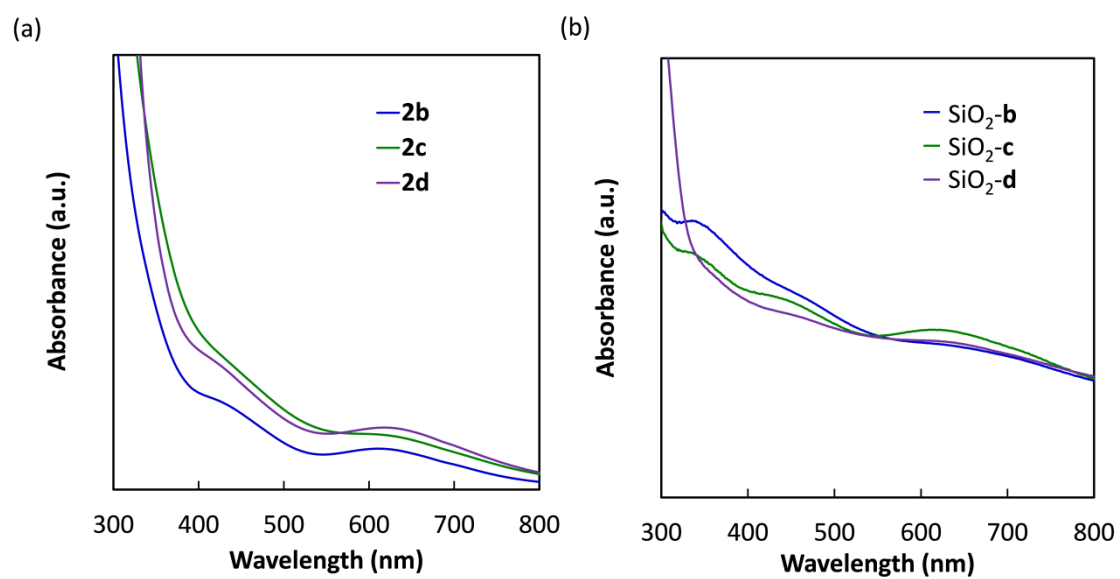


Figure A19 UV/vis (DRS) spectra of a) POSS-supported catalysts (**2a-2d**) and b) SiO₂-supported catalysts (SiO₂-**b-d**).

D. Assignment and analytical method in NMR for polyethylene

Figure S10 reports typical $^{13}\text{C}\{^1\text{H}\}$ and ^1H NMR spectra of the obtained PE (entries 3 and 5 in **Table 1**). The chemical shift was referenced to methyl carbon (1.98 ppm) and methyl proton (0.09 ppm) of hexamethyldisiloxane (HMDS) in $^{13}\text{C}\{^1\text{H}\}$ and ^1H NMR, respectively. The peak assignments have been done based on Refs. [1] and [2]. The fractions of methyl branches and the saturated ends were determined from $^{13}\text{C}\{^1\text{H}\}$ NMR based on the following equations.

$$\text{Eq. (1)} \quad \text{Fraction of methyl branch } (/1000C) = I_{B1}/I_{\text{totalC}} \times 1000$$

$$\text{Eq. (2)} \quad \text{Fraction of saturated end } (/1000C) = I_S/I_{\text{totalC}} \times 1000$$

$$\text{Eq. (3)} \quad I_{B1} = (I_{1B1} + I_{brB1} + I_{\alpha B1})/4$$

$$\text{Eq. (4)} \quad I_S = (I_{1S} + I_{2S} + I_{3S})/3$$

$$\text{Eq. (5)} \quad I_{\text{totalC}} = I_{\text{Main chain}}$$

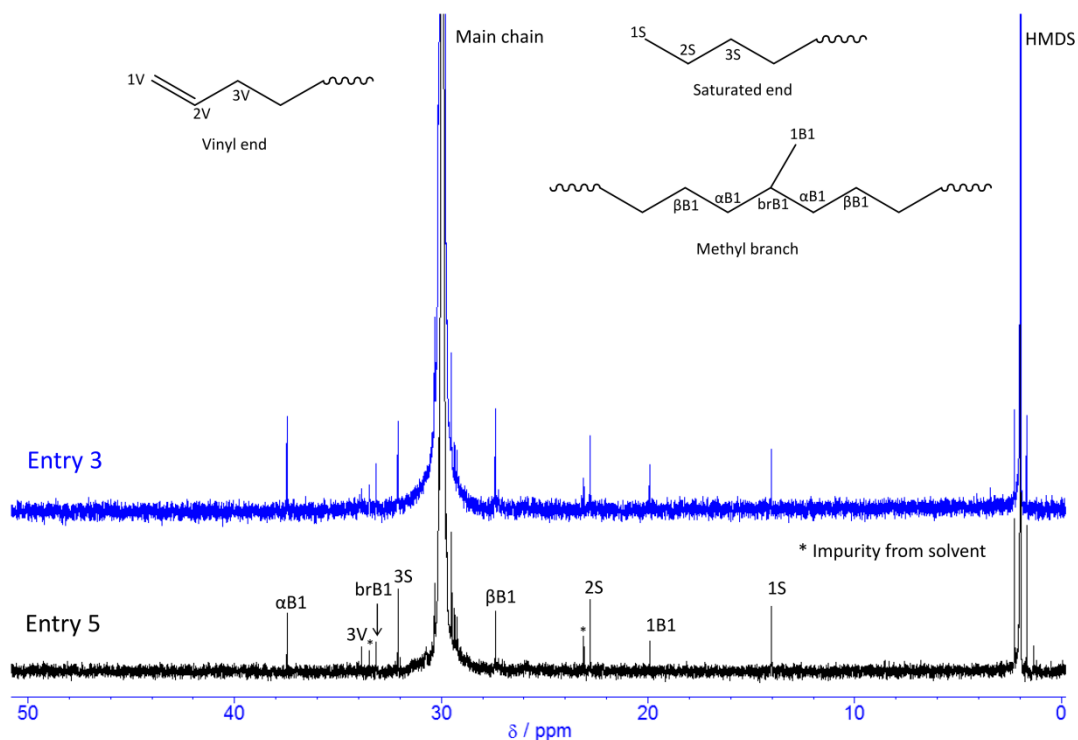


Figure A20 $^{13}\text{C}\{^1\text{H}\}$ NMR spectra of typical PE (100 MHz).

The fraction of the vinyl ends were determined from ^1H NMR based on the following equations.

$$\text{Eq. (6)} \quad \text{Fraction of vinyl end } (/1000C) = I_{\text{Vi}}/I_{\text{total}} \times 1000$$

$$\text{Eq. (7)} \quad I_{\text{Vi}} = (I_{1\text{V}} + I_{2\text{V}})/3$$

$$\text{Eq. (8)} \quad I_{\text{total}} = (I_{\text{Main chain}})/2$$

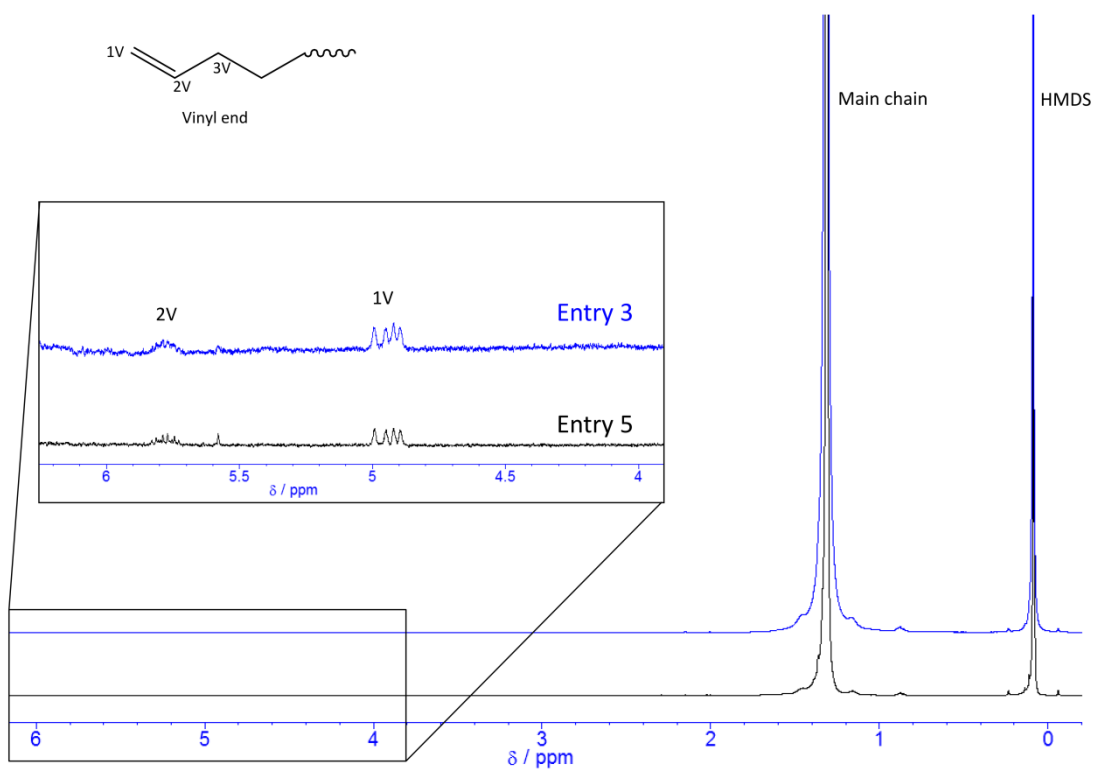


Figure A21 ^1H NMR spectra of typical PE (400 MHz).

References

- [1] B. Qu, X. Qu, Y. Xu, U. Jacobsson, B. Rånby, K. E. Russell and W. E. Baker, *Macromolecules*, 1997, **30**, 1408.
- [2] E. W. Hansen, R. Blom and O. M. Bade, *Polymer*, 1997, **38**, 4295.

Chapter 3

Active Site Nature of a Silsesquioxane-Supported Homogeneous Phillips Catalyst

3.1 Introduction

Phillips catalyst has been employed as ethylene polymerization catalyst in industry, since its discovery over half a century.¹⁻³ However the controlling of molecular weight, molecular weight distribution and copolymerization is insufficient. For example, the representative ethylene polymerization catalyst such as Ziegler-Natta catalyst and metallocene catalyst can control the molecular weight of produced polyethylene (PE) by chain transfer reaction using hydrogen. Due to the Phillips catalyst has low hydrogen response, it was conducted by controlling the calcination and polymerization temperature or addition of inorganic salts (e.g. Al_2O_3 and TiO_2)⁴⁻⁶ but the control in a wide range is not performed. In the copolymerization, α -olefin predominantly introduce to the low molecular weight composition. Thus, it is difficult to influence the mechanical properties. It is necessary to study the relationship between the catalyst structure and the performance to improve the performance of the Phillips catalyst.

The different chemical structure of silica surfaces is the main factor to determine the active site nature due to the catalyst performance largely depends on calcination temperature. Three types of silanol groups (isolated, vicinal, geminal) and siloxane bonds are heterogeneously present on dehydrated silica surface.⁷ It means that the complexity of the chemical environment of active site involved in eliciting of various catalyst performances. The activity site structure during polymerization and the mechanisms have been studied by surface organometallic chemistry studies that an organometallic complex is supported on the silica surface⁸⁻²⁴ and *in-situ* spectroscopic analysis²⁵⁻³⁰. However, the catalyst performance is reflected as the summation of all the active site contained in the sample. Therefore, a model catalyst having a single structure is required to evaluate a relationship between active site structure and the performance.

Polyhedral oligomeric silsesquioxanes (POSS) has a similar chemical structure and properties with silica and high compatibility for organic solvents.^{31,32} Due to it forms bonds with various metal species, the complex is regarded as a model molecular catalyst. $[(c\text{-C}_6\text{H}_{11})\text{Si}_7\text{O}_{11}(\text{OSiMe}_3)]\text{CrO}_2$ reported by Feher *et al.* is known as a sole example for Phillips catalyst.³³ A series of POSS-supported chromium catalysts possessing various functional groups using $(t\text{-Bu})_7\text{Si}_7\text{O}_9(\text{OH})_3$ and investigated their catalytic ethylene polymerization performance in Chapter 2. As the result, it was found that introducing a functional group influenced on catalyst performance. Especially, PPh_2 group improved the activity and change molecular weight distribution of the produced PE in a wide range of 10^3 to 10^6 orders. Thus, it was shown that the relationship between the catalyst structure and the performance can be easily evaluated by using the POSS-supported chromium catalyst having a homogeneous catalyst structure.

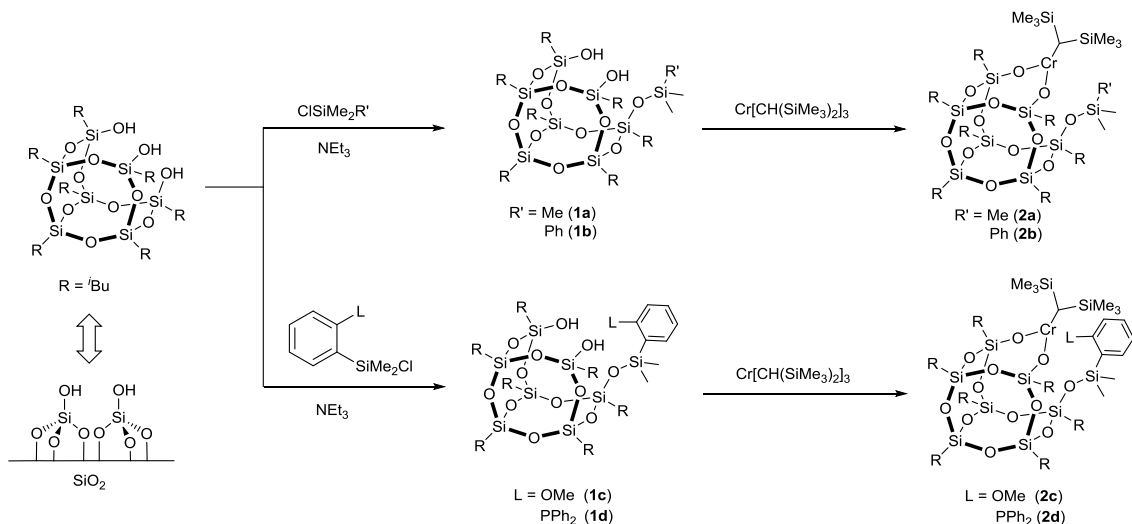
Phillips catalyst has specific properties which show ethylene polymerization activity without using a alkylaluminum. However alkylaluminum is often added to maintain high activity and remove impurities in the industrial process. Although it is known that addition of an excessive amount of alkylaluminum causes undesired reaction such as chain transfer reaction and suppression of activity by cleavage of Si-O-Cr bond, the study of the influence to homogeneous model catalysts is less. Recently, borate-type activator such as $\text{B}(\text{C}_6\text{F}_5)_3$ or $\text{Ph}_3\text{CB}(\text{C}_6\text{F}_5)_4$ is utilized to enhance the activity, however, its effect for chromium molecular catalyst is also not well known. It is unnecessary to consider the reaction between the activator and silica by utilizing the homogeneous model catalyst, so its effect can be clearly evaluated. In this chapter, influences of activator on catalyst performance were investigated using POSS-supported chromium molecular catalyst which can clearly evaluate the properties of active sites.

3.2 Experimental

Materials

All experiments were carried out under a nitrogen atmosphere using Schlenk techniques. Toluene and 1-octene were dried over molecular sieves 4A and N₂ bubbling. Triethylaluminum (TEA) and tri-*iso*-butylaluminum (TIBA) were donated by Tosoh Finechem Co. Tri-*n*-octylaluminum (TNOA) was purchased from Aldrich. Ph₃CB(C₆F₅)₄ was purchased from Tokyo Chemical Industry. (*i*Bu)₇Si₇O₉(OH)₂(OSiMe₃) (**1a**), (*i*Bu)₇Si₇O₉(OH)₂(OSiMe₂Ph) (**1b**), (*i*Bu)₇Si₇O₉(OH)₂[OSiMe₂C₆H₄(OMe-2)] (**1c**) and (*i*Bu)₇Si₇O₉(OH)₂[OSiMe₂C₆H₄(PPh₂-2)] (**1d**) were synthesized according to the literature. Each chlorosilane coupling reagents [Me₃SiCl, PhMe₂SiCl, C₆H₄(OMe-2)Me₂SiCl and C₆H₄(PPh₂-2)Me₂SiCl (2.90 mmol)] were added dropwise to a solution of (*i*Bu)₇Si₇O₉(OH)₃ (2.00 g, 2.53 mmol) and trimethylamine (3.5 ml, 25 mmol) in THF (40 ml). The reaction mixture was stirred overnight at room temperature. Et₃N·HCl as a byproduct was removed by filtration and the solvent was evaporated under reduced pressure. The resultant solid was purified through recrystallization in hexane or dichloromethane. The structures were confirmed by ¹H, ¹³C{¹H}, ²⁹Si{¹H} NMR spectroscopy. A series of POSS-supported catalysts [(*i*Bu)₇Si₇O₁₁(OSiMe₃)]CrCH(SiMe₃)₂ (**2a**), [(*i*Bu)₇Si₇O₁₁(OSiMe₂Ph)]CrCH(SiMe₃)₂ (**2b**), {(*i*Bu)₇Si₇O₁₁[OSiMe₂C₆H₄(OMe-2)]}CrCH(SiMe₃)₂ (**2c**) and {(*i*Bu)₇Si₇O₁₁[OSiMe₂C₆H₄(PPh₂-2)]}CrCH(SiMe₃)₂ (**2d**) were synthesized according to the literature. Cr[CH(SiMe₃)₂]₃ (212 mg, 0.40 mmol) was added to a solution of **1a-1d** (0.40 mmol) in heptane or toluene (20 ml). The mixture was stirred at reflux for 6 h, followed by the removal of the solvent under vacuum. The obtained product was used in

the ethylene polymerization without further purification. The structures were confirmed by $^{29}\text{Si}\{^1\text{H}\}$ NMR spectroscopy.



Scheme 1 Synthesis route of POSS-supported chromium catalysts.

Measurements

Gel permeation chromatography (GPC) measurements were performed on a Waters ALC/GPC 150C with polystyrene gel columns (Shodex AD806 M/S) at 140 °C using ortho-dichlorobenzene as an eluent. The primary structure of PE was determined by $^{13}\text{C}\{^1\text{H}\}$ NMR using a Bruker BioSpin AVANCE III 400 FT-NMR spectrometer at 120°C. A polymer sample was dissolved in a mixture of 1,2,4-trichlorobenzene and 1,1,2,2,-tetrachloroethane-*d*₂ (4,1, v/v). UV-Vis spectra were recorded on JASCO V770 UV-VIS-NIR spectrophotometer.

Polymerization reaction

Toluene (200 mL) was added and saturated with ethylene at 0.5 MPa for 30 min. Alkylaluminum (0.2 mmol) and POSS-supported chromium catalyst (8.0 μmol) were added and ethylene polymerization was conducted for 30 min with or without

$\text{Ph}_3\text{CB}(\text{C}_6\text{F}_5)_4$ (8.0 μmol). The obtained polymer was recovered by filtration and dried under vacuum at 60 °C. In case of ethylene/1-octene copolymerization, 1-octene (25, 50, 100, 200 mmol) was introduced into the reactor prior to monomer saturation.

3.3 Results and Discussion

Ethylene polymerization with different alkylaluminum

In considering the mechanistic aspect of the activity enhancement by the phosphino group, a molecular modeling study (not shown) precluded the association between chromium and phosphor due to a steric reason. Then, it was hypothesized that the phosphino group would weakly interact with the activator so as to affect the activity of the nearby chromium center. In **Figure 1a**, the ethylene polymerization activity of **2a** and **2d** was plotted along the concentration of TNOA. Both the catalysts were scarcely activated below the Al amount of 10 equiv. and reached the maxima at 25 equiv., followed by the deactivation due to the excess amount. A similar tradeoff between the activation and deactivation by an alkylaluminum activator is also known for usual Phillips catalysts. Next, the type of alkylaluminum was varied with the Al amount fixed at 25 equiv. (**Figure 1b**). The activity order among TEA, TIBA and TNOA was explained by considering the balance of the activation and deactivation: the activity became the lowest for TEA because its highest reactivity promoted the deactivation. The activity became lower for TNOA than for TIBA since the largest bulkiness of TNOA contributed to the suppression of not only the deactivation but also the activation. Comparing **2b** with **2a**, the introduction of steric hindrance around the chromium center suppressed the deactivation, thus giving higher activity for TEA. At the same time, it prohibited larger activators to approach the chromium center, thus lowering the activity

for TIBA and TNOA. The introduction of the diphenylphosphino group further enlarged the steric hindrance, but the influence on the activation/deactivation behavior was opposite to that for **2b**. The activity of **2d** became even lower than that of **2a** when TEA was used (more deactivation), while the activity became much higher when bulkier TIBA and TNOA was employed (more activation). Thus, it seems plausible that the diphenylphosphino group makes the chromium center more efficiently exposed to the activator through weak coordination of a lone pair of phosphor to the Lewis acidic aluminum center. It must be noted that the association between phosphor and aluminum was hardly detected in $^{31}\text{P}\{^1\text{H}\}$ NMR as it might be too labile.

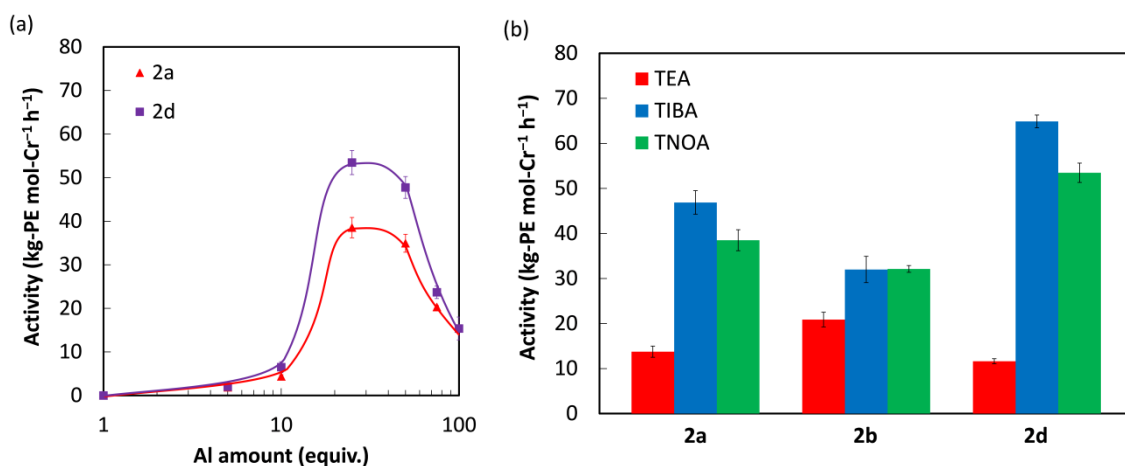


Figure 1 Dependence of the ethylene polymerization activity of **2a**, **2b**, **2d** (a) on the amount of TNOA and (b) on the type of alkylaluminium at 25 equiv.

Ethylene Polymerization with TIBA/ $\text{Ph}_3\text{CB}(\text{C}_6\text{F}_5)_4$

Borate activators such as $\text{Ph}_3\text{CB}(\text{C}_6\text{F}_5)_4$ are employed to improve the activity of transition metal catalysts for olefin polymerization, however the understanding of its effect for Phillips catalyst is lacking. It is possible to evaluate the effect more definitely on the Phillips catalyst using a POSS-supported chromium molecular catalyst having a

single structure. Ethylene polymerization was investigated using a combination of $\text{Ph}_3\text{CB}(\text{C}_6\text{F}_5)_4$ with TIBA which provided the highest activity for POSS-supported chromium catalyst. Ethylene polymerizations using **2a** and **2d** in the presence or absence of $\text{Ph}_3\text{CB}(\text{C}_6\text{F}_5)_4$ were conducted and the results were summarized in **Table 1**.

Table 1 The results of ethylene polymerization with TIBA/ $\text{Ph}_3\text{CB}(\text{C}_6\text{F}_5)_4$ ^a

Run	Catalyst	Temp. (°C)	$\text{Ph}_3\text{CB}(\text{C}_6\text{F}_5)_4$ (equiv.)	Activity (kg-PE/mol-Cr·h)	$M_w^b (\times 10^{-3})$	M_w/M_n^b
1		0	0	1.8 ± 0.7	2000	7
2		30	0	16 ± 0.8	2200	16
3	2a	50	0	29 ± 1.7	2400	22
4		0	1	5.4 ± 0.5	2000	62
5		30	1	78 ± 6	1700	30
6		50	1	58 ± 5	2100	48
7		0	0	12 ± 0.5	2000	11
8		30	0	59 ± 1	1800	28
9	2d	50	0	53 ± 4	1600	40
10		0	1	89 ± 9	1400	60
11		30	1	374 ± 9	660	9
12		50	1	334 ± 34	930	27

^a Polymerization conditions: toluene 200 mL, ethylene 0.5 MPa, catalyst 8.0 μmol , TIBA 0.2 mmol, $\text{Ph}_3\text{CB}(\text{C}_6\text{F}_5)_4$ 8.0 μmol , reaction time 30 min.

^b Determined by GPC.

The activity of both catalyst was improved by $\text{Ph}_3\text{CB}(\text{C}_6\text{F}_5)_4$ and they showed higher activity at 30, 50 °C than 0 °C. Especially, the activity of **2d** greatly enhanced and the activity increasing rate of **2d** was higher than **2a**. It was presumed that the chromium active species was ionized and stabilized by $\text{Ph}_3\text{CB}(\text{C}_6\text{F}_5)_4$ or the concentration of activator around the active site was increased due to the diphenylphosphino group reacted with $\text{Ph}_3\text{CB}(\text{C}_6\text{F}_5)_4$ and alkylaluminum interacted

with the adduct.

The GPC profiles of the produced PEs are shown in **Figure 2**. In case of **2a**, molecular weight of the produced PE was not changed by polymerization temperature and addition of $\text{Ph}_3\text{CB}(\text{C}_6\text{F}_5)_4$. On the other hand, the molecular weight distribution of produced PEs using **2d** without $\text{Ph}_3\text{CB}(\text{C}_6\text{F}_5)_4$ showed unimodal at 0°C and bimodal at $30, 50^\circ\text{C}$. It indicated that PPh_2 group is involved in the formation of active species that produces low molecular weight PE and it causes to induce a chain transfer reaction. Moreover the low molecular weight fraction was increased by addition of $\text{Ph}_3\text{CB}(\text{C}_6\text{F}_5)_4$. It suggested that PPh_2 group involved in making active site species provide low molecular weight PE and $\text{Ph}_3\text{CB}(\text{C}_6\text{F}_5)_4$ enhances the activity.

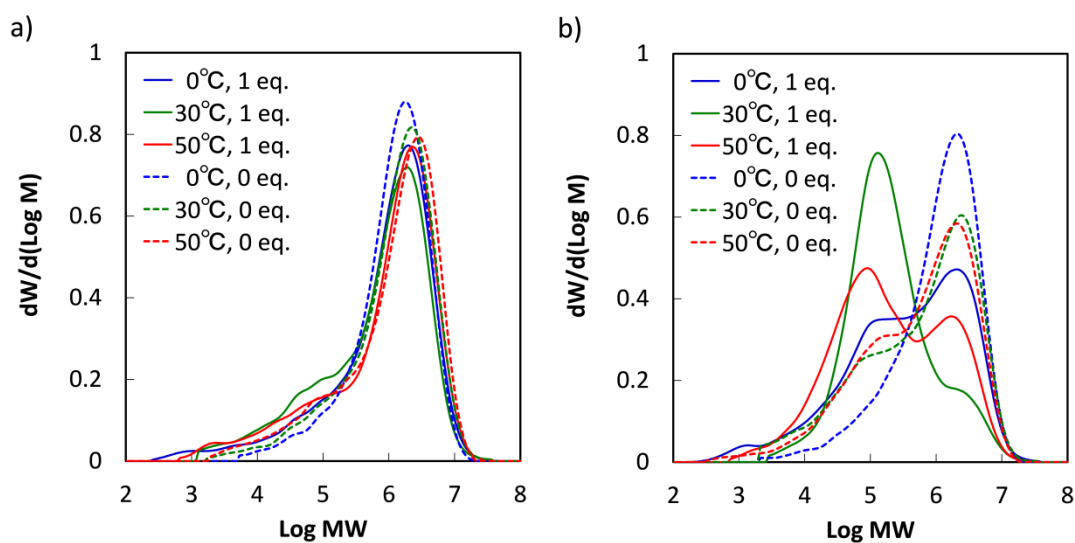


Figure 2 Molecular weight distribution of the produced PE using a) **2a** and b) **2d**.

UV-vis spectrum measurement

In order to clarify the influence of activator on the active site structure, TIBA and TIBA/ $\text{Ph}_3\text{CB}(\text{C}_6\text{F}_5)_4$ were added to catalysts **2a** and **2d** and the catalyst structures were analyzed by UV-vis spectrum measurement. POSS-supported chromium catalyst

(0.010 mmol) was dissolved in toluene (2 mL) at 30 ° C under a nitrogen atmosphere and TIBA (0.25 mmol) or both of $\text{Ph}_3\text{CB}(\text{C}_6\text{F}_5)_4$ (0.010 mmol) and TIBA were added into the solution, respectively. Thereafter, the polymerization was conducted with a continuous supply of ethylene at 1 atm and monitored by UV-vis spectrum measurement for 30 min. The results are summarized in **Figure 3**.

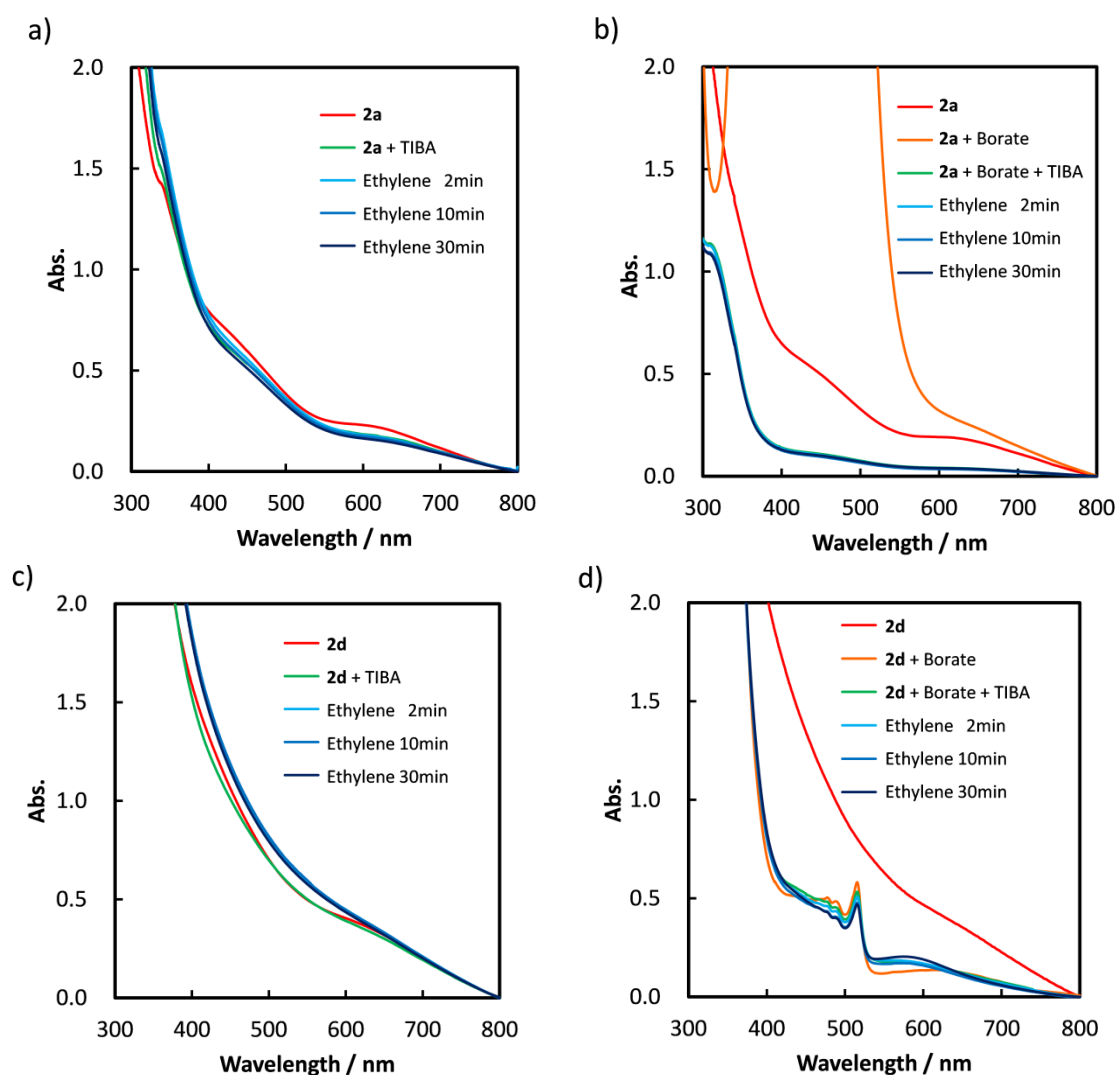


Figure 3 UV-vis spectra of the POSS-supported chromium catalysts (**2a** and **2d**), the catalysts reacted with activators and their ethylene polymerization a) **2a** with TIBA, b) **2a** with TIBA/ $\text{Ph}_3\text{CB}(\text{C}_6\text{F}_5)_4$, c) **2d** with TIBA and d) **2d** with TIBA/ $\text{Ph}_3\text{CB}(\text{C}_6\text{F}_5)_4$.

The both of **2a** and **2d** have an absorption band at 625 nm derived from the d-d transition of Cr (III) species. It was clarified that TIBA has no influence on the catalyst structure since the adsorption band was not changed in both of **2a** and **2d** by the addition of TIBA. Although the spectrum did not change in ethylene polymerization, the PEs were produced in the both solutions. Therefore, it can be considered that the alkyl-Cr (III) species exists as a polymerization active species. In the mixture of **2a** and $\text{Ph}_3\text{CB}(\text{C}_6\text{F}_5)_4$, the absorption peak derived from unreacted $\text{Ph}_3\text{CB}(\text{C}_6\text{F}_5)_4$ was observed at 425 nm. The unreacted $\text{Ph}_3\text{CB}(\text{C}_6\text{F}_5)_4$ peak was disappeared by addition of TIBA, however the peak of Cr (III) specie did not change. It is known that $\text{Ph}_3\text{CB}(\text{C}_6\text{F}_5)_4$ can easily react with TIBA and the following reactions occur (**Scheme 2**).³⁴ Trityl cation extracts hydrogen from the *iso*-butyl group of TIBA to generate aluminum cations. It promptly exchanges ligands with $\text{B}(\text{C}_6\text{F}_5)_4^-$ and the electrophilicity of the boron activator decreases. Thus, it was considered that the influence on the polymerization performance for **2a** was small because of an insufficient ionization for the active species or an alteration of TIBA. In contrast, $\text{Ph}_3\text{CB}(\text{C}_6\text{F}_5)_4$ was not observed in the catalyst **2d** and a new absorption peak was observed at 515 nm. Since the similar peak was also confirmed in the reaction of $(^i\text{Bu})_7\text{Si}_7\text{O}_9(\text{OH})_2[\text{OSiMe}_2\text{C}_6\text{H}_4(\text{PPh}_2-2)]$ (**1d**) with $\text{Ph}_3\text{CB}(\text{C}_6\text{F}_5)_4$, it is thought that there is an interaction between $\text{Ph}_3\text{CB}(\text{C}_6\text{F}_5)_4$ and diphenylphosphino group. It is known phosphine compounds form the adducts with trityl cation.³⁵ For example, PPh_3 gives the adduct $[\text{Ph}_3\text{PCPh}_3][\text{B}(\text{C}_6\text{F}_5)_4]$ at room temperature, so it is inferred that the same reaction occurs in **2d**. It was indicated that the electronic state of the chromium species was changed since the peak of Cr (III) specie at 625 nm was shifted to 580 nm by the addition of TIBA. It is inferred that $\text{Ph}_3\text{CB}(\text{C}_6\text{F}_5)_4$ was released from the diphenylphosphino group by TIBA and it

Table 2 Ethylene/1-octene copolymerization **2a** and **2d** with TIBA/Ph₃CB(C₆F₅)₄^a

Run	Catalyst	Ph ₃ CB(C ₆ F ₅) ₄ (equiv.)	1-Octene (mmol)	Yield (g)	Activity (kg-PE/mol-Cr·h)	Hexyl content ^b (mol%)
1	2a	1	0	0.329	82	n.d. ^c
2		1	25	0.182	45	0.32
3		1	50	0.083	21	0.50
4		1	100	0.080	20	0.58
5		1	200	0.058	14	0.68
6		0	0	0.064	16	
7		0	25	0.039	10	
8		0	50	0.036	9	
9		0	100	0.034	9	n.d. ^c
10		0	200	0.025	6	
11	2d	1	0	1.50	374	n.d. ^c
12		1	25	1.20	301	0.26
13		1	50	1.02	256	0.38
14		1	100	0.792	198	0.67
15		1	200	0.563	141	0.67
16		1	bulk ^d	0.069	17	1.98
17		0	0	0.236	59	
18		0	25	0.172	43	
19		0	50	0.157	39	
20		0	100	0.141	35	n.d. ^c
21		0	200	0.125	31	
22		0	bulk ^d	0.062	16	0.79

^a Polymerization conditions: toluene 200 mL, ethylene 0.5 MPa, catalyst 8.0 μmol, TIBA 0.2 mmol, Ph₃CB(C₆F₅)₄ 8.0 μmol, reaction time 30 min, temperature 30 °C.

^b Determined by ¹³C{¹H} NMR.

^c Not detected.

^d The polymerization was conducted in the absence of ethylene and toluene.

It was considered that 1-octene coordinated to the chromium active site, but the insertion reaction almost does not proceed. However, hexyl branched structure was

confirmed without $\text{Ph}_3\text{CB}(\text{C}_6\text{F}_5)_4$ in the bulk condition. Therefore, it can mention that the catalysts possess certain copolymerization ability with α -olefins. In the condition of addition of $\text{Ph}_3\text{CB}(\text{C}_6\text{F}_5)_4$ it was found that the $\text{Ph}_3\text{CB}(\text{C}_6\text{F}_5)_4$ improved the catalyst activities and hexyl branch content. The reason is that the POSS-supported chromium catalysts were cationized by $\text{Ph}_3\text{CB}(\text{C}_6\text{F}_5)_4$ and 1-octene coordination and insertion reaction was accelerated.

3.4 Conclusions

The influence of activator was investigated using POSS-supported chromium catalyst which can evaluate the nature of chromium active site for Phillips catalyst at molecular level. As a result of examining the effect of various alkylaluminum (AlEt_3 , Al^iBu_3 , Al^nOt_3) as an activator, it was found that AlEt_3 having compact alkyl group and high reactivity suppresses the activity. The suppression of activity by AlEt_3 was decreased for **2b** and **2d** which has the steric hindrance around the active site and there is an optimal addition amount of the alkylaluminum to maximize the activity. Thus, it was shown that the polymerization performance was determined by the balance between activation and deactivation of chromium center by alkyl aluminum. The activity of both of **2a** and **2d** was improved by the combination of $\text{Ph}_3\text{CB}(\text{C}_6\text{F}_5)_4$ with Al^iBu_3 in ethylene homo-polymerization. $\text{Ph}_3\text{CB}(\text{C}_6\text{F}_5)_4$ did not influence the molecular weight of PE produced by **2a**, however the low molecular weight fraction produced by **2d** was increased. It was found that the effect of $\text{Ph}_3\text{CB}(\text{C}_6\text{F}_5)_4$ amplifying for the activity depends on the active species. In the ethylene/1-octene copolymerization, the addition of $\text{Ph}_3\text{CB}(\text{C}_6\text{F}_5)_4$ leads to improve the copolymerization ability with α -olefins. It is thought that diphenylphosphino group can capture $\text{Ph}_3\text{CB}(\text{C}_6\text{F}_5)_4$ and the adduct influences on the catalyst performance. Therefore, it was clarified that the catalytic function can be adjusted by a design of a functional group and a choice of an activator.

3.5 References

- [1] J. P. Hogan, R. L. Banks, U.S. Patent 1958, 2,825,721.
- [2] M. P. McDaniel, *Adv. Catal.*, 1985, **33**, 47.
- [3] M. P. McDaniel, *Adv. Catal.*, 2010, **53**, 123.
- [4] P. J. DesLauriers, M. P. McDaniel, D. C. Rohlfig, R. K. Krishnaswamy, S. J. Secora, E. A. Benham, P. L. Maeger, A. R. Wolfe, A. M. Sukhadia and B. B. Beaulieu, *Polym. Eng. Sci.*, 2005, **45**, 1203.
- [5] P. J. DesLauriers, C. Tso, Y. Yu, D. L. Rohlfig and M. P. McDaniel, *Appl. Catal. A: Gen.*, 2010, **388**, 102.
- [6] M. P. McDaniel, M. B. Welch, M. J. Dreiling, *J. Catal.*, 1983, **82**, 118.
- [7] T. Pullukat, R. E. Hoff, *Catal. Rev.-Sci. Eng.* 1999, **41**, 389.
- [8] J. Amor Nait Ajjou, S. L. Scott, *Organometallics*, 1997, **16**, 86.
- [9] J. Amor Nait Ajjou, S. L. Scott, V. Paquet, *J. Am. Chem. Soc.*, 1998, **120**, 415.
- [10] J. Amor Nait Ajjou, G. L. Rice, S. L. Scott, *J. Am. Chem. Soc.*, 1998, **120**, 13436.
- [11] J. Amor Nait Ajjou, S. L. Scott, *J. Am. Chem. Soc.*, 2000, **122**, 8968.
- [12] M. C., Beaudoin, O, Womiloju, A. Q. Fu, J. A. N. Ajjou, G. L. Rice, S. L. Scott, *J. Mol. Catal. A: Chem.*, 2002, **190**, 159.
- [13] S. L. Scott, A. Fu, L. A. MacAdams, *Inorg. Chim. Acta*, 2008, **361**, 3315.
- [14] O. M. Bade, R. Blom, M. Ystenes, *Organometallics*, 1998, **17**, 2524.
- [15] H. Ikeda, T. Monoi, Y. Sasaki, *J. Polym. Sci., Part A: Polym. Chem.*, 2003, **41**, 413.
- [16] K. Tonosaki, T. Taniike, M. Terano, *Macromol. React. Eng.*, 2011, **5**, 332.
- [17] M. P. Conley, M. F. Delley, G. Siddiqi, G. Lapadula, S. Norsic, V. Monteil, O. V. Safonova, C. Copéret, *Angew. Chem. Int. Ed.*, 2014, **53**, 1872.
- [18] M. F. Delley, M. P. Conley, C. Copéret, *Catal. Lett.*, 2014, **144**, 805.

- [19] M. F. Delley, F. Núñez-Zarur, M. P. Conley, A. Comas-Vives, G. Siddiqi, S. Norsic, V. Monteil, O. V. Safonova, C. Copéret, *Proc. Natl. Acad. Sci. U. S. A.*, 2014, **111**, 11624.
- [20] M. F. Delley, F. Nuñez-Zarura, M. P. Conley, A. Comas-Vives, G. Siddiqi, S. Norsic, V. Monteil, O. V. Safonova, C. Copéret, *Proc. Natl. Acad. Sci. U. S. A.*, 2015, **112**, E4162.
- [21] P. Mania, S. Conrad, R. Verel, C. Hammond, I. Hermans, *Dalton Trans.*, 2013, **42**, 12725.
- [22] C. A. Demmelmaier, R. E. White, J. A. van Bokhoven, S. L. Scott, *J. Phys. Chem. C*, 2008, **112**, 6439.
- [23] C. A Demmelmaier, R. E. White, J. A. van Bokhoven, S. L. Scott, *J. Catal.*, 2009, **262**, 44.
- [24] L. Zhong, M.-Y. Lee, Z. Liu, Y.-J Wanglee, B. Liu, S. L. Scott, *J. Catal.*, 2012, **293**, 1.
- [25] E. Groppo, C. Lamberti, S. Bordiga, G. Spoto, A. Zecchina, *Chem. Rev.* 2005, **105**, 115.
- [26] A. Zecchina, E. Groppo, *Proc. R. Soc. A*, 2012, **468**, 2087.
- [27] E. Groppo, K. Seenivasan, C. Barzan, *Catal. Sci. Technol.*, 2013, **3**, 858.
- [28] E. Groppo, C. Lamberti, G. Spoto, S. Bordiga, G. Magnacca, A. Zecchina, *J. Catal.*, 2005, 236, 233.
- [29] E. Groppo, C. Lamberti, S. Bordiga, G. Spoto, A. Zecchina, *J. Catal.*, 2006, 240, 172.
- [30] E. Groppo, A. Damin, C. O. Arean, A. Zecchina, *Chem. Eur. J.*, 2011, 17, 11110.

- [31] R. Duchateau, *Chem. Rev.*, 2002, **102**, 3525.
- [32] E. A. Quadrelli, J.-M. Basset, *Coord. Chem. Rev.*, 2010, **254**, 707.
- [33] F. J. Feher, R. L. Blanski, *J. Chem. Soc., Chem. Commun.*, 1990, 1614.
- [34] M. Bochmann, M. J. Sarsfield, *Organometallics* 1998, **17**, 5908.
- [35] L. Cabrera, G. C. Welch, J. D. Masuda, P. Wei, D. W. Stephan, *Inorg. Chim. Acta* 2006, **359**, 3066.
- [36] K. Kimura, S. Yuasa, Y. Maru, *Polymer*, 1984, **25**, 441.

Chapter 4

Tandem Catalysis by Soluble Polynorbornene Supported Half-Titanocene Catalysts for Olefin Polymerization

Introduction

Catalysis is an important research field from both of academic and industrial viewpoint. Generally, catalysts can be classified roughly into two types, "molecular catalyst" and "solid catalyst". Molecular catalyst has a single active site and is soluble in a solvent. The clear structure leads to direct understanding of the reaction mechanism and a systematic catalyst design for the required catalyst performance. On the other hand, the solid catalyst is excellent in multifunctionality because multiple components having different properties can be accumulated on the surface of the solid material. In olefin polymerization catalyst, which is a representative industrial catalyst, both solid catalysts such as Ziegler-Natta (ZN) catalyst¹ and Phillips catalyst^{2,3} and molecular catalyst such as metallocene⁴ catalyst and phenoxy-imine complex catalyst (FI catalyst)⁵ have been developed. In the solid catalyst, optimization of the catalyst multifunctionality is carried out by controlling various chemical and physical structural factors ranging from atoms to the particle size scale. However, systematic catalyst design is difficult due to its complexity. On the other hand, molecular catalyst can precisely design catalytic functions such as activity and selectivity since the relationship between the catalyst structure and the polymer structure is one-to-one correlated. However, it is difficult to design multifunctionality for synthesizing polymers with complicated structures. Therefore, in order to create an ideal polymerization catalyst capable of freely controlling the polymer structure, development of a novel polymerization catalyst that combines the concept of homogeneous and heterogeneous catalyst is desired.

Recently, in order to synthesize a polymer having a structure which can not be achieved with a single site catalyst, tandem catalyst which is a mixture of two different

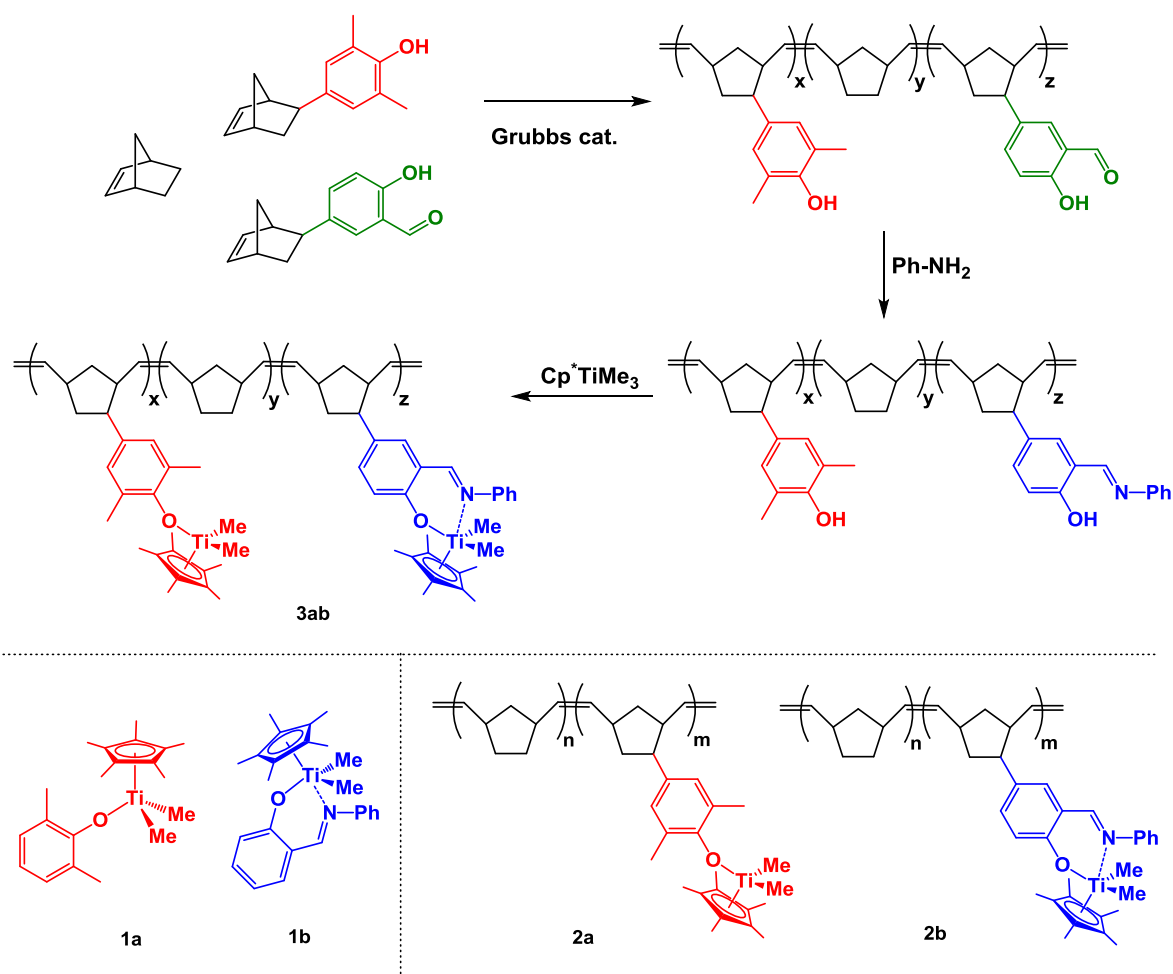
types of single site catalysts and binuclear catalyst having two kinds of metal centers in the same molecule are actively studied.⁶⁻¹¹ For example, Marks *et al.* compared a tandem catalyst that mixed a Ti complex having high copolymerization ability for α -olefin and a Cr complex synthesizing 1-hexene selectively from ethylene with a binuclear complex in which respective complexes are bonded in a single molecule.^{12,13} They clarified that binuclear catalyst produced polymer with a higher branch content than tandem catalyst, and a binuclear catalyst that has a shorter carbon linkage more efficiently incorporates 1-hexene. This fact indicates that the distance between the comonomer producing site and the copolymerization site plays a vital role. However, the designable catalyst structure is restricted because of the synthesis of ligands is complicated to bond multiple metal sites on the same molecule. Also, it is difficult to adjust the balance of the catalytic function since catalyst sites with different functions can be introduced only at the same proportion. Therefore, a new catalyst design concept is necessary to integrate and control the cooperative effect for catalyst multi-functionalization.

Our laboratory has proposed polymer-supported catalyst as a new concept that simultaneously realizes precise structural design and multifunctionality of polymerization catalyst.¹⁴ In ring-opening metathesis polymerization (ROMP) of norbornene using Grubbs catalyst, it can produce monodisperse polymer with controlling molecular weight and introduce various functional groups as side chain because of living polymerization and high tolerance to polar functional group.¹⁵⁻¹⁷ Thus, it is possible to synthesize a polymer support precisely designed with primary structure such as coordination groups, composition ratio, composition distribution and molecular weight. Polynorbornene (PNB) forms a random coil state in a dilute system and the size

of the random coil depends on environmental factors such as solvent and reaction temperature. It is promising to control of active site density and constrain generated macromonomer. Therefore, development of a polymer chain supported catalyst capable of adjusting the coordination effect between active sites by compatibility of precise design and functional accumulation can be expected to create catalyst performance that could not be achieved with conventional catalysts.

Phenoxy-imine type catalyst named FI catalyst is known as an excellent catalyst in its high designability. The catalyst performance can be easily tuned since it is possible to control the molecular weight and the terminal structure of the polymer produced by the choice of the substituent of ligand and the reaction conditions.¹⁸⁻²⁰ On the other hand, $\text{Cp}^*\text{Ti}(\text{OAr})\text{X}_2$ ($\text{X} = \text{Cl}, \text{Me}$) complex developed by Nomura et al. has not only very high olefin polymerization activity but also high copolymerization with bulky comonomer.^{21,22} In this chapter, I focused on PNB-supported catalyst combining FI catalyst and $\text{Cp}^*\text{Ti}(\text{OAr})\text{X}_2$ catalyst and the effect of polymer chains on catalyst performance was investigated. A whole synthesis strategy of PNB-supported catalyst is described in **Scheme 1**. There are four basic steps: (i) Norbornene derivatives bearing aryloxy or salicylaldehyde group were synthesized by reductive Heck coupling reaction; (ii) PNB-supports were synthesized by ROMP reaction using Grubbs catalyst; (iii) salicylaldehyde group was converted to phenoxy-imine group using *p*-toluenesulfonic acid; and (iv) PNB-supported catalyst was synthesized by grafting Cp^*TiMe_3 . PNB-supported catalysts **2a** and **2b** were synthesized and the polymerization performances were compared with the molecular analogues **1a** and **1b**. The terpolymer PNB-supported catalyst **3ab** was also synthesized and compared with tandem molecular (**1a** + **1b**) and PNB-supported catalyst (**2a** + **2b**) systems to investigate the influence on

the polymerization performance.



Scheme 1 Synthesis of polynorbornene-supported catalyst and the reference catalyst.

Experimental

Materials

All experiments were carried out under anitrogen atmosphere using Schlenk techniques. Hexane, ethyl acetate and methanol were purchased from Kanto Kagaku Co. Ltd and used without further purification. Anhydrous toluene, diethylether, tetrahydrofuran (THF), and dichloromethane were used as received from Kanto Kagaku Co. Ltd. N,N-Dimethylformamide (DMF) and toluene for polymerization were dried over molecular sieves 4A and nitrogen bubbling. Triethylamine (Kanto Kagaku Co. Ltd.) was distilled from calcium hydride and stored under nitrogen. 2,5-Norbornadiene, 4-bromo-2,6-dimethylphenol, 5-bromosalicylaldehyde, aniline, bis(triphenylphosphine)palladium(II)dichloride ($\text{Pd}(\text{PPh}_3)_2\text{Cl}_2$), *p*-toluenesulfonic acid, and trityltetrakis(pentafluorophenyl)borate ($\text{Ph}_3\text{CB}(\text{C}_6\text{F}_5)_4$) were purchased from Tokyo Chemical Industry. Formic acid was purchased from Wako Pure Chemical Industries. Ammonium formate ($\text{NH}_4\text{CO}_2\text{H}$), Grubbs 1 st generation catalyst, and ethyl vinyl ether were purchased from Sigma-Aldrich. Trimethylpentamethylcyclopentadienyltitanium (IV) (Cp^*TiMe_3) was purchased from Strem Chemicals. $\text{Cp}^*\text{Ti}(\text{O}-2,6\text{-Me}_2\text{C}_6\text{H}_3)\text{Me}_2$ (**1a**) and $\text{Cp}^*\text{Ti}[\text{O}-2\text{-(PhN=CH)C}_6\text{H}_4]\text{Me}_2$ (**1b**) were synthesized according to the literatures.^{23,24} Tri-*iso*-butylaluminum (TIBA) was donated by Tosoh Finechem Co.

Measurements

^1H and $^{13}\text{C}\{^1\text{H}\}$ NMR spectra were recorded on a Bruker AVANCE III 400 FT-NMR spectrometer using CDCl_3 and chemical shifts were referenced to the residual peak. The molecular weight distribution of PNB support was determined by gel permeation chromatography (GPC, Shimadzu SCL-10A) equipped with a RID-10A

detector using THF as an eluent. Differential scanning calorimeter (DSC) measurement was performed on Mettler Toledo DSC 822. A PE sample was heated from 25 °C to 180 °C at 10 °C/min, then kept at 180 °C for 10 min and cooled down to 25 °C at 10 °C/min.

Norbornene comonomer synthesis

4-(bicyclo[2.2.1]hept-5-en-2-yl)-2,6-dimethylphenol

4-bromo-2,6-dimethylphenol (5.00 g, 24.9 mmol), 2,5-norbornadiene (9.1 ml, 89.6 mmol), PdCl₂(PPh₃)₂ (0.699 g, 0.996 mmol), trimethylamine (10.4 ml, 74.7 mmol) and formic acid (1.9 ml, 49.8 mmol) were added to DMF (14 ml) and stirred at 80 °C for 16 h. The reaction mixture was extracted with ethyl acetate/hexane (1/4 in v/v). The organic layer was washed with water and dried with Na₂SO₄. After evaporation, the crude product was purified by silica gel column chromatography with ethyl acetate/hexane (1/9 in v/v), which gave as colorless solid (4.16 g, 19.4 mmol, Yield 78%). ¹H NMR (400 MHz, CDCl₃): δ 1.37-1.46 (m, 1H, CH₂), 1.52-1.64 (m, 2H, CH₂), 1.65-1.74 (m, 1H, CH₂), 2.25 (s, 6H, CH₃), 2.60 (dd, *J* = 9.6 Hz, 1H, CH), 2.83 (bs, 1H, CH), 2.95 (s, 1H, CH), 4.49 (s, 1H, OH), 6.15 (dd, *J* = 7.4 Hz, 1H, H=CH), 6.24 (dd, *J* = 7.4 Hz, 1H, C=CH), 6.90 (s, 2H, ArH). ¹³C {¹H} NMR (125 MHz, CDCl₃): δ 16.2 (CH₃), 33.6 (CH₂), 42.3 (CH), 42.3 (CH), 43.0 (CH₂), 45.9 (CH), 48.7(CH), 122.8 (C aromatic), 127.9 (C aromatic), 137.3 (CH), 137.5 (CH), 137.8 (C aromatic), 150.1 (C aromatic).

4-(bicyclo[2.2.1]hept-5-en-2-yl)salicylaldehyde

5-bromosalicylaldehyde (5.00 g, 24.9 mmol), 2,5-norbornadiene (9.1 ml, 89.6

mmol), PdCl₂(PPh₃)₂ (0.699 g, 0.996 mmol), trimethylamine (10.4 ml, 74.7 mmol) and formic acid (1.9 ml, 49.8 mmol) were added to DMF (14 ml) and stirred at 80°C for 16 h. The reaction mixture was extracted with ethyl acetate/hexane (1/4 in v/v). The organic layer was washed with water and dried with Na₂SO₄. After evaporation, the crude product was purified by silica gel column chromatography with ethyl acetate/hexane (1/7 in v/v), which gave as colorless liquid (3.31 g, 15.4 mmol, Yield 62%). ¹H NMR (400 MHz, CDCl₃): δ 1.49 (dd, 2H, CH₂), 1.66–1.72 (m, 2H, CH₂), 2.69 (t, 1H, CH), 2.88 (s, 1H, CH), 2.99 (s, 1H, CH), 6.17-6.19 (m, H=CH), 6.24-6.26 (m, 1H, C=CH), 6.93 (d, *J* = 8.0 Hz, 1H, ArH), 7.43(s, 1H, ArH), 7.46 ppm (d, *J* = 8.0 Hz, 1H, ArH), 9.88 (s, 1H, CHO), 10.86 (s, 1H, OH). ¹³C {¹H} NMR (125 MHz, CDCl₃): δ 33.79 (CH₂), 42.45 (CH), 42.79 (CH), 45.78 (CH₂), 48.31 (CH), 117.56 (CH), 120.43 (C aromatic), 131.81 (CH), 137.14 (CH), 137.64 (CH), 137.80 (C aromatic), 159.75 (C aromatic), 196.86 (C, CHO).

Ring opening metathesis polymerization

2-norbornene (19.0 mmol) and the synthesized comonomers (1.00 mmol, 5.0 mol%) were dissolved in CH₂Cl₂ (27.5 mL). A solution of the Grubbs first-generation catalyst (0.100 mmol) in CH₂Cl₂ (12.5 mL) was added and stirred at room temperature for 3 h. Excess ethyl vinyl ether was added and stirred for further 30 min to quench the reaction. The mixture was precipitated in methanol and diethyl ether to yield powder and the obtained polymer was dried under vacuum.

Ligand conversion

PNB-support bearing salicylaldehyde at side chain (1.00 g) was dissolved in

toluene (25 mL). 10 equivalent of aniline and 1 equivalent of *p*-toluenesulfonic acid were added to the solution and stirred under reflux for 6 h. The mixture was casted into methanol and the precipitated polymer was dried under vacuum.

Synthesis of PNB-supported catalysts (**2a**, **2b** and **3ab**)

Cp*TiMe₃ (0.050 mmol) was dissolved in toluene (0.5 mL). A solution of PNB supports (1 equivalent with respect to Cp*TiMe₃) in toluene (4.5 mL) was added and stirred at room temperature for 10 min and then, the solvent was removed under reduced pressure.

Ethylene polymerization

Toluene (300 mL) and TIBA (0.125 mmol) were added into a stainless steel stirred reactor. The temperature was kept at 0 or 30 °C and ethylene gas was filled at 0.6 MPa for 30 min. Cp*TiMe₂[O-2,6-Me₂C₆H₃] (**1a**), Cp*TiMe₂[O-2-(PhN=CH)C₆H₄] (**1b**) or Cp*TiMe₃ grafted PNB-supported catalysts (**2a**, **2b**, **3ab**) (2.5 μmol per Ti) and Ph₃CB(C₆F₅)₄ (2.5 μmol) were added and ethylene polymerization was conducted for 10 min.

PE film preparation and tensile test

The synthesized PE was milled by a cryogenic sample crusher JFC-300 (Japan Analytical Industry Co. Ltd.) and impregnated with of 0.5 wt% Inrganox 1010 as a stabilizer. The PE sample was melted at 190, 200, or 210 °C for 5 min and pressed at 210 °C under 20 MPa for 5 min and then, quenched at room temperature for 10 min. Tensile properties of the PE films were measured by a tensile tester (Abe Dat-100). A

stress strain curve was acquired at 20 °C and at a crosshead speed of 10 mm/min. At least five specimens were examined for each sample.

Results and Discussion

Synthesis and characterization of PNB-supports

Copolymerizations between norbornene with comonomers bearing aryloxo (PNB-A1) or salicylaldehyde group (PNB-B1) were performed using Grubbs 1st generation catalyst. The ratio of norbornene/catalyst was fixed at 200 mol/mol and the comonomer feed ratio was adjusted to be 5.0 mol%. For the terpolymer (PNB-C1), the contents of each functional group was controlled to be 2.5 mol%, respectively. The obtained polymers were characterized by ^1H NMR spectra measurement (**Figure 1**). The signals of aliphatic hydrocarbon (H_1 and H_{4-7}) and unsaturated hydrocarbon ($\text{H}_{2,3}$) derived from PNB backbone were observed, respectively. PNB is composed of a mixture of *trans* and *cis* isomers and the *trans* isomer was dominantly produced. It is consistent with the usual tendency in ROMP using Grubbs 1st generation catalyst. From the ^1H NMR spectrum of PNB copolymer bearing aryloxo group, a singlet signal at 2.21 ppm derived from methyl group, a broad signal at 4.42 ppm derived from hydroxyl group and a singlet signal at 6.18 ppm derived from aromatic proton were observed, respectively. Since the integral ratio was 6 : 1 : 2, it was confirmed that 2,6-dimethylaryloxo group could be introduced. The integral ratio of 2,6-dimethylaryloxo group and $\text{H}_{2,3}$ of the polymer backbone signals was 0.05 : 2. Thus, the functional group content was derived as 5.0 mol%. In the PNB copolymer bearing salicylaldehyde group, three kinds of aromatic proton signal as δ 6.91 (d, 1 H), 7.32 (s, 1 H), 7.35 (d, 1 H), a singlet signal at 9.85 ppm derived from aldehyde group and a

broad signal at 10.85 ppm derived from hydroxyl group were observed. Analysis on the terpolymer similarly revealed that the signals of aryloxo group and salicylaldehyde group were detected and the contents were 2.5 mol%, respectively. Therefore, a terpolymer was successfully synthesized with the contents of the two side chain functional groups controlled quantitatively.

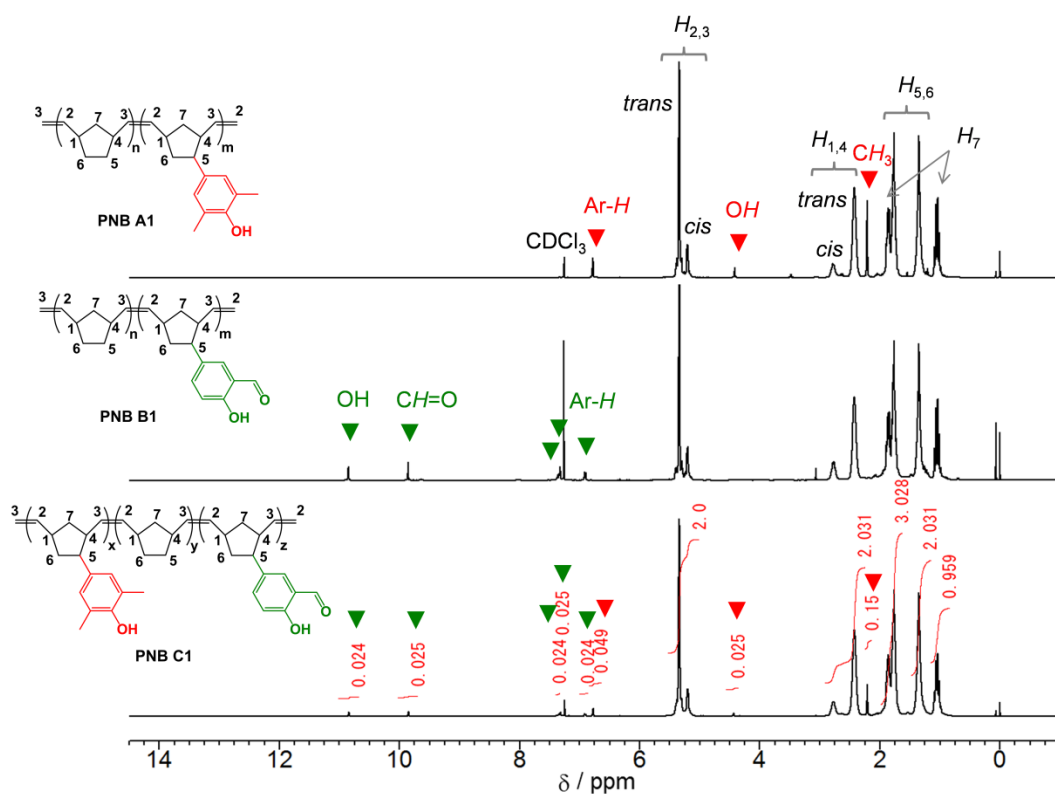


Figure 1 ^1H NMR spectra of copolymers bearing aryloxo (PNB-A1, top) or salicylaldehyde group (PNB-B1, middle) and their terpolymer (PNB-C1 bottle).

Subsequently, the salicylaldehyde group of PNB support was converted to imine. The polymers (PNB-B1, C1) and aniline were dissolved in toluene and heated under reflux in the presence of *p*-toluenesulfonic acid as an acid catalyst. The reaction mixture was precipitated from methanol and the collected copolymer (PNB-B2) and terpolymer (PNB-C2) were characterized by ^1H NMR measurements (**Figure 2-3**). Copolymer bearing salicylaldehyde group is also shown as reference.

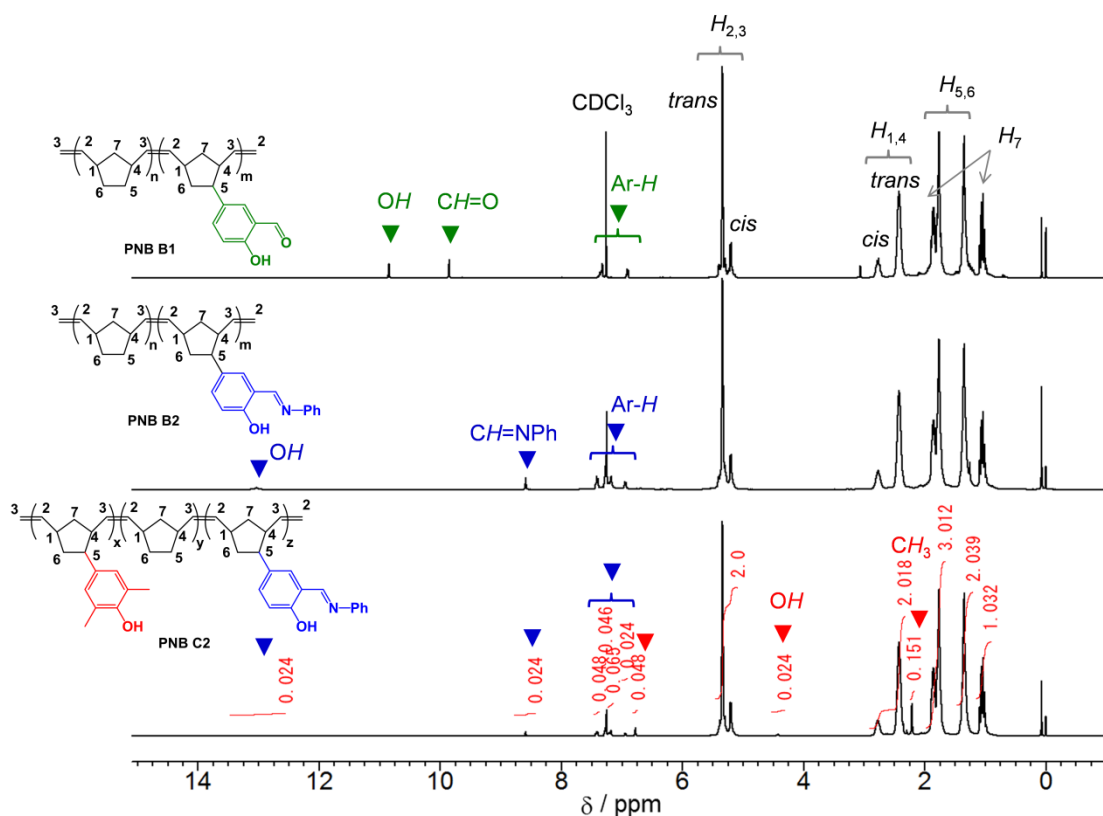


Figure 2 ^1H NMR spectra of copolymers bearing salicylaldehyde (PNB-B1, top), phenoxy-imine group (PNB-B2, middle) and the terpolymer (PNB-C2, bottle).

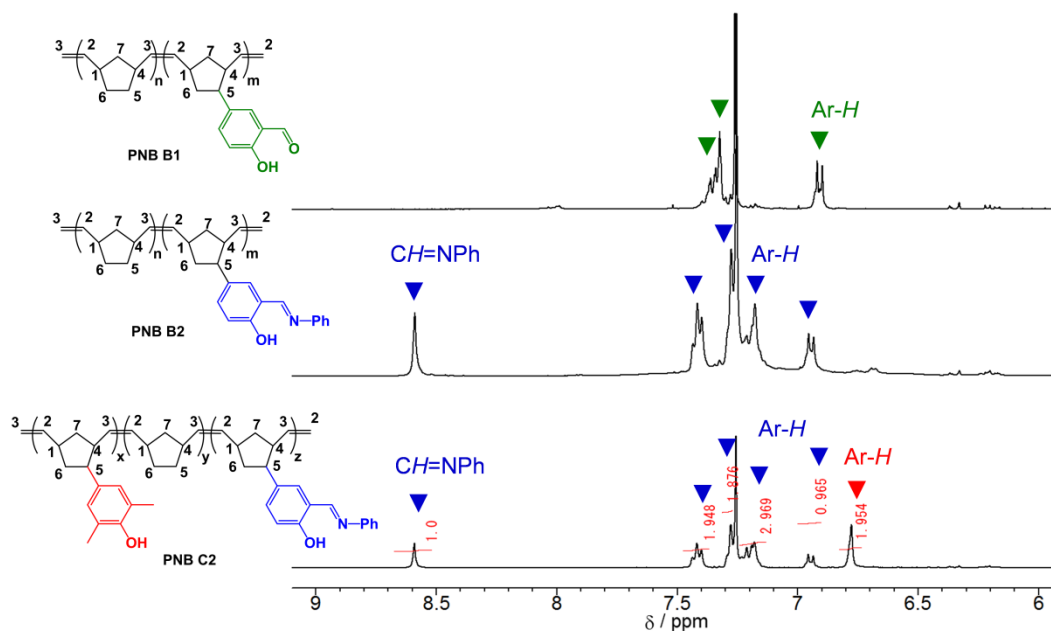


Figure 3 ^1H NMR spectra of the side chain conversion to phenoxy-imine group in the aromatic region.

The aldehyde group signal observed at 9.85 ppm in the PNB-B1 completely disappeared and a new singlet signal derived from the imine group was confirmed at 8.59 ppm. The broad signal of hydroxyl group also shifted from 10.85 to 13.03 ppm. In **Figure 3**, the aromatic proton signals which were clearly different with salicylaldehyde appeared in total eight number of protons, though they were overlapped with the residual hydrogen signal in the deuterated solvent. It was presumed that the triplet signal of two protons at 7.42 ppm was derived from the phenyl group and the number of aromatic signals were consistent with the target structure. It was confirmed that the salicylaldehyde group in the copolymer was completely converted into phenoxy-imine. In PNB-C2, the content of phenoxy-imine group and 2,6-dimethylaryloxo group was 2.4 mol%, respectively. Therefore, the synthesis of terpolymer PNB-C2 having both of 2,6-dimethylaryloxo and phenoxy-imine group was succeeded.

Table 1 summarizes the characterization results for the synthesized polymers. In all polymers, almost quantitative comonomer incorporation were observed and the molecular weight distributions were close to one. Although the obtained M_n values were higher than estimated values from the initial comonomer/catalyst ratio, the deviation frequently arises in ROMP using Grubbs 1st generation catalyst since the propagation rate is much higher than the initiation rate.²⁵ Moreover, all the numbers of pendant group per chain were almost constant and the terpolymer has both of the functional groups in the same ratio. These results indicated that the polymer structures were precisely controlled and the series of PNB-support bearing different functional group can be obtained.

Table 1 Results of PNB support synthesis^a.

Run	Sample	Pendant group	Comonomer content ^b (mol%)	$M_n^d \times 10^{-4}$	M_w/M_n^d	Pendant group /chain ^e
1	PNB-A1	aryloxo	4.9	6.3	1.11	33
2	PNB-B1	salicylaldehyde	5.0	5.4	1.28	29
3	PNB-B2	phenoxy-imine	5.0	6.8	1.14	31
4	PNB-C1	aryloxo	2.5	6.2	1.22	16
		salicylaldehyde	2.5			16
5	PNB-C2	aryloxo	2.4	6.3	1.13	16
		phenoxy-imine	2.4			16

^a Polymerization conditions: Norbornenes 20.0 mmol, catalyst 0.100 mmol, CH₂Cl₂ 30 mL, temperature 30°C, reaction time 3 h.

^b Calculated from ¹H NMR.

^c Determined by GPC.

^d Calculated from the M_n value and the comonomer content.

Synthesis and characterization of PNB supported catalysts

Each PNB-supported catalyst was synthesized by grafting Cp^{*}TiMe₃ to the obtained polymers (PNB-A1, B2, C2). ¹H NMR measurement results are shown in **Figure 4**. In the spectrum of **2a**, the hydroxyl group was completely disappeared after the grafting of Cp^{*}TiMe₃ and the methyl group of side chain was shifted from 2.21 to 2.14 ppm. The new signals derived from Cp-CH₃ and Ti-CH₃ group were confirmed at 1.93 and 0.42 ppm while the original Cp^{*}TiMe₃ are observed at 1.95 and 0.74 ppm, respectively. The proton ratio of these signals and methyl group of side chain was consisted with the desired product. Thus Cp^{*}TiMe₃ was quantitatively grafted onto the PNB-support. In the spectrum of **2b**, the hydroxyl group derived from the phenoxy-imine group completely disappeared after the grafting and CH=NPh signal was shifted from 8.59 ppm to 8.92 ppm. It was also confirmed that the grafted Cp-CH₃ and Ti-CH₃ group were appeared at 1.89 and 0.48 ppm. Although, Cp-CH₃ signal was

overlapped with the norbornene backbone $H_{5,6,7}$, $Ti-CH_3$ signal was observed as six protons. Therefore, it was found that Cp^*TiMe_3 was completely grafted onto the PNB-support. The corresponding signals were observed in **3ab**.

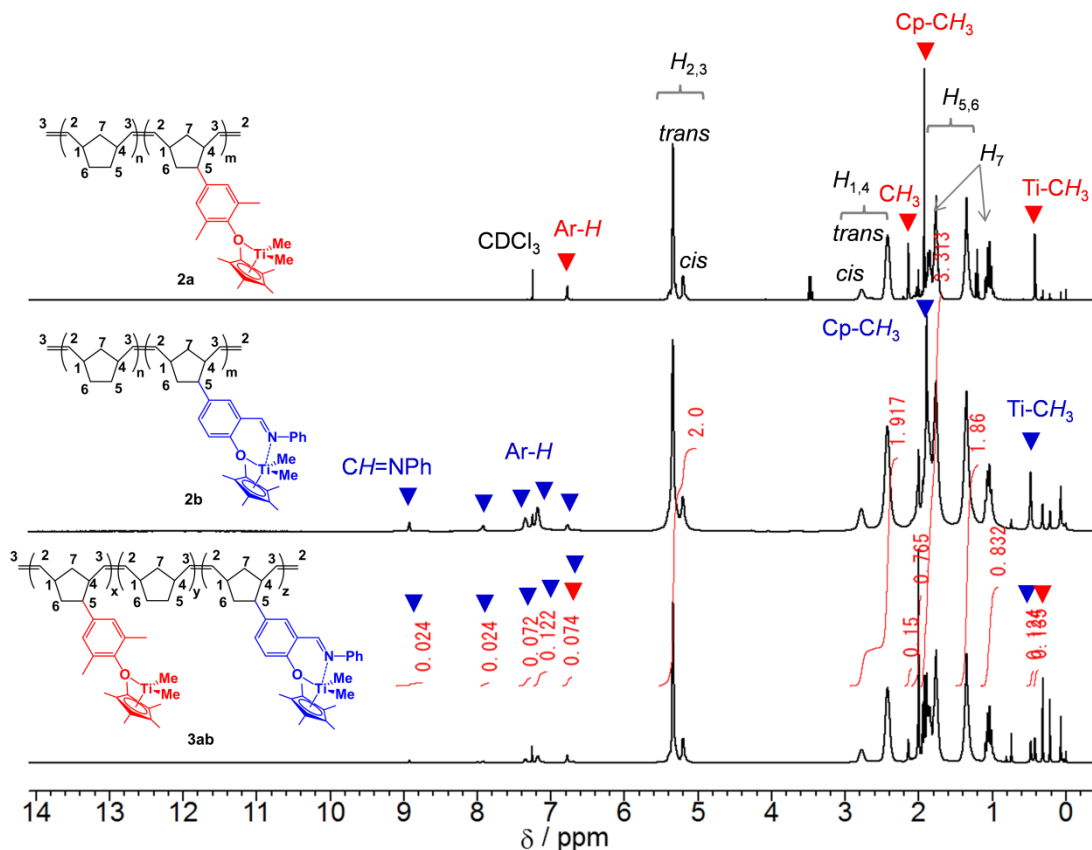


Figure 4 1H NMR spectra of Cp^*TiMe_3 grafted PNB-supported catalysts **2a** (top), **2b** (middle) and **3ab** (bottle).

Ethylene polymerization

Ethylene polymerization was performed using seven kinds of catalyst such as molecular catalysts (**1a**, **1b**), their tandem catalyst (**1a+1b**), PNB-supported catalysts (**2a**, **2b**), their tandem catalyst (**2a+2b**) and terPNB-supported catalyst (**3ab**) and the results were summarized in **Table 2**. The both of molecular catalysts **1a** and **1b** showed high polymerization activity at 0 °C, while it largely decreased at 30 °C. It indicates that

the catalysts are unstable and it tends to be deactivated by heat. This tendency was also confirmed in the tandem molecular catalyst **1a+1b**. The polymer chain-supported catalysts **2a** and **2b** showed lower activity than that respective molecular catalyst at the 0 °C. It is considered that the activation by the activator is suppressed by the polymer support, while the suppression of activity at 30 °C was decreased compared to the molecular catalysts. The tandem PNB-supported catalyst showed similar or slightly lowers activity than the average value of **2a** and **2b**. On the other hand, it was found that the polymerization activity of the PNB-supported catalyst **3ab** was higher than that of the average value of **2a** and **2b** and the tandem PNB-supported catalyst at 0 °C.

Table 2 Ethylene polymerization results using respective catalysts.^a

Run	Cat. ($\mu\text{mol-Ti}$)	Temp. ($^{\circ}\text{C}$)	Activity (kg-PE/mol-Ti-h)	T_m^b ($^{\circ}\text{C}$)	T_c^b ($^{\circ}\text{C}$)	X_c^b (%)
1	1a (2.5)	0	20200 \pm 2000	141.2	119.7	75
2	1a (2.5)	30	8340 \pm 220			
3	1b (2.5)	0	19900 \pm 340	137.8	118.5	75
4	1b (2.5)	30	10200 \pm 990			
5	1a (1.25) + 1b (1.25)	0	25800 \pm 1900	140.8	119.2	78
6	1a (1.25) + 1b (1.25)	30	6890 \pm 540			
7	2a (2.5)	0	14700 \pm 190	139.0	120.7	71
8	2a (2.5)	30	8860 \pm 1460			
9	2b (2.5)	0	10700 \pm 820	139.0	121.0	74
10	2b (2.5)	30	12300 \pm 260			
11	2a (1.25) + 2b (1.25)	0	8860 \pm 130	138.8	120.8	73
12	2a (1.25) + 2b (1.25)	30	9500 \pm 570			
13	3ab (2.5)	0	15900 \pm 1020	137.6	119.3	70
14	3ab (2.5)	30	10200 \pm 930			

^a Polymerization conditions: toluene 300 mL, ethylene 0.6 MPa, catalyst 2.5 μmol , TIBA 0.125 mmol, $\text{Ph}_3\text{CB}(\text{C}_6\text{F}_5)_4$ 8.0 μmol , reaction time 10 min.

^b Determined by DSC.

Tensile test

Tensile test of PEs synthesized with tandem molecular catalyst (**1a+1b**), tandem PNB supported catalyst (**2a+2b**) and terPNB-supported catalyst (**3ab**) was carried out. The results are shown in **Figure 5**. There was almost no difference in elastic deformation range in all of the samples. The order of elongation at break was **3ab** > **1a+1b** > **2a+2b** and PE produced by **3ab** was not broken. It seems to be derived from the fusibility due to difference of mixing degree of the produced polymers. It is presumed that the polymer is present in a nonuniform manner using the tandem polymer supported catalyst (**2a+2b**) since the polymer is independently generated from the catalyst sites **a** and **b**. Therefore, it is considered that the fusibility at the interface between the polymers declined and it became easy to break. On the other hand, in the the polymer produced by catalyst **3ab** was uniformly blended and fused easily.

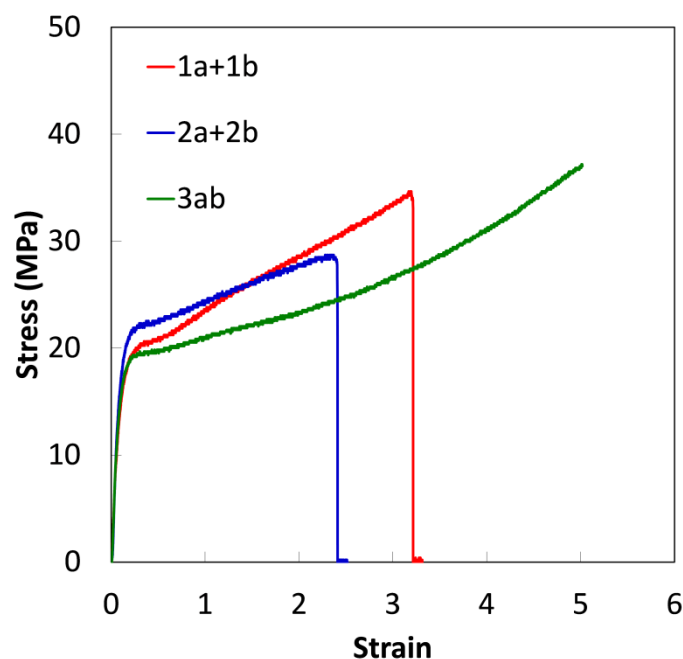


Figure 5 Stress-strain curves for PE produced by **1a+1b**, **2a+2b** and **3ab**.

Conclusions

In order to bridge the gap between molecular and solid catalysts, polymer supported olefin polymerization catalyst was suggested. A series of polynorbornene (PNB) bearing aryloxo group and/or phenoxy-imine group were synthesized by ring-opening polymerization using Grubbs catalyst. Copolymers and terpolymer controlled the structure precisely were successfully obtained and Cp^*TiMe_3 was grafted onto these PNB-support. While the activity of PNB-supported catalyst was lower than the molecular catalyst at low temperature, the deactivation at room temperature was suppressed by grafting onto PNB-support. It was found that a catalyst supported on the one polymer chain show higher activity than just mixing the each PNB-supported catalysts. From the tensile test, it indicated the ternary PNB supported catalyst provided a homogeneously dispersed polyethylene (PE) which generating from different active sites, whereas the tandem catalyst provided heterogeneously dispersed PE. It was succeeded to propose a catalyst having a precise active site structure and a unique catalyst behavior using a polymer supported catalyst.

References

- [1] E. Albizzati, U. Giannini, G. Collina, L. Noristi, L. Resconi, in: E.P. Moore Jr. (Ed.), *Polypropylene Handbook*, Hanser, New York, 1996, Chapter 2, pp. 11–98.
- [2] M. P. McDaniel, *Adv. Catal.* 1985, **33**, 47.
- [3] M. P. McDaniel, *Adv. Catal.*, 2010, **53**, 123.
- [4] L. Resconi, L. Cavallo, A. Fait, F. Piemontesi, *Chem. Rev.* 2000, **100**, 1253.
- FI
- [5] H. Makio, H. Terao, A. Iwashita, T. Fujita, *Chem. Rev.* 2011, **111**, 2363.
- [6] D. J. Arriola, E. M. Carnahan, P. D. Hustad, R. L. Kuhlman, T. T. Wenzel, *Science* **2006**, *312*, 714.
- [7] H. Li, T. J. Marks, *Proc. Natl. Acad. Sci. U.S.A.* 2006, **103**, 15295.
- [8] M. Delferro, T. J. Marks, *Chem. Rev.* 2011, **111**, 2450.
- [9] J. P. McInnis, M. Delferro, T. J. Marks, *Acc. Chem. Res.* 2014, **47**, 2545.
- [10] M. Stürzel, S. Mihan, R. Mülhaupt, *Chem. Rev.* 2016, **116**, 1398.
- [11] H. Suo, G. A. Solan, Y. Maa, W.-H. Sun, *Coord. Chem. Rev.* 2018, **372**, 101.
- [12] S. Liu, A. Motta, M. Delferro, T. J. Marks, *J. Am. Chem. Soc.* 2013, **135**, 8830.
- [13] S. Liu, A. Motta, A. R. Mouat, M. Delferro, T. J. Marks, *J. Am. Chem. Soc.* 2014, **136**, 10460.
- [14] A. Thakur, R. Baba, P. Chammingkwan, M. Terano, T. Taniike, *J. Catal.* 2018, **357**, 69.
- [15] S. T. Nguyen, L. K. Johnson, R. H. Grubbs, *J. Am. Chem. Soc.* 1992, **114**, 3974.
- [16] C. W. Bielawskia, R. H. Grubbs, *Prog. Polym. Sci.* 2007, **32**, 1.
- [17] G. C. Vougioukalakis, R. H. Grubbs, *Chem. Rev.* 2010, **110**, 1746.

- [18] H. Makio, N. Kashiwa, T. Fujita, *Adv. Synth. Catal.* 2002, **344**, 477.
- [19] M. Mitani, J. Saito, S. Ishii, Y. Nakayama, H. Makio, N. Matsukawa, S. Matshui, J. Mohri, R. Furuyama, H. Terao, H. Bando, H. Tanaka, T. Fujita, *Chem. Rec.* 2004, **4**, 137.
- [20] A. E. Cherian, E. B. Lobkovsky, G. W. Coates, *Macromolecules* **2005**, *38*, 6259.
- [21] K. Nomura, N. Naga, M. Miki, K. Yanagi, A. Imai, *Organometallics* 1998, **17**, 2152.
- [22] K. Nomura, K. Oya, Y. Imanishi, *Journal of Molecular Catalysis A: Chemical* 2001, **174**, 127.
- [23] K. Nomura, N. Naga, M. Miki, K. Yanagi, *Macromolecules* 1998, **31** 7588.
- [24] H. Zhang, S. Katao, K. Nomura, J. Huang, *Organometallics* 2007, **26**, 5967.
- [25] T. L. Choi, R. H. Grubbs, *Angew. Chem. Int. Ed.* 2003, **115**, 1785.

Chapter 5

General Conclusion

This dissertation discussed the establishment of catalyst combining the concepts of solid and molecular catalyst through the study of molecular catalyst that mimics solid catalyst structure with a systematic design and polymer-supported catalyst possessing well defined active site structures and multifunctionality.

In Chapter 1, general introductions introduced the definition and importance of catalysis, olefin polymerization catalysts, approaches using heterogeneous and homogenous catalysts and bridging catalysts in olefin polymerization and the objectives of this dissertation.

In Chapter 2, polyhedral oligomeric silsesquioxanes (POSS) supported Phillips-type molecular catalysts for ethylene polymerization were synthesized to minimize the heterogeneity of solid support surfaces. A series of POSS-supported chromium catalysts with different active-site environments were obtained by the introduction of different functional groups. Their ethylene polymerization performances were influenced by the functional groups. Especially, diphenylphosphino group improved the activity and provided a bimodal polyethylene (PE). The similar result was confirmed in diphenylphosphino group modified silica supported catalyst. It was revealed that the design strategy based on the support functionalization can be transferred to SiO₂-supported chromium catalysts.

In Chapter 3, a series of POSS-supported chromium catalyst was used with various alkyl aluminum (AlEt₃, Al^{*i*}Bu₃, Al^{*n*}Ot₃) and Ph₃CB(C₆F₅)₄ to reveal the influences on the catalyst performance. The activity of POSS-supported chromium catalyst with alkylaluminum was determined by the balance of activation and deactivation. In contrary, Al^{*i*}Bu₃/Ph₃CB(C₆F₅)₄ system constantly enhance the activity since it stabilized the chromium site as cationic species. In particular, the catalyst having

diphenylphosphino group was improved the activity and influenced the molecular weight distribution. The co-catalyst system also enhanced the ethylene/1-octene copolymerization activity. It was revealed that the choice of functional group and activator is crucial for determination the catalyst performance.

In Chapter 4, a new type olefin polymerization catalyst which can accumulate multiple active sites with clear structure on one polymer chain was investigated to bridge the gap between solid and molecular catalyst. A series of polynorbornene (PNB)-support possessing different functional groups were synthesized by ring-opening metathesis polymerization using Grubbs catalyst. Copolymers and terpolymer possessing aryloxo group and/or phenoxyimine group were synthesized. The structure of PNB-supports were controlled precisely and Cp^*TiMe_3 were grafted on them successfully. The terPNB-supported catalyst exhibited higher activity compared with a mixture of each PNB-supported catalyst having sole active site species. Polyethylene produced by the terPNB-supported catalyst showed good elongation property compared with tandem molecular/PNB-supported catalyst systems. It indicated that ternary PNB-supported catalyst produced uniformly dispersed PE which generating from different active sites. It was found that PNB-supported catalyst has a unique catalyst features and is promising for develop a novel catalyst class.

Thus these results in this work suggests a series of model molecular catalysts with systematic design is a useful tool for the better understanding of a solid catalyst performance and the bridging of multiple active site on polymer chains shows unique catalyst performance. The results in this dissertation can be applied to other catalyst systems and will contribute developments of catalyst chemistry.

Acknowledgments

I would like to express my sincere gratitude to Associate Professor Dr. Toshiaki Taniike. This work would never have been achieved without his kind helps. I am deeply grateful to Professor Dr. Minoru Terano, Assistant Professor Patchanee Dr. Chammingwan, Research Assistant Professor Dr. Toru Wada and Research Assistant Professor Dr. Ashutosh Thakur for many helpful discussion and advices. I am deeply grateful to Dr. Kazuhiro Yamamoto, Japan Polychem Co., for his help on GPC experiments and for his suggestions. I deeply appreciate Professor Dr. Shinya Maenosono, Associate Professor Dr. Shinohara Ken-ichi, Associate Professor Dr. Shun Nisimura, Professor Dr. Hideki Kurokawa for valuable advices and comments. Finally, I wish to express my gratitude to all the laboratory members for their kind encouragements. Especially, I deeply appreciate all colleagues in olefin polymerization catalyst group for their helps and suggestions on the experiments.

Ryuki Baba

Achievements

Publications

Original Articles

1. The influence of functional groups on the ethylene polymerization performance of silsesquioxane-supported Phillips-type catalysts

Ryuki Baba, Ashutosh Thakur, Patchanee Chammingkwan, Minoru Terano, Toshiaki Taniike

Dalton Trans., 2017, **46**, 12158.

2. Synthesis of aryloxy-containing half-titanocene catalysts grafted to soluble polynorbornene chains and their application in ethylene polymerization: Integration of multiple active centres in a random coil

Ashutosh Thakur, Ryuki Baba, Patchanee Chammingkwan, Minoru Terano, Toshiaki Taniike

J. Catal., 2018, **357**, 69.

3. Activation and deactivation of Phillips catalyst for ethylene polymerization using various activators

Yanning Zeng, Patchanee Chammingkwan, Ryuki Baba, Toshiaki Taniike, Minoru Terano

Macromol. React. Eng., 2017, **11**, 1600046.

Presentations

International Conferences

1. Design of coordination environment of silsesquioxane-supported chromium catalyst for ethylene polymerization

World Polyolefin Congress 2015, Tokyo, Japan, Nov. 2015.

2. Synthesis of silsesquioxane-supported chromium catalyst bearing hemilabile ligand for ethylene polymerization

DU-JAIST Indo-Japan Symposium on Chemistry of Functional Molecules/Materials, Delhi, India, Feb, 2016.

3. Design of coordination environment of chromium species by hemilabile ligand of silsesquioxane-supported catalyst

4th Blue Sky Conference on Catalytic Olefin Polymerization, Sorrento, Italy, June, 2016.

Domestic Conferences

1. 分子構造の異なるシルセスキオキサン担持型クロム触媒の合成とエチレン重合特性

第64回高分子討論会、仙台、2015年、9月

2. シルセスキオキサンを利用したクロム触媒の配位環境設計とエチレン重合特性の検討

第45回石油・石油化学討論会、名古屋、2015年、11月

3. Hemilabile型シルセスキオキサン担持クロム触媒における配位環境設計とエチレン重合特性

第65回高分子学会年次大会、神戸、2016年、5月

4. ホスフィン修飾シリカを担体とした Phillips触媒の重合特性

第65回高分子討論会、横浜、2016年、9月